University of Nevada, Reno

Early Visual Processing in Autism Spectrum Disorder as Assessed by Visual Evoked Potentials

A thesis submitted in partial fulfillment of the requirements for the degree of Master of Science in Psychology

By

Natalie F. Leslie Fournier

Dr. Jeffrey J. Hutsler/Thesis Advisor

May, 2022

THE GRADUATE SCHOOL

We recommend that the thesis
prepared under our supervision by

Natalie F. Leslie Fournier

entitled

Early Visual Processing in Autism Spectrum Disorder as Assessed by Visual Evoked Potentials

be accepted in partial fulfillment of the
requirements for the degree of

MASTER OF SCIENCE

Jeffrey J. Hutsler , Ph.D.
Advisor

Michael A. Crognale, Ph.D
Committee Member

Debra C. Vigil, Ph.D.
Graduate School Representative

David W. Zeh, Ph.D., Dean
Graduate School

May, 2022

Abstract

Understanding early visual processing and the integrity of the visual pathways in Autism Spectrum Disorder (ASD) could help to develop a potential neuromarker. If these early stages of visual perception are compromised it could be impacting higher cognitive abilities that are necessary for social perception. For example, atypical visual behaviors such as poor eye gaze, difficulty with facial expression, and difficulty processing motion have been highly documented in social and nonsocial domains in ASD. These symptoms have been linked to abnormal sensory processing suggesting possible impairments in the magnocellular visual pathway (M-pathway). To assess early visual processing and the integrity of the visual pathways we used achromatic pattern-reversal along with a motion-onset and offset stimuli in children and adolescents with and without a diagnosis of ASD. Visual-evoked potentials (VEPs) were used to investigate early visual processing in adolescents with ASD compared to neurotypicals (NTs). For pattern-reversal, we used a black-and-white checkerboard with two different sizes (1° and 0.25°) and four different contrast levels (0.025 contrast, 0.05 contrast, 0.1 contrast, and 0.98 contrast). To study motion-onset and offset we used an expanding and contracting 'dartboard.' These stimuli were displayed to a total of seven male ASD and eight male NT subjects, ranging in age from 10-15 years old. VEPs were recorded on the scalp midline over the occipital (Oz) and parietal (Pz) cortices. For pattern-reversal, we examined the negative component N75, and the positive component P100. For motion-onset and motion-offset, we explored the positive component P100 and the negative component N135. VEPs responses were analyzed using measures of peak latency, peak amplitude, mean amplitude, and fractional

area latency. Our results point to a disruption of the M-pathway where the ASD subjects often showed hyper-responsiveness to lower contrast stimuli presented at the largest check size. Individual waveforms in ASD subjects were variable, and may not be useful as a reliable early neuromarker. Some measures of the VEP seem to be related to symptom severity as assessed by the GARS-2, although these results never reached significance. For motion-onset, the ASD group presented larger amplitudes for the components P100 and N135 at electrode size Oz. Alterations to early visual processing in the ASD group suggest specific difficulties in the magnocellular system which could be causing a cascade of symptoms that impairs social communication. Although individual waveform variability limits the use of VEPs as a neuromarker, there is some potential relationship to symptom severity that deserves further study.

Acknowledgements

We thank the participants and parents who volunteered in our study, as well as the individuals who helped in clinical assessments, particularly Celia N. Zisman for some of the early EEG recordings and Sean O'Neil for assisting with plot-contrast responses. I also thank my principal investigator, family, and female friends for their eternal support who have inspired me to follow a STEM career against all odds.

Table of Contents

List of Tables

List of Figures

Author Contributions

Early stages of this project were a collaborative effort across two research groups: the Cognitive and Brain Science (CBS) and the Applied Behavioral Analysis (ABA) programs within the Department of Psychology at the University of Nevada, Reno. Both groups contributed their expertise: CBS with EEG data collection; and ABA with their knowledge of individuals with ASD as well as habituation techniques and participant training.

1. Introduction

Autism spectrum disorder (ASD) is a neurodevelopmental condition with impairments in social communication and social interaction, as well as repetitive patterns of behavior, interests, or activities. These classic characteristics in ASD can range from mild to severe. The prevalence today of ASD is about 1 in every 54 children (CDC, 2020). The diagnosis is still largely based on behavioral criterion, and no current medical test consistently identifies the condition. Because of this, diagnosis cannot take place until these behaviors manifest themselves in early childhood. One major goal of ASD research is to identify potential markers that could identify at-risk individuals earlier in development. The present work explores the utility of well-characterized scalp-recording techniques to visual stimuli to distinguish between ASD and neurotypical (NT) subjects. Additionally, the utility of visual evoked potential (VEPs) as an early diagnostic marker applied to individual subjects with ASD is assessed, along with the potential relationship between symptom severity and VEP alterations.

Leo Kanner, in the 1940s, was one of the first to describe ASD behaviors in children and noted the presence of both hypo- and/or hyper-responsiveness to sensory stimuli. Since that time, sensory-processing difficulties in ASD have been reported in the auditory, somatosensory, and visual domains. It wasn't until 2013 that the *Diagnostic and Statistical Manual of Mental Disorders, 5th ed.* (DSM-5) added restricted patterns of behavior an individual could exhibit hyper- or hypo-reactivity to sensory input.

Although sensory alterations can occur across domains, here I focus on alterations that may be present in early visual processing. Visual perception alterations in ASD have been demonstrated in a variety of tasks (for a review, see Brown et al., 2020). These

include abnormal eye movements (Howard et al., 2019), altered face processing (Gepner, 2002), and difficulties with motion coherence and biological-motion perception (Dakin & Firth, 2005). Altered behavioral responses in these types of simple visual tasks suggest abnormalities may be present at the earliest stages of visual processing. These types of simple visual impairments may prove to be useful for the early detection of ASD, since they may be perceptible before other behaviors manifest (Bakroon & Lakshminarayanan, 2016; Little, 2018). Such hopes depend upon a better characterization of the functioning of the early visual system in this condition.

1.1. Early Visual Pathways

VEP recordings are focused on the brain responses in the first 500 milliseconds (ms) after a visual stimulus is presented. This makes them ideal for assessing the overall integrity of the early visual pathways that transmit information to the visual cortex. These pathways start at the retina and project to the primary visual cortex (V1) via the lateral geniculate nucleus (LGN) (Callaway, 2005). At this early stage, visual information is already segregated into parallel processing streams and shows selectivity for specific types of visual features. One of these streams, the magnocellular pathway (M-pathway), is essential for detecting motion and sends information to motion-specialized cortical regions, such as the V5/MT (Livingstone & Hubel, 1988; Fujita et al., 2011; Kaplan & Shapley, 1986). In contrast, the parvocellular pathway (P-pathway) carries information to color-sensitive cortical areas such as V4 as well as the rest of the ventral stream (Livingstone & Hubel, 1988; Fujita et al., 2011). These pathways differ in their physiological characteristics as well as their structural characteristics. The specialized fibers of the M-pathway are thick, resulting in faster impulse conduction of information

(Laycock et al., 2007). Other characteristics of the M-pathway include low spatial resolution, color insensitivity, saturation at high contrast, and high temporal resolution. The P-pathway, in contrast, has high spatial resolution, color sensitivity, lower contrast sensitivity, and lower temporal resolution (Livingstone & Hubel, 1988; Liu et al., 2006; Yamasaki et al., 2017). Visual cognitive functions of the M-pathway have been linked to motion processing, planning for actions, and attention (Laycock et al., 2007). Notably, each of these cognitive functions has been reported as being disrupted in ASD subjects. The impact of M-pathway impairments could underlie problems with global visual perception, motion processing, and socially relevant behaviors such as poor processing of eye gaze and facial expressions (Todorova et al., 2019). Several authors have suggested that these impairments might ultimately result in deficient social communication (Sutherland & Crewther, 2010; Brown & Crewther, 2017; Greenaway et al., 2013; Thye et al., 2018).

1.2. ASD VEPs with Traditional Measurement Strategies

Traditionally, VEP recordings taken from scalp locations over the visual cortex have been used to assess the early visual pathways. A standardized version of this recording technique is often used in clinical settings (Odom et al., 2016) to detect neuritis and demyelination of the optic nerve (Walsh et al., 2005). In addition, alterations to VEPs have been found in neurological disorders that include Fragile-X syndrome, attention deficit hyperactivity disorder (ADHD), schizophrenia, and multiple sclerosis (Sayorwan et al., 2018). As an example, VEP responses of children with ADHD show longer latencies and decreased amplitudes for a late negative component that occurs around 200 ms after the presentation of a visual stimulus (Yumnam et al., 2010).

The early visual components (N75 and P100) have also been examined in ASD in a series of studies utilizing both pattern-reversal and motion-onset stimuli (see stimuli examples, pp. 13-15). Such studies have suggested that both latency and peak amplitudes differ between ASD and NT groups, but the precise outcomes are often in disagreement. In a VEP study by Frey et al. (2013), using a checkerboard with a visual angle of 6.4° at a 100- percent contrast, ASD subjects show larger amplitudes and longer peak latencies for component P100 relative to NT participants. In contrast, studies by Kovarski et al. (2016; 2019) using the same paradigm of pattern reversal at 100 percent contrast, but a different check size, have shown a decrease in the amplitude of the P100 in ASD subjects. Despite these differences, studies tend to agree the M-pathway may be preferentially affected in ASD subjects (see Yamasaki et al., 2017, 2011; Brown & Crewther, 2017; Greenaway et al., 2013; Sutherland & Crewther, 2010; Constable et al., 2012).

1.3. Motion-Related Components and Behaviors in ASD

Although reversing checkerboards can activate the M-pathway, motion- specific responses can be elicited with actual moving stimuli. The earliest component often associated with activation in response to motion is the N135. This negative component occurs with a latency around 135 ms and shows a large peak for motion-onset stimuli (Bach & Ullrich, 1996; Kuba et al., 2007; Kubová et al., 1995). Although not many studies have employed motion-onset stimuli, and even fewer have examined motion-offset, when using an expanding and contracting stimulus ASD subjects have shown larger N135 amplitudes specifically to motion-onset when compared to NT subjects (Constable et al., 2012).

Behavioral assessments in ASD subjects also indicate deficits in various motion-processing tasks. For example, measures of motion coherence use more dynamic stimuli such as random dots moving with varying degrees of correlation in one direction. Participants have to detect and report the overall movement direction, and changes in the degree of correlated activity are used as a behavioral method of motion sensitivity. Using this type of stimuli, ASD subjects require approximately a ten percent greater coherent motion to accurately report the direction of movement relative to NT subjects (Spencer et al., 2000; Milne et al., 2002). In addition, other motion-relevant tasks are affected in ASD. These include biological motion and motion-captured facial expressions (Dakin & Firth, 2005; Zane et al., 2019; Van der Hallen et al., 2019; Blake et al., 2003). Taken together, these studies suggest the motion-sensitive magnocellular stream is impaired in individuals with ASD. The ability of the visual system to detect and interpret movement and dynamics of the world is essential, since impairments in this ability have implications for processing basic visual stimuli as well as visually based emotional and social cues. Given the number and variety of studies documenting M-pathway relevant deficits in subjects with ASD, we can safely predict there may be motion-relevant alterations in the cortical responses of ASD subjects.

1.4. VEPs as a Biomarker and an Index of Symptom Severity

Of importance, it has been proposed that VEPs could be a potential diagnostic tool in ASD. To use VEPs as a diagnostic tool, waveforms from individuals have to conform to the group averages reported in the studies shown previously. However, none of these studies have reported individual waveforms. In addition, abnormalities in

individual waveforms and the early stages of visual processing could be related to the expression of symptoms in ASD.

A study by Sayorwan et al. (2018) correlated VEP parameters and symptoms of preschool children with ASD compared to a control group. Severity was assessed with the Autism Treatment Evaluation Checklist (ATEC) and the Vineland Adaptive Behavior Scales 2nd edition (VABS-II). They found ASD subjects present significantly longer N135 latencies that correlated with higher scores on the ATEC in sensory/cognitive awareness and lower scores for the VABS-II in the socialization domain. Another study by Sutherland and Crewther (2010) tested individuals scoring either low or high on the Autism Spectrum Quotient (AQ). They measured local and global processing, motion processing, and visual-pathway integrity assessing reaction time and VEPs recorded at the occipital point (Oz) electrode site. Their results indicate that individuals scoring high on the AQ showed difficulties with motion processing. This means that magnocellular processing is delayed in high-scoring AQ, decreasing the ability to integrate information from feedback communication associated with the magnocellular advantages. ASD subjects with severe forms of autism present more difficulties integrating visual information, which correlates with their severity and differences in latency. However, these differences were found between groups and not at the individual waveforms of each of their participants in response to visual stimuli. It is unknown whether variability in symptoms is associated with early visual components as measured by the VEP. Variability of scalp recordings in patient groups is a well-known phenomenon. In past studies, ASD groups have shown high variability (e.g., Haigh et al., 2015; Butler et al., 2017). Unfortunately, individual waveforms are not always presented in ASD studies.

Studies that have examined individual waveforms in subjects with ASD have reported high interindividual variability among participants both for sensory processing (Kovarski et al., 2019; Milne, 2011) and language (DiStefano et al., 2019). Because one of the goals of this research is to provide a potential early tool for diagnosis, the consistency of individual results in ASD subjects is key to achieving this outcome. In addition, if altered early visual responses are a predictor of the presence of ASD, then symptom severity may be associated with the severity of waveform alterations. An ASD neuromarker would help identify potential individuals earlier in development. This early biomarker of ASD is sought because, as demonstrated, earlier implementation of cognitive behavioral therapy provides the best long-term outcomes for this group (Ung et al., 2014).

1.5. Measuring VEP Waveforms and their Components

Traditional measures of VEP components assess the height and time, respectively, to a component's peak amplitude and peak latency. Both of these are single-point measures that do not consider the shape of the components. An alternative to peak amplitude is the area amplitude measure, an approach that uses a pre-specified time window and computes the average amplitude of the waveform within that window. An alternative to peak latency is the fractional area latency, also known as the 50 percent latency measurement, which assesses the area under the waveform that occurs between two preselected time points. The latency of the waveform is the time point that divides the area of the waveform in half. Relative to traditional measures, these measures are meant to address the assumption of traditional measures that individual components can be considered in isolation without the influence of adjacent waveforms. In other words, assessing amplitude and latency over a window is less susceptible to artifacts that can be

produced by adjacent waveforms and waveform averaging. Both approaches to measuring the amplitudes of individual scalp components are depicted in Figure 1. For mean amplitude measurements, a time window is defined for each component being measured and the mean voltage within that window is then calculated. For peak amplitudes, one determines the maximum amplitude reached within the defined time window for each component (Luck, 2005). In terms of results, mean amplitude presumably provides a result more robust to the influence of noise in the data. In addition, it is suitable for the comparison of two groups or conditions with a different number of trials. It is also not as susceptible to latency variability (Luck, 2005, 2014). In contrast, peak amplitude could be influenced by noise/variability in the data, which would likely affect the component's time and amplitude (Luck, 2005). The greatest downside of using mean amplitudes is determining which measurement window to apply to the subjects, where mean amplitudes could considerably vary depending on the window, while peak amplitude would be less dependent on the specific window when the largest waveform peak is being measured (Luck & Gaspelin, 2017).

Both approaches for measuring the latency of a component—peak latency and fractional area latency--are depicted in figures 1 & 2. Peak latency measurements find the time it takes to reach the maximum amplitude within a specific time window. There are some shortcomings to this approach, as peak latency measurements are highly sensitive to noise and change as noise increases in the data, largely because the measure heavily depends on the shape of the component's waveform (Luck, 2005). In contrast, fractional area latency computes the area under the event-related potential (ERP) waveform over a given time range and often finds the time point corresponding to the median value (Luck,

2005). Woodman (2010) explains that the 50 percent latency measurements can precisely measure the differences in latencies between two conditions even when the measurement window does not contain the whole component of interest or if some overlap of other components exists. Thus, this method is useful when components fail to present a clear peak. This is especially true of late components such as the N135, where the data can be noisy with multiple peaks (Kiesel et al., 2008; Luck, 2005, 1998). Due to theoretical differences between these techniques and the proposed advantage of these alternate measures, a comparison of the outcomes of the different measures in ASD has not been performed. This is particularly important in assessing patient groups where the components can vary and create overlap leading to measurement artifacts.

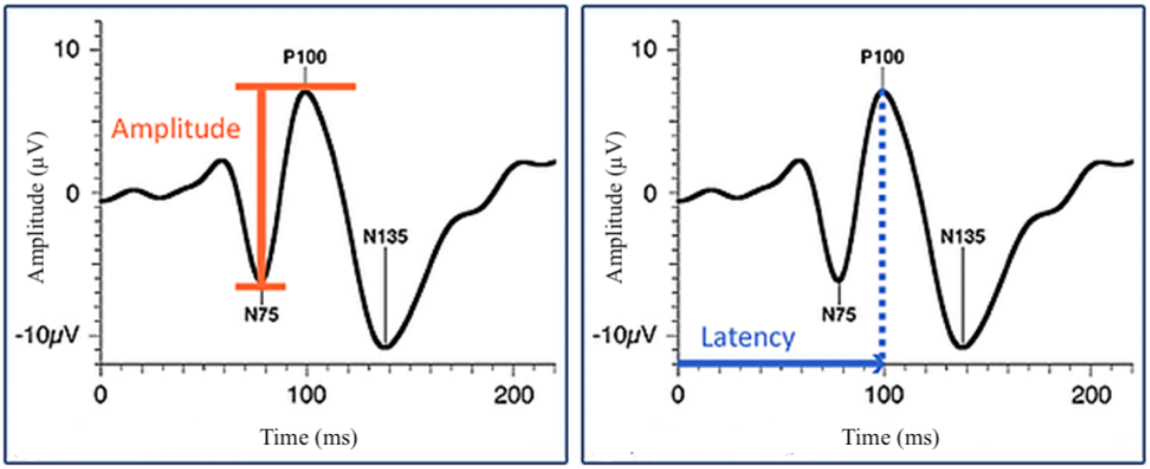

Figure 1. Measurements for peak amplitude and peak latency. Traditional measures of individual components in the VEP waveform. VEP peak amplitude is depicted on the left, in orange, while; peak latency is shown on the right panel, in blue (modified from Odom et al., 2016).

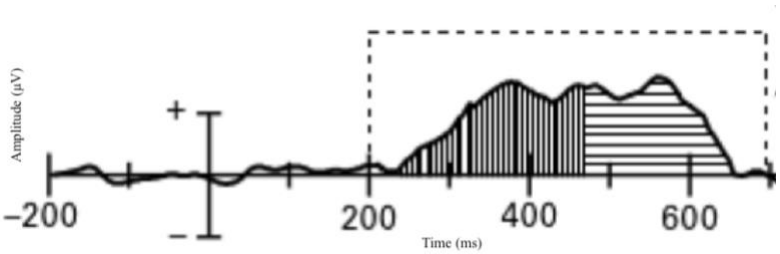

Figure 2. ERP graphs of the measurement for fractional area latency. In this example, the algorithm measures the area of the positive region between 200 and 600 ms and finds the latency of the point dividing this area into two equal regions. The 50 percent fractional area latency is depicted here (source: Luck, 2005).

1.6. Current Research Questions

The aim of this study is to investigate early visual processing in children and adolescents with and without a diagnosis of ASD. In addition, we assessed a standard clinical VEP paradigm along with visual stimuli not currently used in clinical settings. These included presenting stimuli with varying contrasts, as well as motion-onset and motion-offset stimuli to better assess for specific problems within the magnocellular visual pathways. The goal is to provide a potential biomarker based upon VEPs that can assess the early stages of visual processing. The following questions were addressed:

1) Can standard clinical-reversing checkerboard stimuli differentiate early visual responses between ASD and NT subjects?
2) Do ASD and NT subjects differ in their responses to both low and high contrast stimuli, or do differences in responses occur only with low-contrast stimuli?
3) Do motion-onset and motion-offset responses differentiate visual responses between ASD and NT subjects?

4) What do individual waveforms reveal about differences across individuals with ASD, and is there a relationship between individual VEP waveforms and assessments of symptom severity?
5) Do mean amplitude and fractional area latency measures differ from peak amplitude and peak latency measures in their assessment of the VEP?

2. Method

2.1 Participants

Participants were recruited with the assistance of Larry Williams, PhD, from the autism treatment program at the University of Nevada, Reno. A diagnosis of ASD was made according to DSM-IV criteria (subject diagnoses were completed prior to implementation of DSM-V criteria) along with the Autism Diagnostic Observation Schedule (2012). Symptomatology was further assessed with the Gillian Autism Scale (GARS-2, 2nd ed.; ASD: 84.87 ± 11.9). For pattern-reversal, a total of eight male participants with ASD were age-matched with six NT males between the ages of ten to fifteen (ASD: 13.25 ± 1.83; NT: 11.8 ± 1.77). For motion-onset/offset, a total of seven male participants with ASD were matched for chronological age with seven male NT subjects between the ages of ten to fifteen years. None of the ASD participants carried a comorbid diagnosis of intellectual disability and/or epilepsy. The subjects with ASD were habituated to the sensor attachment procedure for several sessions until movement criterion for the recording procedure was achieved. During the experiment, all participants were seated comfortably in a chair while staying as still as possible and were asked to look at the screen and fixate on a red cross for each stimulus. During the recording session, participants were monitored to ensure they were looking at the stimuli

and continued to tolerate the recording sensors. One participant with ASD was eliminated from the study after three habituation sessions due to extreme tactile sensitivities and an inability to adapt to the sensors. One NT participant for the pattern-reversal paradigm was eliminated because of poor signal-to-noise ratios and an insufficient number of trials for analysis. All testing procedures were approved by the University of Nevada, Reno, Internal Review Board. Informed written consent was obtained from the parents or guardians, alongside continuing assent from the participants.

Table 1. Details of adolescents and adults with ASD and NT groups matched for chronological age. Means, standard deviation, and ranges.

Participants	**ASD**	**NT**
N (males)	8	8
Chronological age	13.25 ± 1.83 (range 10-15)	11.8 ± 1.77 (range 10-15)
GARS-2	84.87 ± 11.9	-

2.2. Stimuli and Procedure

The International Society for Clinical Electrophysiology of Vision (ISCEV) specifies specific stimuli and recording conditions. This widely adopted paradigm provides core clinical information and can be used by most clinical electrophysiology settings throughout the world (Odom et al., 2016). These are pattern-reversal VEPs elicited by checkerboard stimuli presented at maximum contrast with large (1°) and small (0.25°) checks. Motion-onset/offset responses have been proposed as another promising method for diagnostic purposes. To elicit the motion-onset/offset response radial stimuli (Kuba et al., 2007), such as a contracting and expanding “dartboards,” were utilized (Bach and Hoffamn, 1999).

The experiment consisted of two passive visual tasks. Two types of stimuli were presented: a pattern-reversal stimulus (Figure 3) and a motion-onset and motion-offset

stimulus (Figure 4). The contrast of the stimuli was calculated using Michelson contrast and direct measurements of the relative differences in luminance. Contrast values are calculated by taking the differences between a stimulus' maximum and minimum values and dividing by their sum.

2.2.1. Pattern-Reversal Stimuli

Pattern reversals consisted of a black and white checkerboard presented at four contrast levels (0.025, 0.05, 0.1, and 0.98) and two check sizes (ISCEV standards, at 1 degree +/- 20 arc minutes per side and 0.25 +/- 20 arc minutes per side) (Odom et al., 2016; see Figure 3). Each reversal lasted 500 milliseconds. Stimuli were presented at a viewing distance of 56 centimeters. The total length of data acquisition was 60 seconds for each combination of check size and contrast for a total of 8 checkerboards presented to each subject in random order.

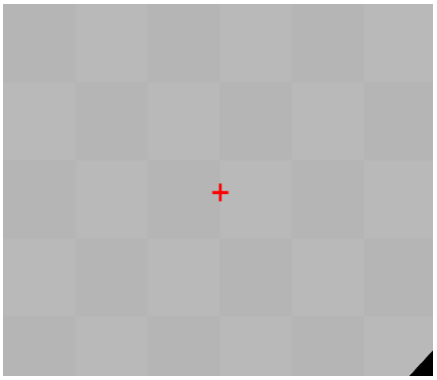

1(a): Checkerboard at 0.025 contrast

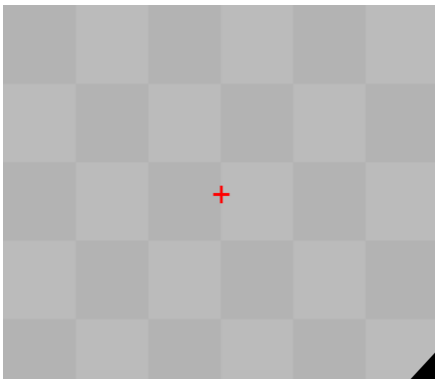

2(b): Checkerboard at 0.05 contrast

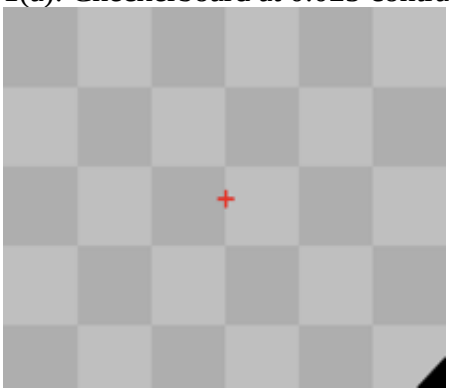

3(c): Checkerboard at 0.1 contrast

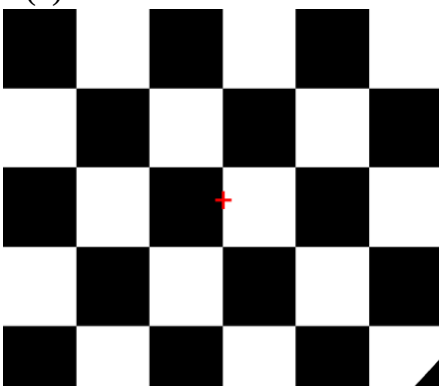

4(d): Checkerboard at 0.98 contrast

Figure 3. Experimental paradigm for pattern reversal. During one experimental block, each checkerboard with two check sizes (1° and 0.25°) were presented in random order with four contrasts (0.025, 0.05, 0.1, and 0.98).

2.2.2. Motion-Onset and Motion-Offset Stimuli

To assess responses to motion-onset/offset, an expanding and contracting "dartboard" (34° in diameter; Bach, 1999) had a contrast of 0.98 (see Figure 4). Motion-onset was generated with the abrupt onset of contraction or expansion of the pattern for 500 ms, followed by a stationary phase for 1500 ms for motion offset. Acquisition length for the expanding and contracting dartboard was 85 seconds with a viewing distance of 42 centimeters. Stimuli were generated using the RealStudio software package (Xojo, Inc) and run on a Dell desktop computer.

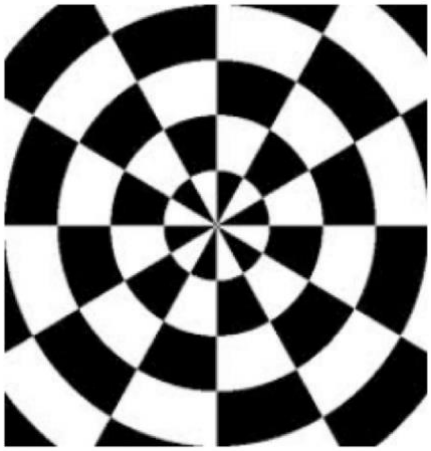

Figure 4. Experimental paradigm for motion onset and motion offset.

2.4. VEP Recording and Preprocessing

Recording sites and procedures were identical for both types of stimuli. Two recording electrodes were placed on the scalp at midline occipital (Oz) and midline parietal-occipital (Pz) locations. The midline central site (Cz) was used as reference, and Fz was used as ground (see Figure 5). Additional electrodes placed laterally to the outer canthus of each eye measured horizontal eye movements. Recordings were made with a BIOPAC MP150 WSW-G Data Acquisition System and input to a 21.5 – inch Core i5/2.7 GHz Apple IMAC computer running the Aqknowledge software package (BioPac, Inc). The signal was recorded at a sampling frequency of 625 Hz for the checkerboard and 1000 Hz for the dartboard. Raw data from the acquisition system was converted into the edf format within Matlab (Mathworks, Natick, MA, United States) files and uploaded for further analysis in EEGLAB and ERPLAB (Matlab Toolbox, MathWorks, Inc.). Data were filtered using an IIR Butterworth filter with a high pass of 0.1 Hz and a low pass of 100 Hz. To remove 60 Hz noise, a notch filter (Parks – McClellan) was applied to the data. The continuous EEG was time-locked, and trials were extracted in a 500 ms time window for the checkerboard (-100 ms pre-stimuli to 400 ms post-stimulus); dartboard

trials were extracted in a 700 ms time window (-200 ms pre-stimulus and 500 post-stimulus; Bach & Hoffmann, 2000). ERPs for the checkerboard were baseline corrected utilizing the 100 ms trace that occurred prior to stimulus onset. Baselines for the dartboard were corrected using the trace that occurred 200 ms prior to stimulus presentation. For artifact detection and rejection, we used semi-automated rejection coupled with visual inspection. First, step-like artifacts, with a voltage threshold between 0.4 and 1 mV, were automatically rejected (Luck, 2005). This was followed by a visual inspection of individual subject eye-movement data and removal of trials where the eyes were not stationary. Using this procedure, rejection rates never exceeded 10 to 15 percent per subject for either the pattern-reversal trials or the motion-onset and motion-offset trials.

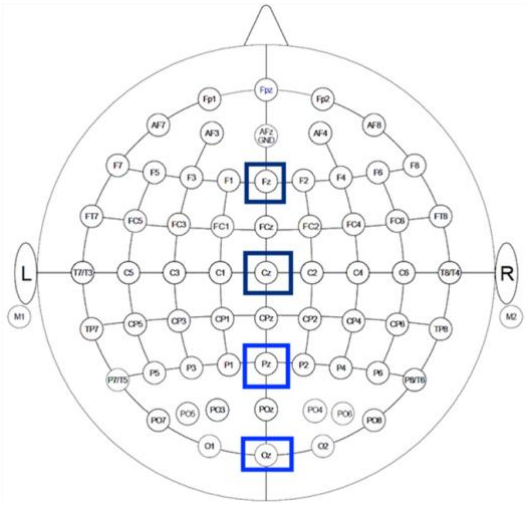

Figure 5. Electrode sites. Electrodes were placed on the scalp at the occipital region (Oz), the parietal region (Pz), the midline central (Cz) as reference, and midline frontal (Fz) as ground. Electrodes were placed laterally to the outer canthi of both eyes.

2.5. ERP Analysis

The first earliest negative component is the N75 is linked to early visual processing stages, and the window was defined as the greatest negative deflection in

between 60 and 100 ms (Shigeto et al., 1998). The N75 component has been proposed to emerge around the central parieto-occipital scalp, the peak of which disappears around 4 percent luminance contrast (Foxe et al., 2008). The first positive component--the P100--occurs around 25 ms after the N75 and has been proposed to represent responses arising from the occipital cortex. It has been suggested that the P100 component in pattern reversal is linked to changes in response to luminance contrast, which increases as contrast increases, and the peak disappears at around 2 percent contrast (Kuba et al., 2007). The P100 was measured by identifying the greatest positive deflection in the 80-130 ms latency range window for pattern-reversal. For motion-onset and motion-offset the greatest positive deflection in the 85-135 latency window was assessed (Bach & Hoffmann, 2000; see Figure 6). The second negative component--the N135--has been suggested to represent responses that are associated with moving stimuli (Kuba et al., 2007; Bach and Ulrrich, 1996). The N135 window was defined as the greatest negative deflection in the 100-205 ms latency range. These windows were chosen using temporal windows assessed by the *viewer window*. This tool is available in ERPLAB and allows the user to see the measured windows and their values (for more information review: López-Calderon & Luck, 2014). We applied those windows to extract amplitudes (peak amplitude and mean amplitude and latencies (peak latency and fractional area latency) for each of the components and recording sites at electrode site Oz for pattern-reversal and electrode site Oz and Pz for motion-onset and motion-offset for ASD subjects and NT group. N75, P100 and N135 components were visually inspected at the occipital (Oz) and parieto-occipital electrodes (Pz).

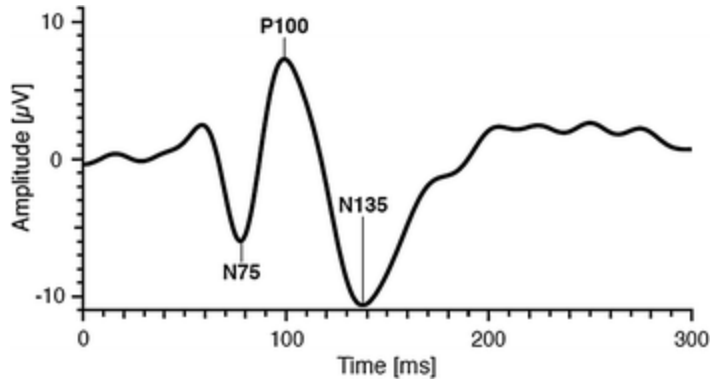

Figure 6. Classic sequence of ERP components plotted in a VEP waveform. In this plotting, positive is up and negative is down. The first negative component reaches a peak around 75 ms (N75). The first positive component (P100) reaches a peak around 100 ms. The second negative component is the N135, which peaks around 135 ms (source: Odom et al., 2016).

2.6. ERP Waveform Analysis

Statistical analysis was completed by matching the NTs and ASDs for chronological age. Analysis of variance with repeated measures (ANOVAs) for peak latency and amplitude of N75, P100 were performed with diagnostic groups (ASD, NT) as between-subjects factors; electrode site (mean values at parieto-occipital vs. occipital electrodes) were performed as within-subjects factors for pattern-reversal. The same analysis was carried out for the P100 and the N135 with Oz and Pz only, with the electrode site as a factor for motion-onset and offset. All data are presented as mean ± standard deviations or standard error of the mean (SEM) with calculations performed using SPSS 24, IBM, Inc.

In addition, effect sizes were calculated with Cohen's d to assess the differences between the two diagnostic groups (ASD vs NT). A Levene's test was used to determine if the variance values differed between the diagnostic groups. Finally, to evaluate the relationship between symptomology and the VEP measures, Pearson's r correlations were calculated.

3. Results

3.1. Can standard clinical reversing-checkerboard stimuli differentiate early visual responses between ASD and NT subjects?

VEPs provide specific types of information regarding the integrity of the visual pathways. Using different checkerboard sizes (as well as different contrast levels; see Section 3.2) the M- and P-pathways can be preferentially activated to investigate their relative contributions to potential visual-response differences between ASD and NT subjects (Ellemberg et al., 1999). Specifically, checkerboards presented at low contrasts and large check sizes (1° visual angle) are more likely to activate the M-pathway, while the P-pathway prefers higher contrasts and small checkerboard sizes (0.25° visual angle; Livingstone & Hubel, 1987). If differences between ASD and NT subjects are present, VEP recordings have the potential to identify the specific visual subpathways that may be involved. We assessed VEP responses to reversing checkerboards at two sizes and four contrast levels. Both the N75 and P100 components were examined.

3.1.1 Checkerboard-Reversal Responses at Electrode Site Oz

To explore group differences between subjects with ASD and NT controls at electrode site Oz, waveforms in response to reversing checkerboards were assessed using time windows around both the N75 and P100 components of the VEP (indicated by arrows in figures 7 and 8; also see Section 2.5). As stated previously, checkerboards are often used clinically at two check sizes (1.00 and 0.25 degrees of visual angle), and here we emulated those stimuli and employed the traditional measures of peak amplitude and peak latency. In addition, four contrast values were assessed, since group differences may not be apparent at maximum-contrast settings used in the clinic.

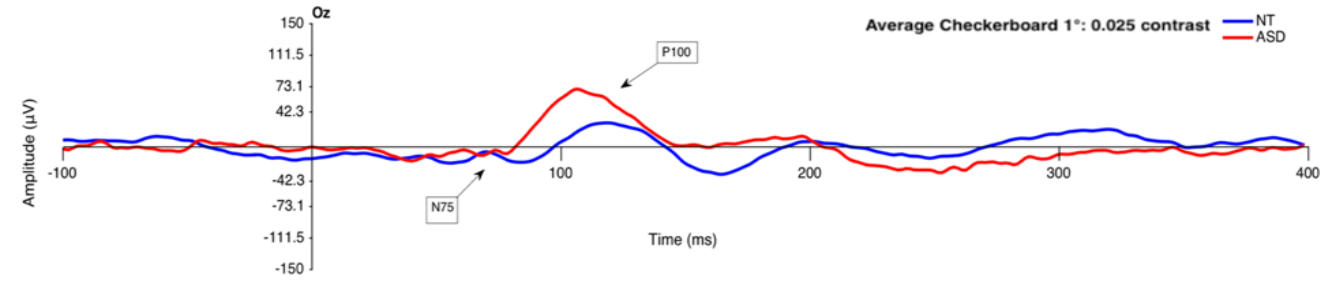

(A)

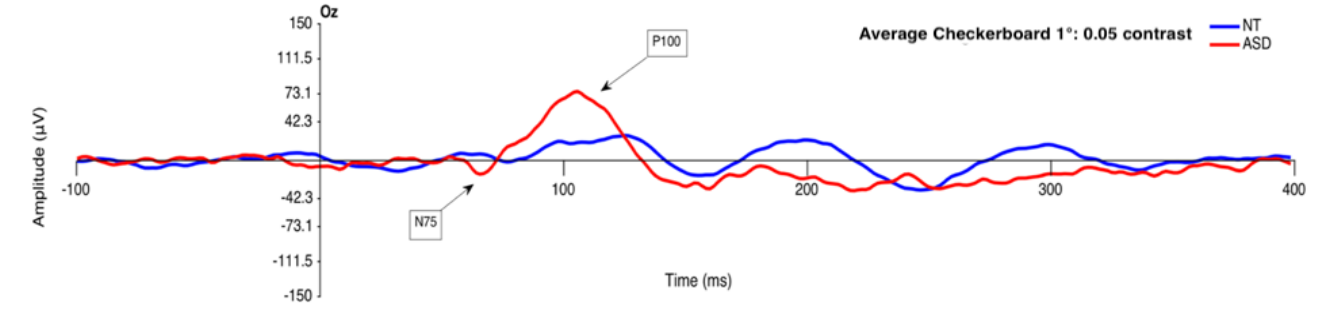

(B)

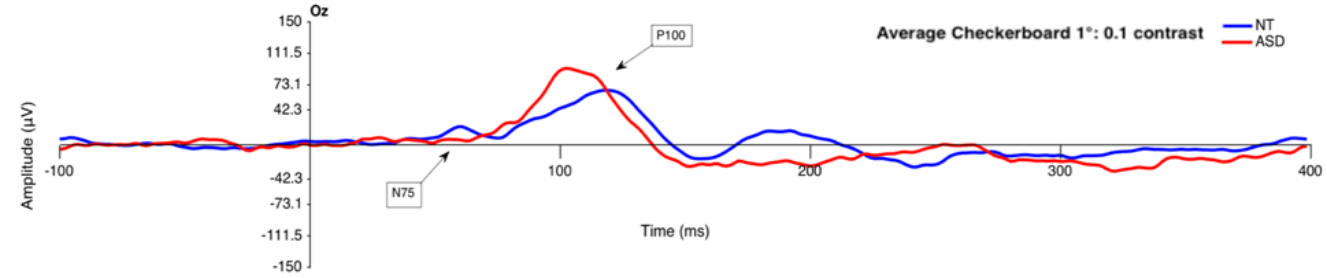

(C)

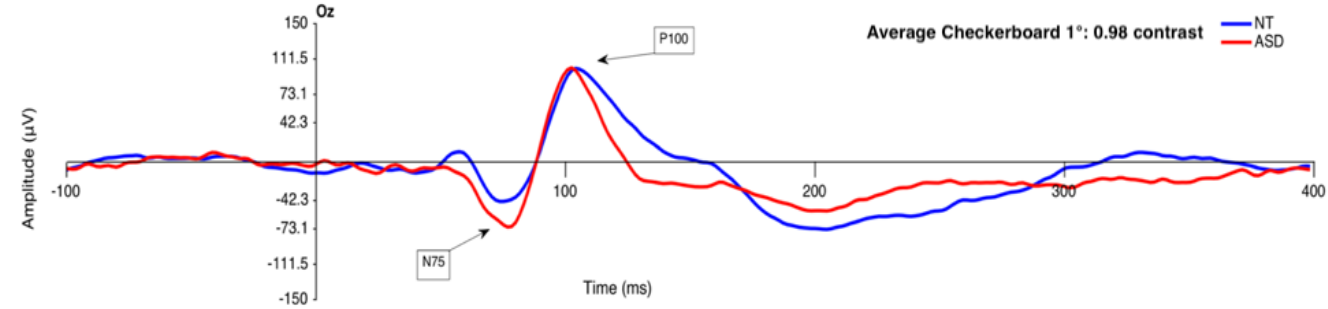

(D)

Figure 7. Grand-average ERP waveforms at the Oz electrode for checkerboard at a 1° visual angle. Comparisons of NT and ASD averaged responses to the large checkerboard presented at the following contrasts: (A) 0.025, (B) 0.05, (C) 0.1, and (D) 0.98.

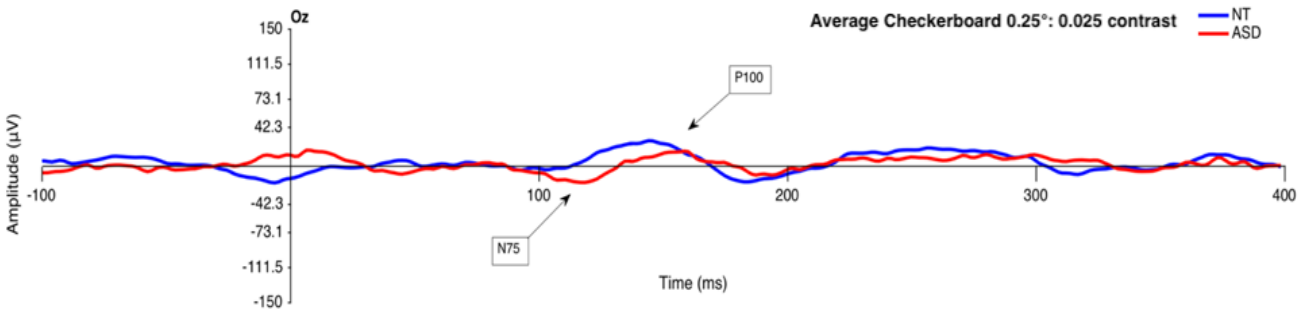

(A)

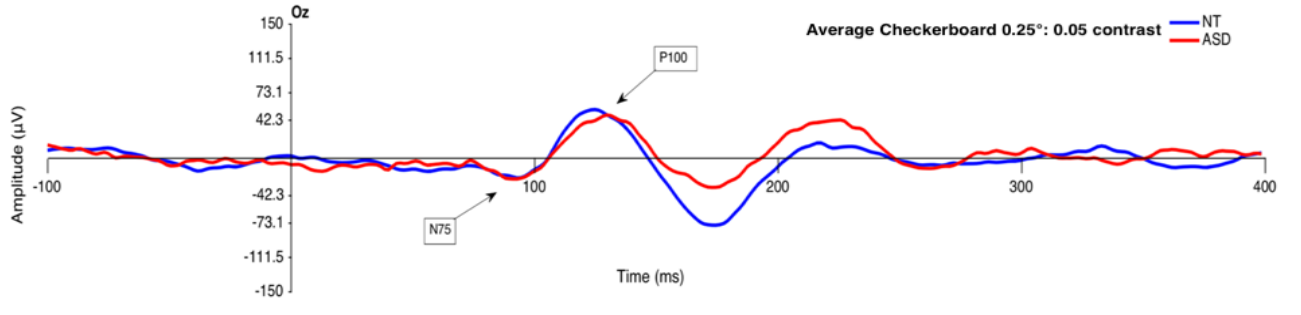

(B)

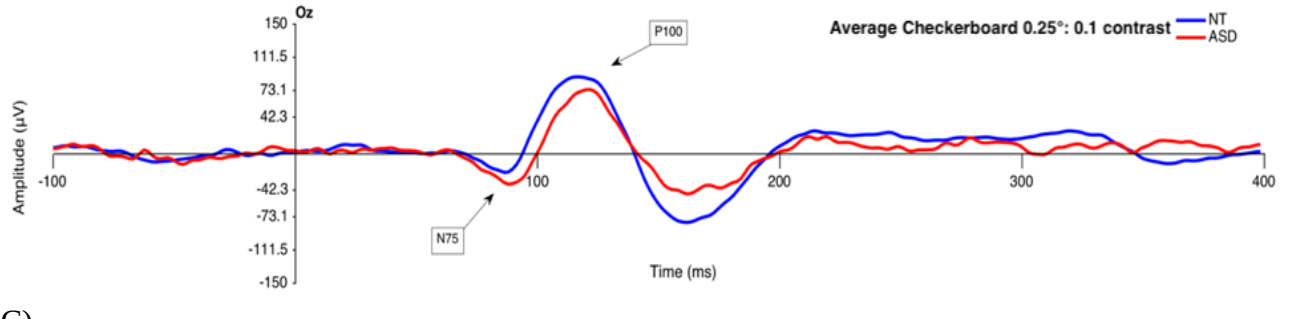

(C)

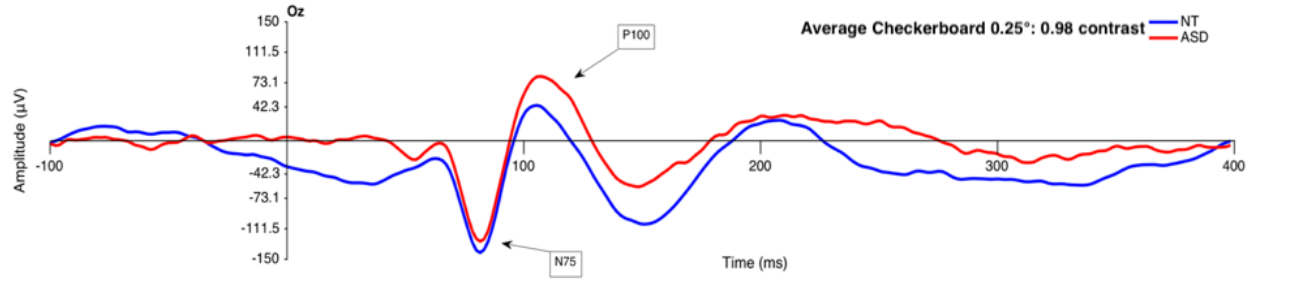

(D)

Figure 8. Grand-average ERPs waveforms for checkerboard at a 0.25° visual angle. Comparisons of NT and ASD averaged responses to the small checkerboard presented at the following contrasts: (A) 0.025, (B) 0.05, (C) 0.1, and (D) 0.98.

Peak Amplitudes

N75 Peak Amplitudes

The ANOVA analysis (Table 2) for component N75 at electrode site Oz showed significant effects for check size (at Oz, ASD: -10 ± 30 μV, NT: -30 ± 30 μV, $F_{(1,12)}$ = 19.237, p = .001; see Figure 7.A) and contrast ($F_{(3,36)}$ = 13.824, p > 0.001; see figures 7 and 8) as well as a two-way interaction between check size and contrast (ASD: -.02 ± .01 μV; at Oz, NT: -.01 ± .02 μV, $F_{(3,36)}$ = 16.283, p > 0.001; see Figure 7.B). Main effects and interactions were nonsignificant for diagnosis at component N75 for peak amplitudes.

The significant interaction found between check size and contrast was largely expected. The interaction arises from minimal differences found at the lower contrast levels between the large and small checks. Along with large amplitudes for the small check size relative to the large check size at the highest contrast (0.98; see figures 9 and 10). A lack of significant effects for diagnosis, either as a main effect or an interaction, indicates that from a practical perspective the N75 component may not readily distinguish between ASD and NT subject groups. This lack of differences applies to both check sizes as well as the four contrast values.

Table 2. ANOVA for peak amplitudes for component N75 at electrode site Oz.

Criteria	SS	DF	MS	F-value	P-value
Diagnosis	.002	1	.002	.350	.565
Check Size	.029	1	.029	19.237	.001
Check Size x Diagnosis	5.959E-5	1	5.959E-5	.039	.847
Contrast	.166	3	.055	13.821	<.001
Contrast x Diagnosis	.004	3	.001	.373	.773
Check Size x Contrast	.039	3	.013	16.289	<.001
Check Size x Contrast x Diagnosis	.001	3	.000	.308	.819

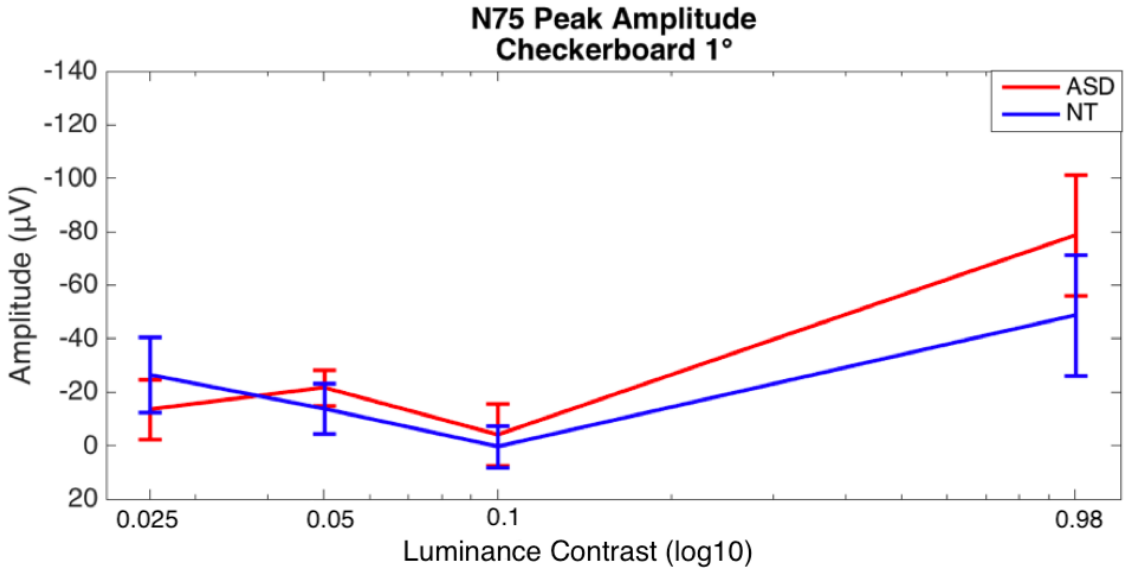

Figure 9. Contrast-response function for component N75 peak amplitudes for ASD versus NT at the larger checkerboard size for the four contrasts (0.025, 0.05, 0.1, and 0.98). Error bars represent standard error of the mean (SEM).

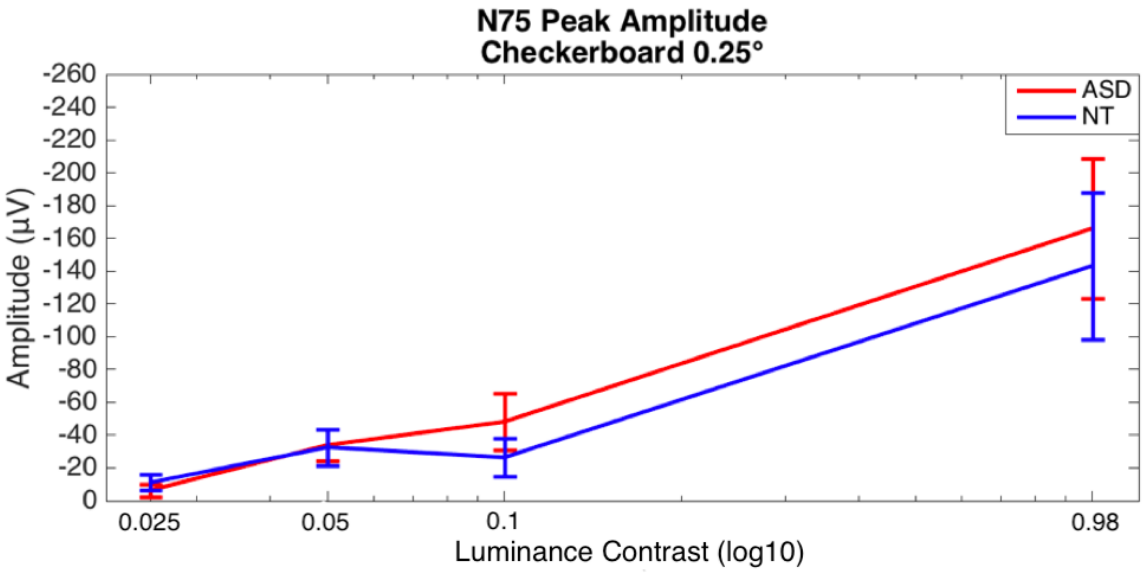

Figure 10. Contrast-response function for component N75 peak amplitudes for ASD versus NT at checkerboard size 0.25° visual angle at electrode Oz for four contrasts (0.025, 0.05, 0.1, and 0.98). Error bars represent SEM**.**

P100 Peak Amplitudes

The ANOVA analysis for component P100 (Table 3) showed a significant effect for check size (ASD: large check at Oz, 111 ± 54 μV; small check at Oz, 82 ± 42 μV; NT: large check at Oz, 75 ± 33; small check at Oz, 91 ± 83 μV, $F_{(1,12)} = 12.141$, $p = 0.005$; see figures 7.B and 8.B). In addition, a significant effect was found for contrast (ASD: 72 ± 52 μV, NT: 33 ± 27, $F_{(3,36)} = 16.024$, $p < .001$; see Figure 7.D). In this analysis, diagnosis showed nonsignificant main effects and interactions but did reveal several medium to large effect sizes for the large checkerboard between the ASD and NT groups. These effects occurred at 0.025 contrast (d = 0.9), 0.05 contrast (d = 1.09), and 0.1 contrast (d = 0.7) but not for the highest contrast value (.98; d = 0.2). In comparison, for the small check sizes only the highest contrast level (0.98) showed a similar effect size (d = 0.7; see figures 11 and 12).

The greater positive amplitudes found in the ASD subjects at a combination of the largest check size and the lowest contrast values suggest hyper-reactivity that may be attributable to the M-pathway (Figure 11). This contention is supported by the lack of group differences at both the highest contrast level for the large check size and at almost all the contrast levels of the small check size (Figure 12). The one exception was the highest contrast level (0.98) of the small check sizes. ASD subjects again showed larger amplitudes relative to the NT group; however, the difference appeared to be due to lower positive amplitude values in the NT subjects relative to their responses at the 0.1 contrast level. For NT subjects, the contrast function for the small check sizes *should* asymptote as contrast values increase, but our subjects showed lower average amplitudes (and higher individual variance: see figures 19 to 26 for individual subject waveforms). These results suggest the P100 component could distinguish between ASD and NT subjects when elicited with low-contrast and low-frequency stimuli. Given the large effect sizes we found, these results should be pursued in subsequent studies.

Table 3. ANOVA for peak amplitudes for component P100 electrode site Oz.

Criteria	SS	Df	MS	F-value	P-value
Diagnosis	.011	1	.011	1.609	.229
Check Size	.018	1	.018	12.141	.005
Check Size x Diagnosis	.005	1	.005	3.349	.092
Contrast	.072	3	.024	16.024	<.001
Contrast x Diagnosis	.001	3	.000	.192	.901
Check Size x Contrast	.008	3	.003	1.560	.216
Check Size x Contrast x Diagnosis	.011	3	.004	2.021	.128

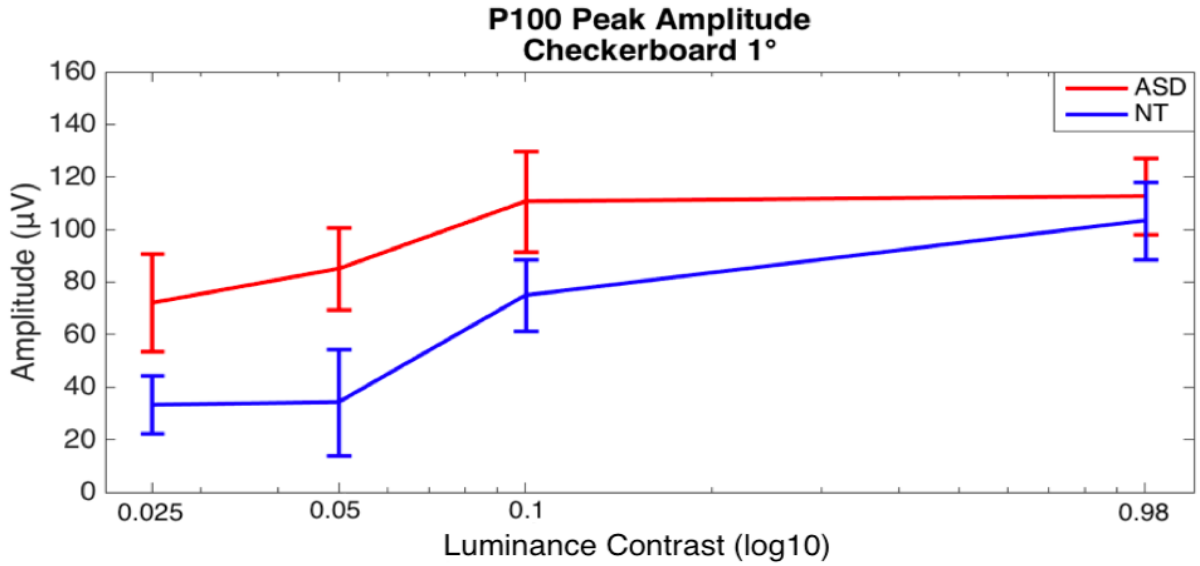

Figure 11. Contrast-response function for component P100 peak amplitudes for ASD versus NT at checkerboard size 1° visual angle at electrode Oz at the four contrasts (0.025, 0.05, 0.1, and 0.98). Error bars represent SEM. ASD peak amplitudes were higher than those found in the NTs at the lower (0.025, 0.05, and 0.1) contrast values. For the 0.98 contrast, ASD and NT subjects showed similar peak amplitudes. These results conform to the prediction that ASD subjects might show hyper-responsivity in the M-pathway since it is preferentially stimulated by low-contrast and larger checks (cf. Figure 12).

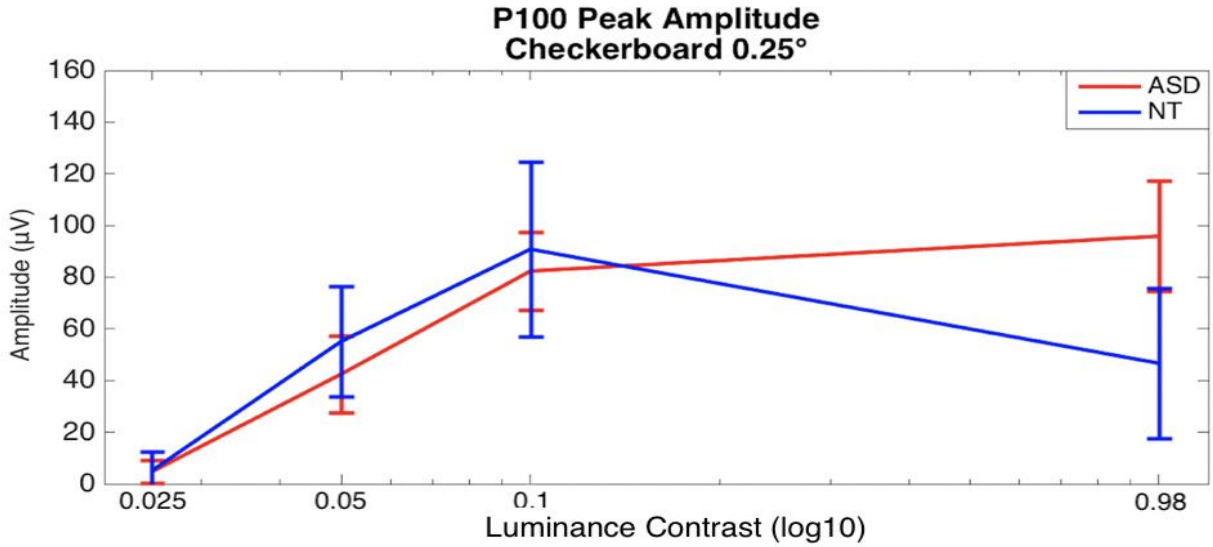

Figure 12. Contrast-response function for component P100 peak amplitudes for ASD versus NT at checkerboard size 0.25° visual angle at electrode Oz at the four contrasts (0.025, 0.05, 0.1, and 0.98). Error bars represent SEM. ASD and NT subjects showed similar response values where amplitudes increase along with contrast. Unusually, at 0.98 contrast, NT subjects showed smaller amplitudes relative to both the ASD subjects and their own responses at the 0.1 contrast level.

Peak-to-Trough Analysis

In the previous analyses, recording baselines were adjusted using pre-stimulus values to reduce the influence of drift on the raw amplitudes. Another way to limit the influence of transient baseline shifts in the recordings was to utilize peak-to-trough measures of the differences between the amplitudes of the N75 and P100 components. Because these measures straddle the baseline, this distance should be somewhat consistent even in the presence of drift away from the baseline. Utilizing the difference between the peak amplitude of the N75 component and the peak amplitude of the P100 component as the dependent measure, an ANOVA model was constructed examining the factors of diagnosis, check size, and contrast. This analysis (Table 4) showed a significant effect for contrast ($F_{(3,36)} = 40.483$, $p < .001$) as well as a two-way interaction between

check size and contrast ($F_{(3,36)} = 7.482$, $p = .001$). Qualitatively, ASD subjects showed larger peak-to-trough differences for the large check sizes independent of the contrast, while NT subjects showed a reduction in peak-to-trough as contrast increased (Figure 13). For the small check size, ASD subjects showed smaller peak-to-trough differences for each of the contrast values compared to the NT subjects who showed larger differences that decreased as contrast increased (Figure 14).

Although diagnosis did not show any main effects or interactions with other variables, we found large effect sizes at the 0.025 contrast (d=1.3) and the 0.1 contrast (d = 1.4) and medium effect sizes for the low contrast (0.025: d = 0.5) and for the high contrast (0.98: d = 0.5). For the small checkerboard, we found medium effect sizes at a 0.98 contrast (d = 6). These results are mostly consistent with the already presented results for the raw peak amplitude of the N75 and P100 (see tables 2 and 3). Once again, ASD subjects showed larger amplitudes for the large check sizes at low contrasts but smaller effects at the small check sizes.

Table 4. ANOVA for peak-to-trough analysis using peak amplitudes at electrode site Oz.

Criteria	SS	Df	MS	F-value	P-value
Diagnosis	.023	1	.023	1.244	.287
Check Size	.001	1	.001	.800	.389
Check Size x Diagnosis	.004	1	.004	2.162	.167
Contrast	.364	3	.121	40.483	<.001
Contrast x Diagnosis	.007	3	.002	.829	.487
Check Size x Contrast	.048	3	.016	7.482	.001
Check Size x Contrast x Diagnosis	.009	3	.003	1.430	.250

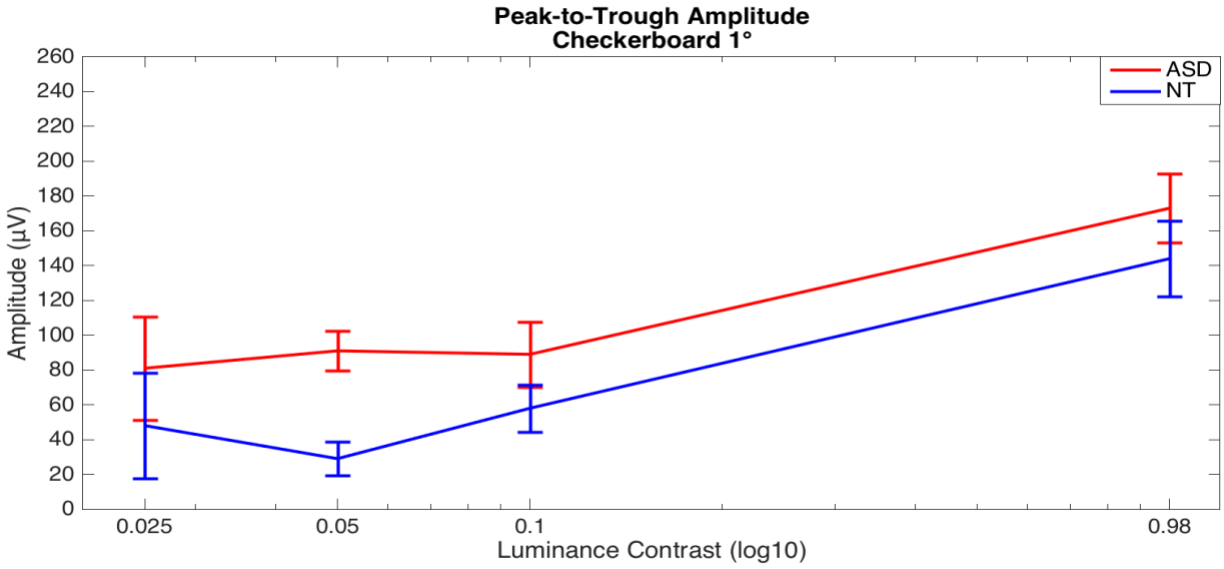

Figure 13. Contrast-response function for peak-to-trough amplitudes for ASD versus NT at checkerboard size 1° visual angle at electrode Oz at the four contrasts (0.025, 0.05, 0.1, and 0.98). Error bars represent SEM.

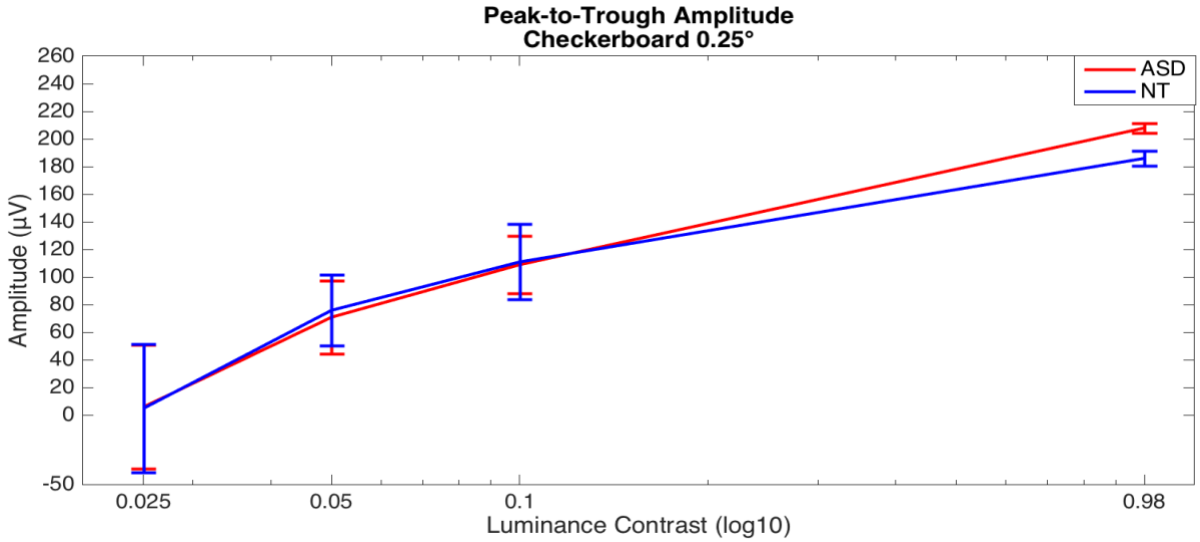

Figure 14. Contrast-response function for peak-to-trough amplitudes for ASD versus NT at checkerboard size 0.025° visual angle at electrode Oz at the four contrasts (0.025, 0.05, 0.1, and 0.98). Error bars represent SEM. ASD and NT subjects show similar peak-to-trough amplitudes at all four contrast levels, with the largest difference occurring at the highest contrast (0.98; d = 0.6).

Peak Latency

In addition to the evaluation of amplitudes, latency measures have the potential to differentiate between ASD and NT subjects. To determine if this was the case, peak latency values were measured for both the N75 and P100 components and, as before, used in a model that considered diagnosis, the two check sizes, and the four contrast levels of the stimuli.

N75 Peak Latency

For peak latency of the N75 component (Table 5), a main effect was found for check size (ASD: large check at Oz, 68.8 ± 7.97 ms; small check at Oz, 79.2 ± 8.29 ms; NT: large check at Oz, 106.7 ± 20.8 ms; small check at Oz, 81.86 ± 1.87 ms, $F_{(1,12)} = 8.643$; $p = .012$; see figures 7.C and 8.D). All other main effects and interactions were non-significant, including those involving diagnosis. Despite these non-significant results, a large effect size ($d = 1.0$) was present for the large checkerboard but only at the 0.1 contrast level. These results, along with an examination of figures 15 and 16, indicate that although the N75 for the large checkerboard may have some promise for distinguishing between ASD and NT subjects at specific contrast values (i.e., faster latencies for ASD subjects), latency of the N75 may not be useful for discriminating between the two groups. In general, peak latency did not show clear differences between the groups (see figures 15 and 16).

Table 5. ANOVA for peak latency for component N75 electrode site Oz.

Criteria	SS	Df	MS	F-value	P-value
Diagnosis	131.750	1	131.750	1.730	.213
Check Size	1405.488	1	1405.488	8.643	.012
Check Size x Diagnosis	78.493	1	78.493	.483	.500
Contrast	32.768	3	10.923	.101	.959
Contrast x Diagnosis	100.242	3	33.414	.310	.818
Check Size x Contrast	687.107	3	229.036	2.183	.107
Check Size x Contrast x Diagnosis	231.610	3	77.203	.736	.538

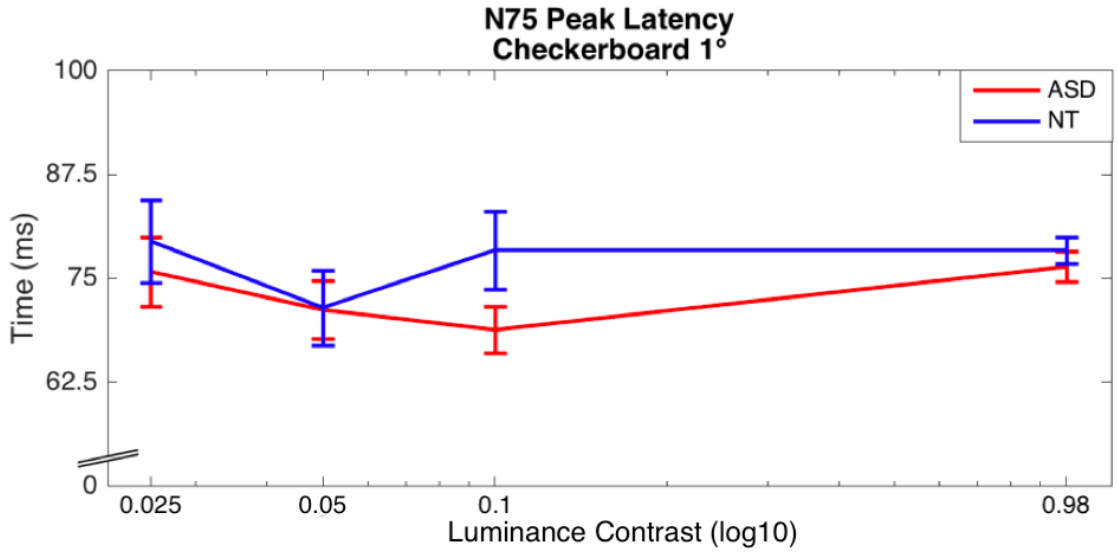

Figure 15. Contrast-response function for component N75 peak latency for ASD versus NT at checkerboard size 1° visual angle at electrode Oz and the four contrasts (0.025, 0.05, 0.1, and 0.98). Error bars represent SEM. Although ASD subjects showed faster N75 latencies at the 0.1 contrast level, this result was not significant, and the spurious nature of this difference relative to the other contrast levels would require further confirmation. In general, N75 latency values at the large check size do not appear to be useful for discriminating between ASD and NT subjects.

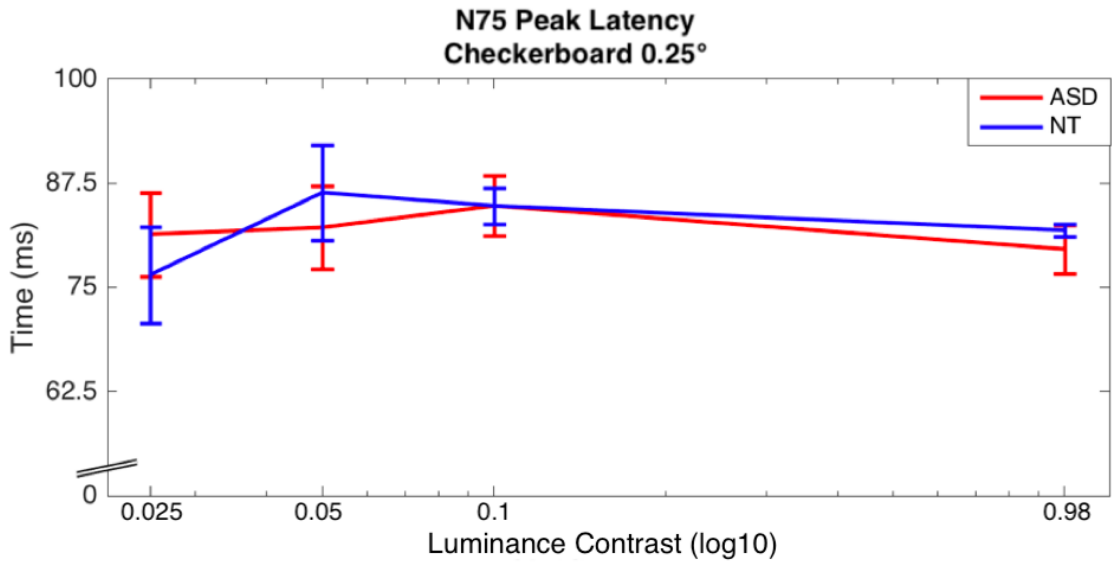

Figure 16. Contrast-response function for component P100 peak latency for ASD versus NT at checkerboard size 0.25° visual angle at electrode Oz for the four contrasts (0.025, 0.05, 0.1, and 0.98). Error bars represent SEM. N75 latencies in response to the small check sizes do not appear to have a utility in discriminating between ASD and NT subjects in this paradigm.

P100 Peak Latency

Component P100 (Table 6) showed a significant two-way interaction between check size and contrast ($F_{(3,36)} = 3.587$, $p = .023$) along with a significant main effect for contrast (at Oz, ASD: 107.8 ± 6.73 ms, NT: 107.4 ± 12.4 ms, $F_{(3,12)} = 5.380$, $p = .004$; see Figure 7.B). Although average latencies were largely the same between the small and large check sizes, these values became short for the lowest contrast value but only at the small check size (cf. figures 17 and 18).

As with the N75, no significant main effects or interactions existed for diagnosis. As before, some large effect sizes were apparent for diagnosis but only for the large check sizes and, even then, only for specific contrast values (0.025; d = 1.19, .1; d = 0.7). Thus, latency measures did not identify clear differences among the ASD subjects for either the N75 or the P100 components.

Table 6. ANOVA for peak latency for component P100 electrode site Oz.

Criteria	SS	Df	MS	F-value	P-value
Diagnosis	191.408	1	191.408	1.705	.216
Check Size	11.293	1	11.293	.087	.774
Check Size x Diagnosis	232.002	1	232.002	1.779	.207
Contrast	2204.608	3	734.869	5.380	.004
Contrast x Diagnosis	9.773	3	3.258	.024	.995
Check Size x Contrast	1288.250	3	429.417	3.587	.023
Check Size x Contrast x Diagnosis	604.181	3	201.394	1.682	.188

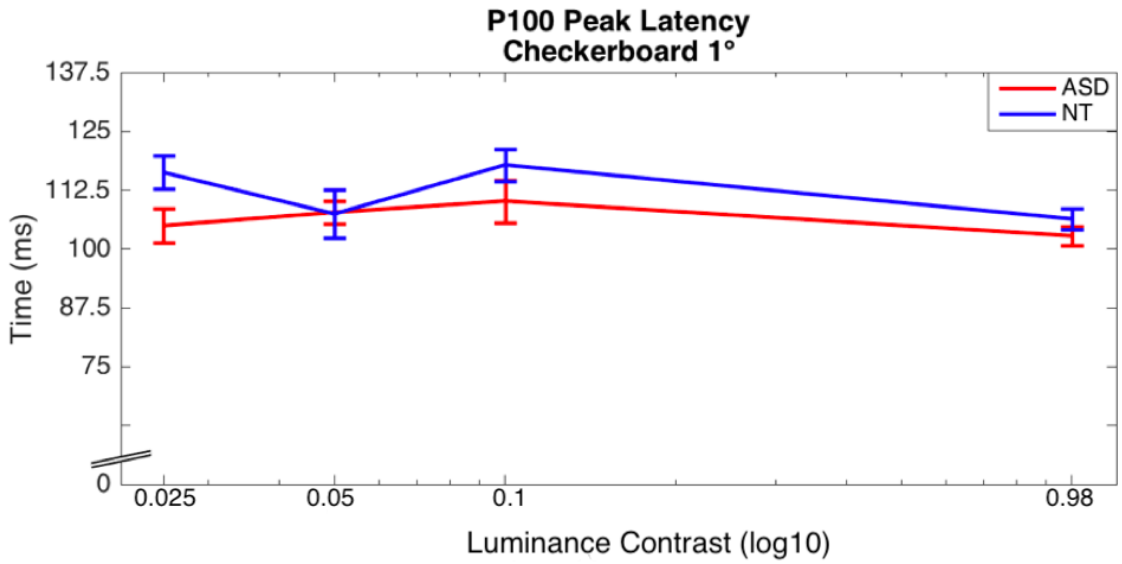

Figure 17. Contrast-response function for component P100 peak latency for ASD versus NT at checkerboard size 1° visual angle at electrode Oz for the four contrasts (0.025, 0.05, 0.1, and 0.98). Error bars represent SEM. Although factors and interactions were non-significant for diagnosis, we found a large effect at 0.1 contrast (d = 0.7) and at 0.025 contrast (d = 1.19). Here, ASD subjects present shorter latencies.

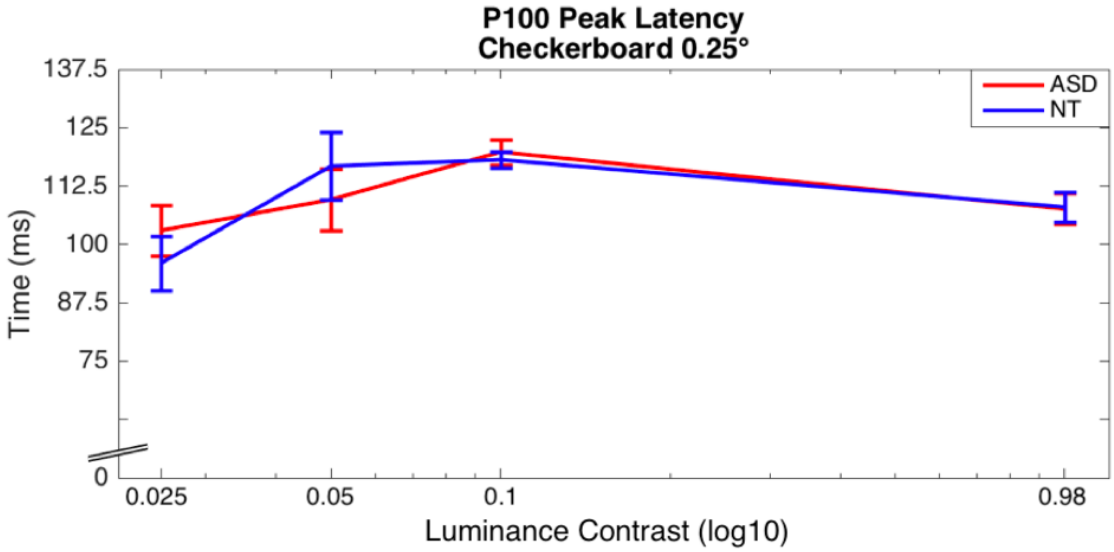

Figure 18. Contrast-response function for component P100 peak latency for ASD versus NT at checkerboard size 0.25° visual angle for the four contrasts (0.025, 0.05, 0.1, and 0.98). Error bars represent SEM.

3.2. Do ASD and NT subjects differ in their responses to both low- and high-contrast stimuli, or do differences in responses occur only with low-contrast stimuli?

The M- and the P-pathways not only can be stimulated by different sizes of the checkerboard (1.0 and 0.25 degrees), but they also can be segregated by contrast sensitivities each of these pathways prefers. Contrast sensitivity provides extra detail of the integrity of the visual pathways where low contrasts are most likely to stimulate the M-pathway, while the P-pathway is stimulated by higher contrast (Ellemberg et al., 1999; Allen, 1986).

Due to the small sample size, the effects involving diagnosis were non-significant. We did, however, find medium (d = 0.5) to large effect sizes (d = 1.19) for contrast between groups. These differences where present more for the large checkerboard at lower contrasts for peak amplitude at the P100 component (d = 0.9 at 0.025 contrast, d = 1.09 at 0.05 contrast, and d = 0.7 at 0.1 contrast) compared to the smaller check, where

we found only a large effect (d = 0.7) at a 0.98 contrast. These results from traditional measurements suggest that low-contrast stimuli employing large reversing checkerboards have the potential to differentiate between the ASD and NT groups. In contrast, clinical protocols for VEP utilize only stimuli at full contrast. Since the M-pathway may be preferentially affected in ASD, the use of full-contrast stimuli would be suboptimal as a method of differentiating between ASD and NT subjects.

3.3. What do individual waveforms reveal about differences across individuals with ASD, and is there a relationship between individual VEP waveforms and assessments of symptom severity?

Although averaged group responses to the reversing checkerboard stimuli provide clues to where differences between ASD and NT subjects may occur, the utility of using VEP measures as a potential diagnostic tool largely depends upon the consistency of individual responses. Here we document the VEP traces of individual subjects to assess the repeatability of these waveforms. In addition, we examine whether simple measures of symptom severity (GARS-2 scores) are associated with quantitative VEP measurements. Together these results are meant to assess the practical utility of using VEP recordings as an indicator of: (1) an ASD diagnosis; and (2) the severity of ASD symptomatology.

3.3.1. Individual Waveforms for the Large Checkerboards at the Four Contrast Levels

To determine whether ASD subjects show consistent responses to each of the stimuli, individual waveforms were plotted for the two checkerboard sizes at each of the four contrast levels. Figures 19, 20, 21, and 22 show the individual waveforms for the

ASD participants (labeled PA) (A: top panel) and the NT participants (labeled PN) (B: bottom panel) at electrode site Oz for the large checkerboard (1° visual angle).

The association between the N75 and P100 peak amplitudes for each ASD subject and individual GARS-2 score are shown in tables 7 through 10, with each table representing the results at a different contrast level from the checkerboard stimuli. Individual components are reported from the lowest to the highest amplitude for ASD and NT subjects. Tables 7 through 14 show ASD subject GARS-2 scores. These values are a crude measure of symptom severity where subjects with scores above 85 are likely to have an ASD diagnosis, scores between 70 and 84 indicate a possible ASD diagnosis, and scores below 69 indicate an unlikely diagnosis. Correlation values were calculated between these individual GARS-2 scores and subject amplitude values at each of the contrast levels, the results of which appear within the relevant table legend. Although the waveform variance may appear higher in the ASD group (cf Panel A to Panel B in figures 19–22), the variance calculated based upon the peak amplitude values for the N75 and P100 at the four contrast levels never differed between the subject groups (evaluated with a Levene's test for equality of variance). It is, however, possible that peak amplitude values based upon a single point do not fully capture the overall fluctuations in the individual waveforms. Regardless of whether variation differs between the two groups, substantial variability exists in the individual traces as a whole. This data makes it unlikely that subject traces can classify individual subjects prior to a formal ASD diagnosis.

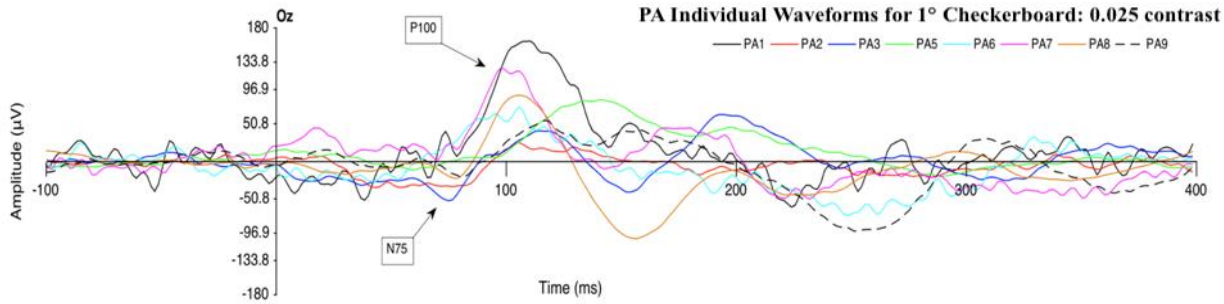

(A)

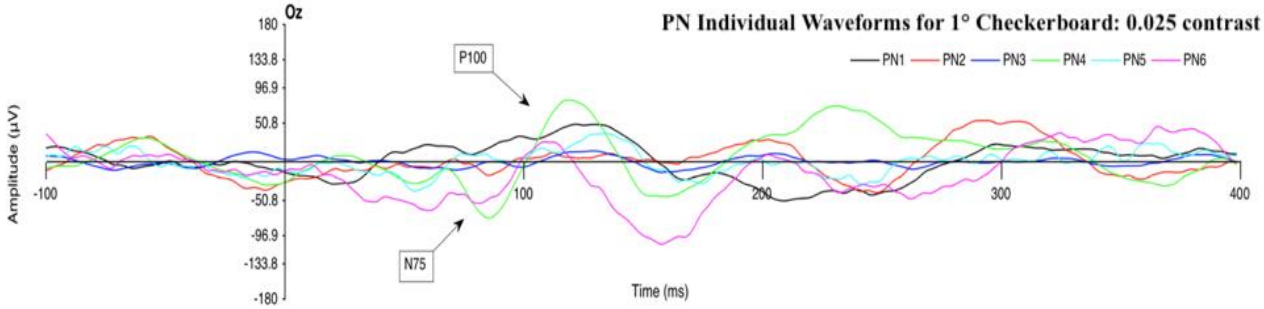

(B)

Figure 19. Checkerboard 1°: 0.025 contrast. Individual waveforms for ASD (A) and NT subjects (B) for the large checkerboard (0.025 contrast).

Table 7. ASD-subject GARS-2 scores, ordered from the lowest to the highest amplitude for components N75 and P100 for the large checkerboard (0.025 contrast). A negative correlation was found between GARS-2 scores and severity in ASD subjects for the components N75 r(6) = -.591 and P100 r(6) = -.257; however these relationships were not significant.

Component N75 ASD			**Component N75 NT**			**Component P100 ASD**			**Component P100 NT**		
ID	GARS -2	PkAmp μV	ID		PkAmp μV	ID	GARS -2	PkAmp μV	ID		PkAmp μV
PA3	85	-53	PN4	-	-74	PA5	76	5	PN2	-	12
PA2	104	-34	PN6	-	-64	PA2	104	25	PN3	-	14
PA8	100	-23	PN2	-	-18	PA3	85	41	PN5	-	18
PA1	76	-22	PN3	-	-11	PA9	87	55	PN6	-	26
PA9	87	-21	PN5	-	-1	PA6	70	74	PN1	-	49
PA5	76	-12	PN1	-	9	PA8	100	89	PN4	-	81
PA7	81	2				PA7	81	126			
PA6	70	54				PA1	76	162			

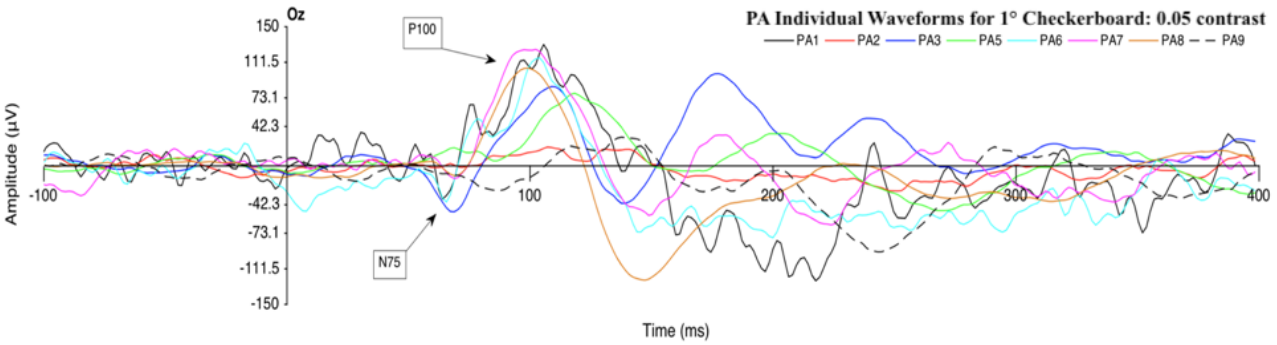

(A)

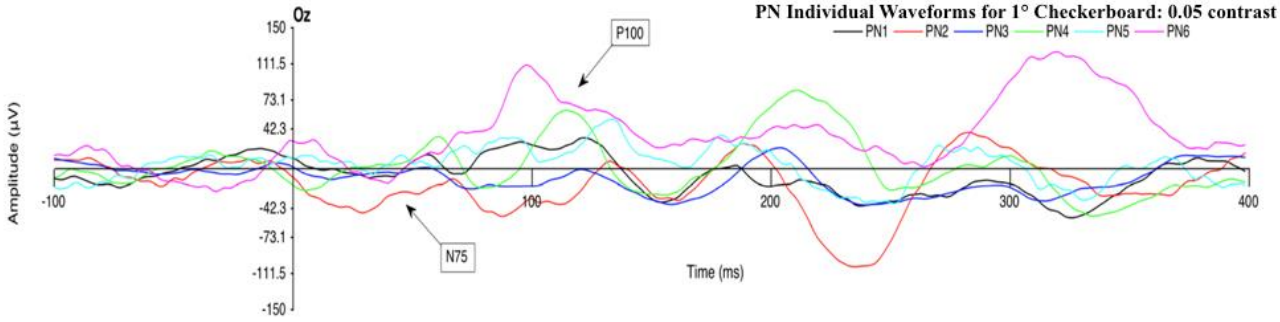

(B)

Figure 20. Checkerboard 1°: 0.05. Individual waveforms for ASD (A) and NT (B) subjects for the large checkerboard (0.05 contrast).

Table 8. GARS-2 scores for the ASD subjects are ordered from the lowest amplitude to the highest amplitude for components N75 and P100 for the large checkerboard at a 0.05 contrast. We found a positive correlation between GARS-2 scores and severity in ASD subjects for the components N75 r(6) = .399 and a negative correlation for P100 r(6) = -.558; however, these relationships were not significant.

Component N75 ASD			**Component N75 NT**		**Component P100 ASD**			**Component P100 NT**		
ID	GARS-2	PkAmp μV	ID	PkAmp μV	ID	GARS-2	PkAmp μV	ID		PkAmp μV
PA3	85	-50	PN2	-51	PA2	104	20	PN2	-	-32
PA6	70	-39	PN3	-22	PA9	87	21	PN3	-	-1
PA1	76	-36	PN4	-21	PA5	76	78	PN1	-	33
PA9	87	-27	PN1	-6	PA3	85	85	PN5	-	33
PA7	81	-14	PN5	2	PA8	100	105	PN4	-	62
PA8	100	-11	PN6	15	PA6	70	116	PN6	-	111
PA2	104	-2			PA7	81	125			
PA5	76	5			PA1	76	131			

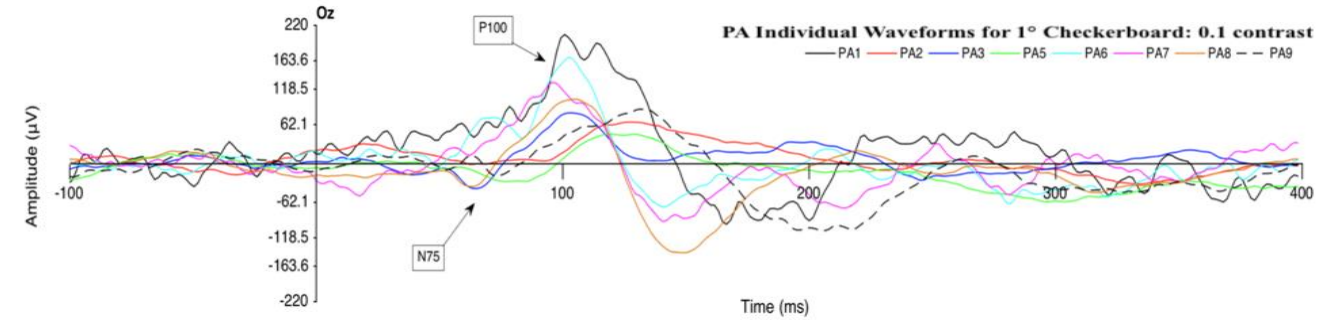

(A)

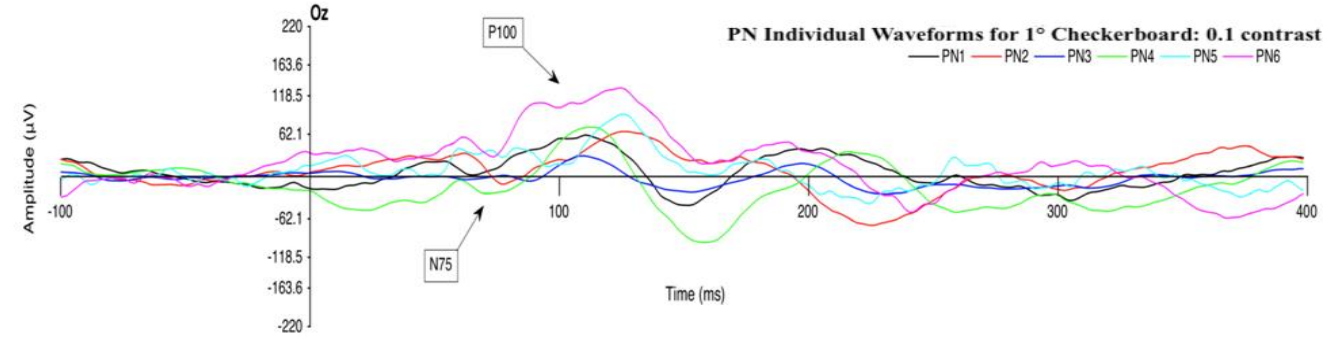

(B)

Figure 21. Checkerboard 1°: 0.1 contrast. Individual waveforms for ASD (A) and NT subjects (B) for the large checkerboard at 0.1 contrast.

Table 9. ASD-subject GARS-2 scores, from the lowest amplitude to the highest amplitude for components N75 and P100 for the large checkerboard (0.1 contrast). A negative correlation was located between GARS-2 scores and severity in ASD subjects for the components N75 r(6) = -0.512 and for P100 r(6) = -0.499; however, these relationships were not significant.

Component N75 ASD			**Component N75 NT**			**Component P100 ASD**			**Component P100 NT**		
ID	GARS-2	PkAmp μV	ID		PkAmp μV	ID	GARS-2	PkAmp μV	ID		PkAmp μV
PA3	85	-40	PN4	-	-25	PA5	76	47	PN3	-	30
PA8	100	-37	PN2	-	-11	PA2	104	66	PN1	-	61
PA5	76	-29	PN3	-	-7	PA3	85	81	PN2	-	66
PA9	87	-20	PN1	-	2	PA9	87	85	PN4	-	72
PA2	104	-2	PN5	-	14	PA8	100	103	PN5	-	91
PA7	81	13	PN6	-	29	PA7	81	129	PN6	-	130
PA6	70	40				PA6	70	169			
PA1	76	42				PA1	76	206			

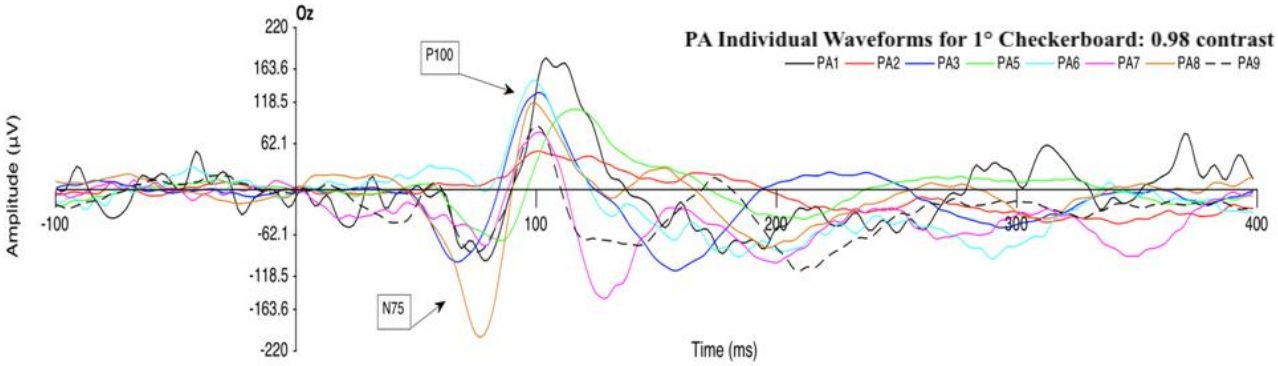

(A)

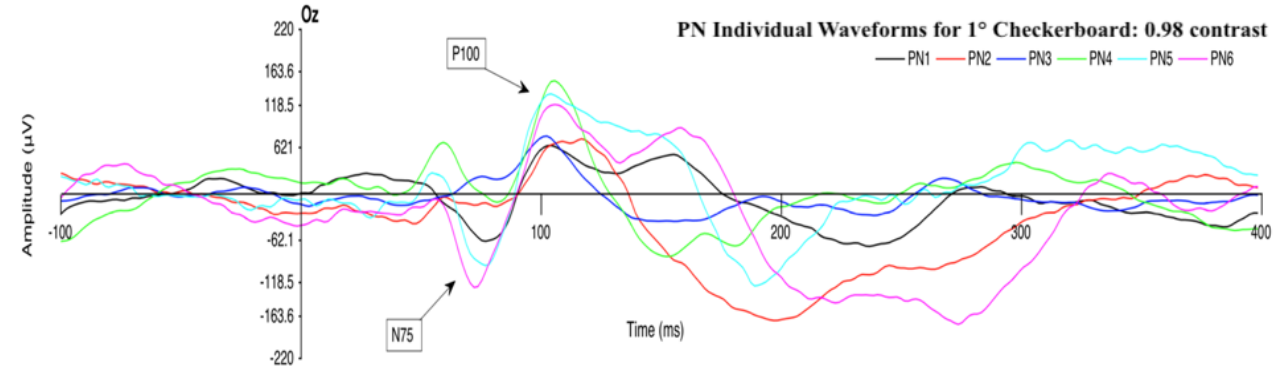

(B)

Figure 22. Checkerboard 1°: 0.98 contrast. Individual waveforms for ASD (A) and NT (B) subjects for the large checkerboard (0.98 contrast).

Table 10. ASD-subject GARS-2 scores, from the lowest to the highest amplitude for components N75 and P100 for the large checkerboard (0.98 contrast). A negative correlation was found between GARS-2 scores and severity in ASD subjects for the components N75 r(6) = -0.253 and for P100 r(6) = -0.612.

Component N75 ASD			**Component N75 NT**			**Component P100 ASD**			**Component P100 NT**		
ID	GARS-2	PkAmp μV	ID		PkAmp μV	ID	GARS-2	PkAmp μV	ID		PkAmp μV
PA8	100	-202	PN6	-	-125	PA2	104	52	PN1	-	65
PA3	85	-99	PN5	-	-96	PA7	81	78	PN2	-	74
PA1	76	-97	PN1	-	-63	PA9	87	86	PN3	-	77
PA9	87	-86	PN2	-	-17	PA5	76	109	PN6	-	120
PA7	81	-77	PN4	-	-11	PA8	100	118	PN5	-	134
PA5	76	-70	PN3	-	19	PA3	85	132	PN4	-	151
PA6	70	-3				PA6	70	148			
PA2	104	4				PA1	76	179			

3.3.2. Individual Waveforms: Small Checkerboard with Four Contrasts

Figures 23, 24, 25, and 26 represent individual waveform responses for ASD and NT subjects at each of the four contrast levels for the small checkerboard (0.25° visual angle). Tables 11, 12, 13, and 14 show the amplitudes for each of the components (N75 and P100) and are ordered from the lowest to the highest amplitude for ASD and NT subjects. Correlations between these amplitudes and the individual GARS-2 scores were calculated; results are shown in the table legends for each contrast level.

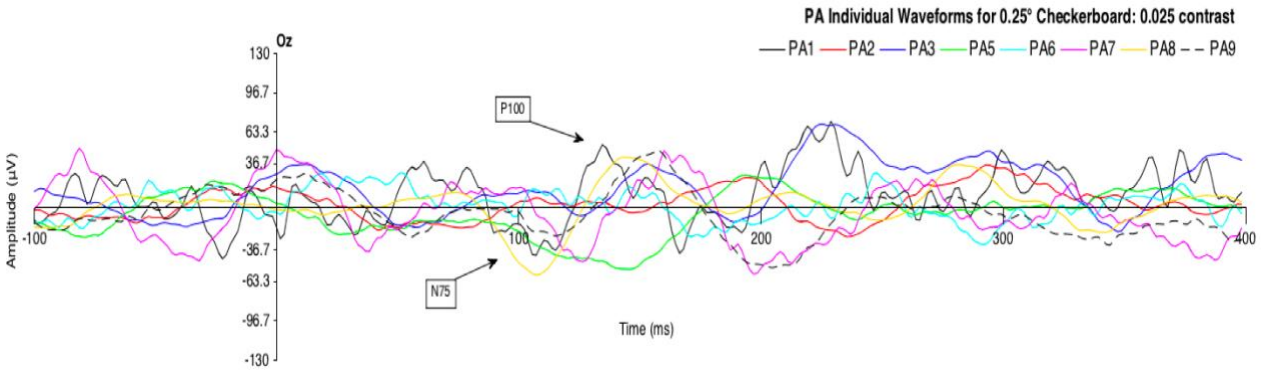

(A)

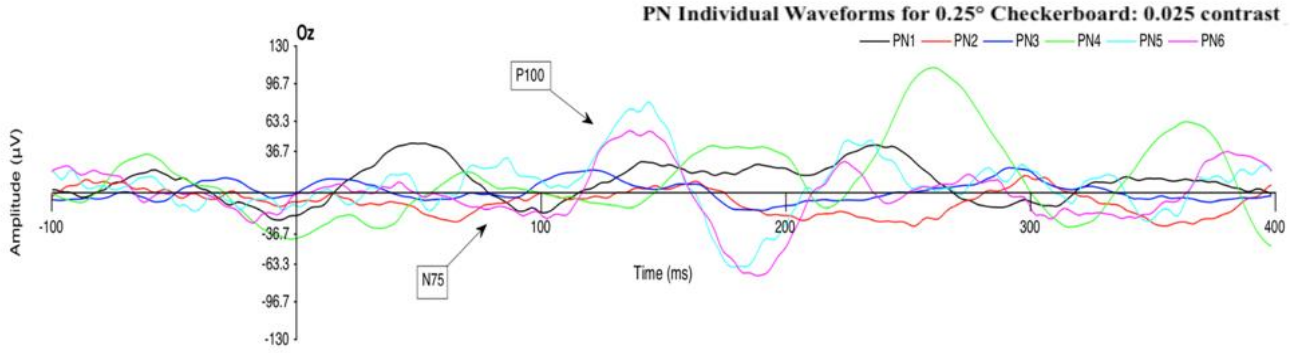

(B)

Figure 23. Checkerboard 0.25°: 0.025 contrast. Individual waveforms for ASD (A) and NT (B) subjects for the small checkerboard (0.025 contrast).

Table 11. ASD-subject GARS-2 scores from the lowest amplitude to the highest amplitude for components N75 and P100 for the small checkerboard (0.025 contrast). Although positive correlations between GARS-2 scores of severity and the amplitudes of both the N75 r(6) = 0.205 and the P100 r(6) = 0.246 were present, they were not significant.

Component N75 ASD			**Component N75 NT**			**Component P100 ASD**			**Component P100 NT**		
ID	GARS-2	PkAmp µV	ID		PkAmp µV	ID	GARS-2	PkAmp µV	ID		PkAmp µV
PA1	76	-22	PN2	-	-26	PA1	76	-14	PN1	-	-13
PA2	104	-18	PN6	-	-21	PA5	76	-11	PN6	-	-12
PA5	76	-13	PN1	-	-16	PA9	87	-2	PN2	-	0
PA6	70	-8	PN3	-	-6	PA2	104	8	PN4	-	5
PA9	87	-5	PN5	-	-2	PA8	100	11	PN3	-	20
PA7	81	-2	PN4	-	4	PA3	85	14	PN5	-	31
PA8	100	7				PA6	70	15			
PA3	85	9				PA7	81	17			

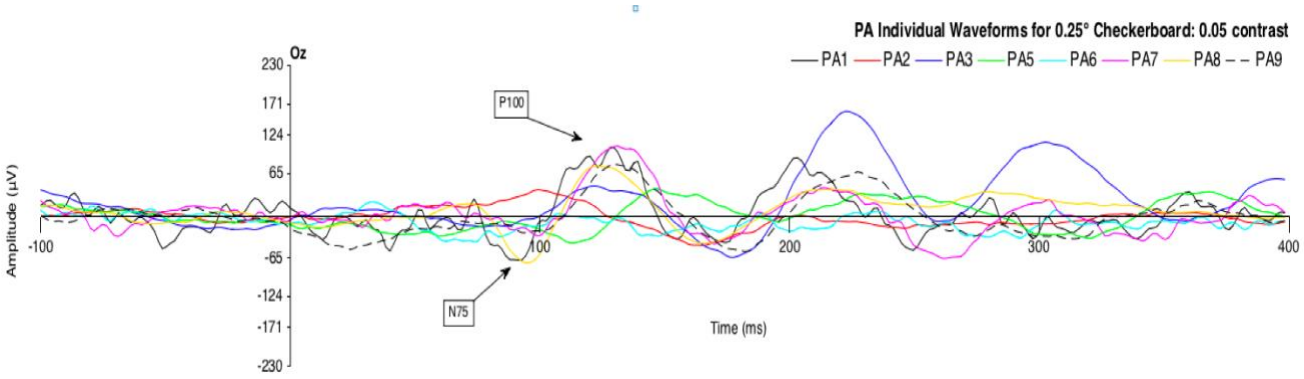

(A)

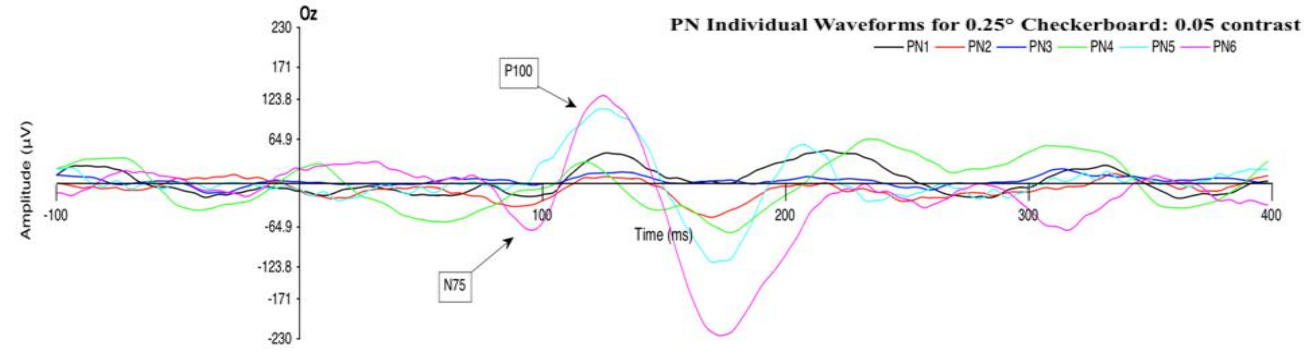

(B)

Figure 24. Checkerboard 0.25°: 0.05. Individual waveforms for ASD (A) and NT subjects (B) for the small checkerboard (0.05 contrast).

Table 12. ASD-subject GARS-2 scores from lowest to highest amplitude for components N75 and P100 for the small checkerboard (0. 05 contrast). We found a positive correlation between GARS-2 scores and severity in ASD subjects for components N75 r(6) = 0.306 and for P100 r(6) = 0.335; however, these relationships were not significant.

Component N75 ASD			**Component N75 NT**			**Component P100 ASD**			**Component P100 NT**		
ID	GARS-2	PkAmp μV	ID		PkAmp μV	ID	GARS-2	PkAmp μV	ID		PkAmp μV
PA8	100	-72	PN6	-	-70	PA5	76	-8	PN3	-	5
PA1	76	-68	PN4	-	-58	PA7	81	-2	PN2	-	10
PA6	70	-40	PN2	-	-35	PA6	70	4	PN4	-	31
PA5	76	-31	PN1	-	-20	PA2	104	40	PN1	-	45
PA7	81	-31	PN5	-	-10	PA3	85	46	PN5	-	110
PA9	87	-26	PN3	-	-3	PA8	100	76	PN6	-	130
PA3	85	-17				PA9	87	79			
PA2	104	13				PA1	76	105			

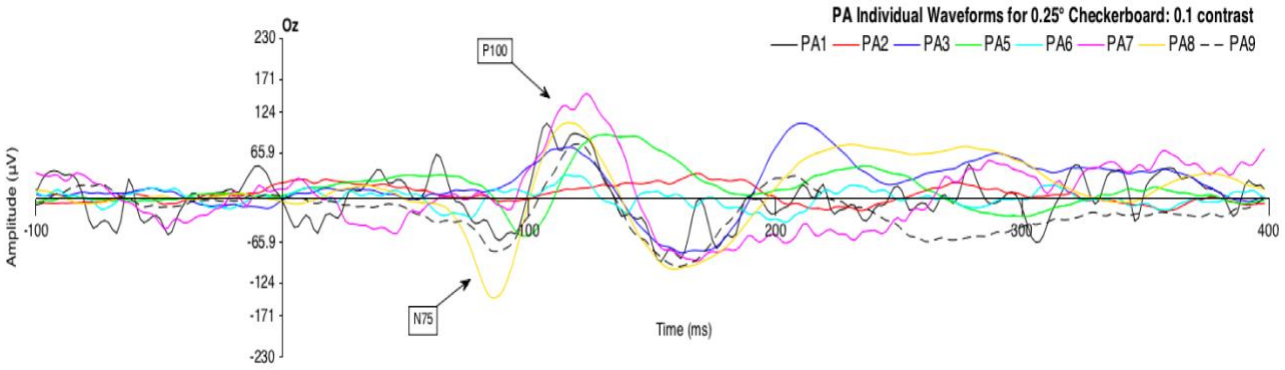

(A)

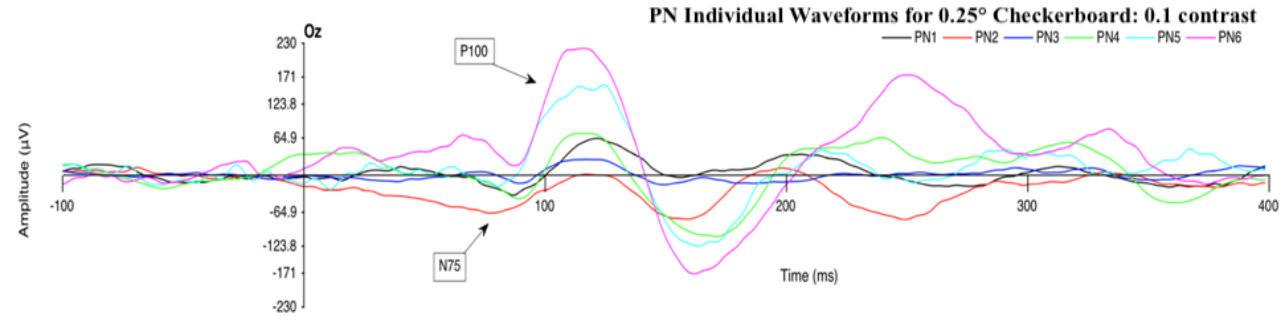

(B)

Figure 25. Checkerboard 0.25°: 0.1. Individual waveforms for ASD (A) and NT subjects (B) for the small checkerboard at 0.1 contrast.

Table 13. ASD-subject GARS-2 scores from the lowest to the highest amplitude for components N75 and P100 for the small checkerboard (0.1 contrast). A negative correlation was found between GARS-2 scores and severity in ASD subjects for the components N75 r(6) = -0.227 and for P100 r(6) = -0.187; however, these relationships were not significant.

Component N75 ASD			**Component N75 NT**			**Component P100 ASD**			**Component P100 NT**		
ID	GARS-2	PkAmp μV	ID		PkAmp μV	ID	GARS-2	PkAmp μV	ID		PkAmp μV
PA8	100	-145	PN2	-	-66	PA2	104	19	PN2	-	2
PA9	87	-78	PN4	-	-41	PA6	70	33	PN3	-	27
PA1	76	-62	PN1	-	-35	PA3	85	73	PN1	-	64
PA5	76	-55	PN5	-	-20	PA9	87	78	PN4	-	73
PA6	70	-29	PN3	-	-14	PA5	76	91	PN5	-	158
PA7	81	-17	PN6	-	17	PA1	76	107	PN6	-	221
PA2	104	-5				PA8	100	108			
PA3	85	5				PA7	81	150			

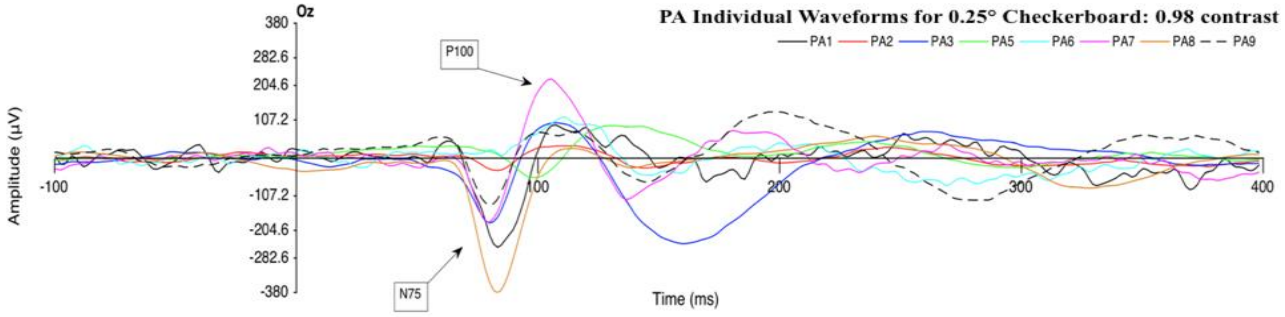

(A)

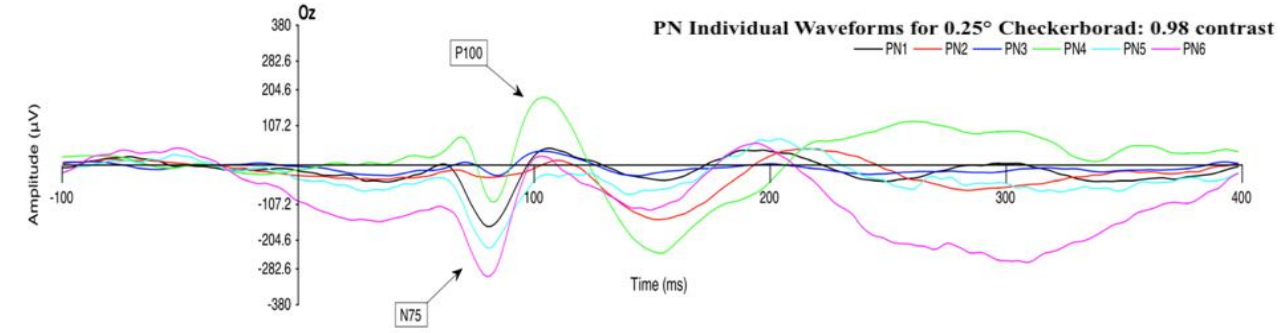

(B)

Figure 26. Checkerboard 0.25°: 0.98 contrast. Individual waveforms for ASD subjects (A) and NT (B) subjects for the large checkerboard (0.98 contrast).

Table 14. ASD-subject GARS-2 scores from the lowest to the highest amplitude for components N75 and P100 for the small checkerboard (0.98 contrast). A negative correlation was found between GARS-2 scores and severity in ASD subjects for components N75 r(6) = -0.237 and for P100 r(6) = -0.609; however, these relationships were not significant.

Component N75 ASD			**Component N75 NT**			**Component P100 ASD**			**Component P100 NT**		
ID	GARS-2	PkAmp μV	ID		PkAmp μV	ID	GARS-2	PkAmp μV	ID		PkAmp μV
PA8	100	-381	PN6		-304	PA8	100	27	PN5	-	-25
PA1	76	-252	PN5	-	-225	PA2	104	34	PN2	-	13
PA3	85	-184	PN1	-	-167	PA9	87	75	PN6	-	24
PA7	81	-181	PN4	-	-101	PA1	76	93	PN3	-	37
PA5	76	-169	PN6	-	-34	PA3	85	99	PN1	-	45
PA9	87	-133	PN3	-	-29	PA5	76	100	PN4	-	184
PA2	104	-35		-		PA6	70	116			
PA6	70	6		-		PA7	81	223			

No significant correlations were found between components, amplitudes, and measures of symptom severity in the ASD subjects. Due to the small sample size and associated low power levels, we examined the proportion of variance that might be explained (R^2) for each of these correlations; R^2 values were adjusted for the small sample size. Although most R^2-adjusted values were under 10 percent, several exceeded 25 percent. These included: negative correlations between the GARS-2 and the amplitude of the P100 at 0.98 contrast for both the large and small check sizes (large checks: adjusted-R^2 = 0.265; small checks: adjusted-R^2 = 0.271); a negative relationship between the GARS-2 and the large check stimuli at lower contrast levels; and a positive correlation between the amplitude of the N75 at the lower contrast levels for the large check sizes (see tables 9–16). We would not have predicted correlations between symptom severity and VEP amplitudes since early sensory responses and the higher-order cognitive alterations found in ASD are unlikely to have a simple relationship. Although none of these correlations are significant and the adjusted R^2 are not high

(likely due to small sample sizes), some of the raw r-values are intriguing and deserve further scrutiny with a larger sample size.

In summary, the variability in individual waveforms show that VEPs do not appear to be useful for reliably distinguishing between ASD and NT subjects on an individual basis. Surprisingly, some measures of the VEP seem to be related to symptom severity as assessed by the GARS-2 although these results never reached significance. Given the small sample size and the number of correlations examined, these tentative associations need to be replicated.

3.4. Do responses to motion-onset and motion-offset stimuli differ between ASD and NT subjects?

Pattern-reversal VEPs are the most common stimuli used in clinical settings, but because ASD subjects seem to show more difficulties in the M-pathway, simple moving stimuli may have additional utility for distinguishing between the two groups (Bach & Ullrich, 1996). Both the P100 and N135 (indicated by the arrows in figures 27 and 28) were assessed in response to motion-onset and offset stimuli using an expanding and contracting dartboard (Figure 4). While the predominant component in pattern-reversal is the P100 that increases in amplitudes with contrast, the N135 component is the most predominant for motion-onset stimuli (Kubová et al., 1995). In contrast, the N75 component is not as reliable and stable for motion-onset and offset compared to the N135 (Kremláček et al., 2004). The analysis model for expanding and contracting dartboards explored: the type of component (P100 & N135), the diagnosis (ASD & NT), the type of movement (motion-onset & motion-offset), and the two electrode locations (Oz & Pz; see Figure 5).

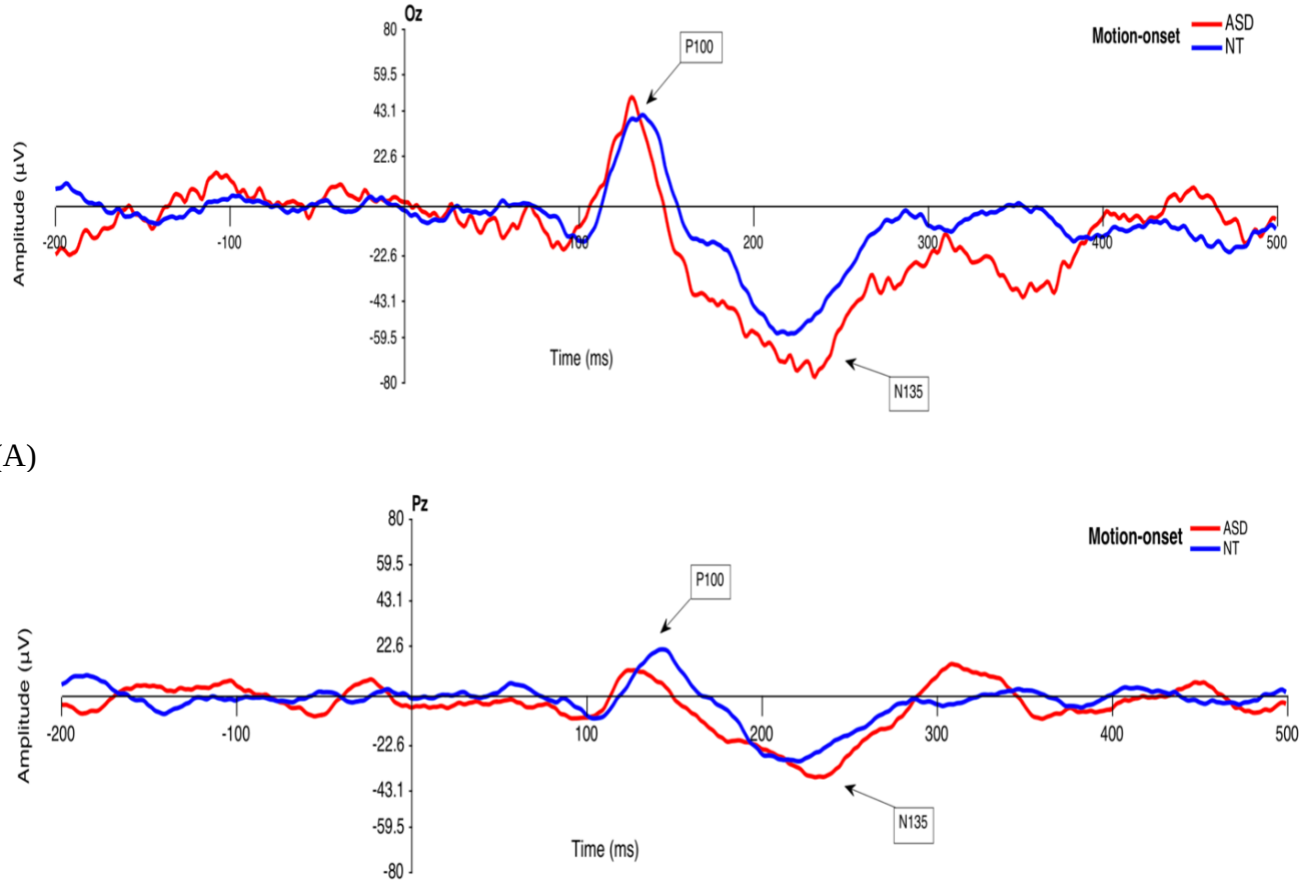

(A)

(B)

Figure 27. Grand-average ERP waveform at Oz (A) and Pz (B) electrodes for motion-onset. Comparisons of NT and ASD averaged responses to motion-onset of the dartboard at electrode site Oz (A) and Pz (B). For component N135 at Oz, ASD subjects show increased late negativity compared to NT subjects. For electrode site Pz, component P100, ASD subjects show smaller amplitudes and shorter latencies; for component N135, ASD subjects continue to show increased late negativity relative to the NT group, similar to our findings at site Oz.

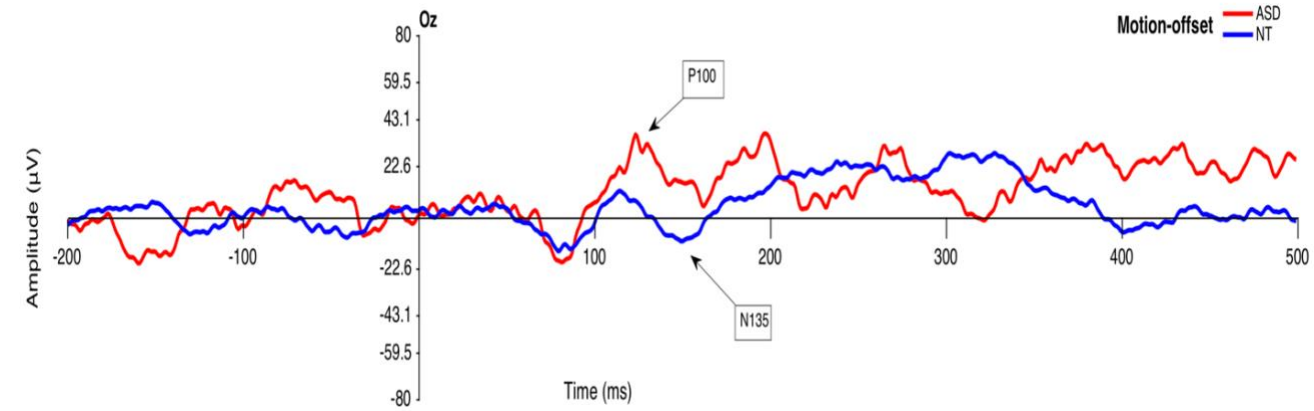

(A)

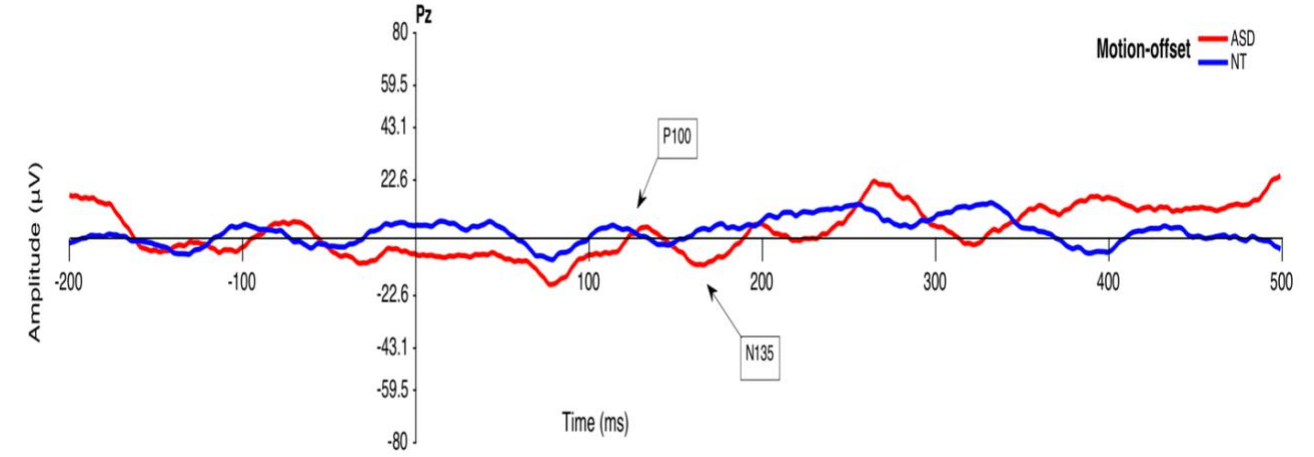

(B)

Figure 28. Grand-average ERP waveform at Oz (A) and Pz (B) electrodes for motion-offset. Comparisons of NT and ASD averaged responses to motion-offset at electrode site Oz (A) and Pz (B). At Oz, ASD subjects show larger amplitudes and long latencies for component P100. For component N135, ASD subjects present a positive N135 compared to the NT group. For component N135, ASD subjects show an increased late negativity.

Motion-Onset and Offset Peak Amplitudes

A significant three-way interaction was observed between the component (P100 & N135), the type of movement (onset and offset), and the recording site (Oz & Pz; $F_{(1,13)} = 6.154$, $p = 0.028$). Two-way interactions were found between the components (P100 v. N135) and the type of motion (onset v. offset; $F_{(1,13)} = 15.124$, $p = 0.002$), as well as between the components (P100 v. N135) and the recording site (Oz v. Pz) ($F_{(1,13)} =$

9.982, p = 0.008). These two two-way interactions were subsumed by the three-way interaction. Diagnosis showed a non-significant main effect and did not participate in any significant interactions.

At site Oz, the N135 amplitudes were smaller for motion offset relative to motion onset. The P100 also showed smaller motion-offset amplitudes relative to motion onset. This pattern of results at electrode site Oz differed from that of electrode site Pz, thus accounting for the three-way interaction (see Figure 29). In contrast, the main effect of diagnosis was non-significant, and diagnosis did not participate in any significant higher-order interactions (see Table 15). We did find a large-effect size difference between the ASD and NT subjects for component P100 at electrode site Oz for motion-offset (d = 0.7) and a medium effect for motion-onset (d = 0.5). For component N135, a large-effect size for motion-offset was found at electrode site Oz (d = 1) and a medium effect for motion-onset at electrode site Pz (d = 0.5).

Although we observed intriguing differences between the NT and ASD waveforms, especially for motion-offset, our current results do not suggest onset and offset VEPs can reliably differentiate between the ASD and NT subjects. Based upon the effect sizes reported, motion-onset for both the P100 and N135 components revealed the largest group differences at electrode site Oz. All other notable effects were considered to be of medium size according to Cohen. These included specific medium effects for motion offset of the P100 at electrode site Oz and the N135 at electrode site Pz. In summary, qualitatively the ASD subjects showed higher amplitudes for the P100 for both motion onset and offset at electrode site Oz. In contrast, the N135 motion onset, but not offset, showed higher amplitudes for the ASD subjects.

Table 15. ANOVA for peak amplitudes for ASD subjects and NT subjects.

Effect	SS	Df	MS	F-value	P-value
Diagnosis	5.447E-5	1	5.447E-5	.033	.858
Component	.09	1	.09	56.609	<.001
Component x Diagnosis	.004	1	.004	2.687	.125
Motion-onset/offset	.006	1	.006	2.653	.127
Motion-onset/offset x Diagnosis	.000	1	.000	.123	.731
Recording Site	.000	1	.000	.820	.382
Recording Site x Diagnosis	.001	1	.001	3.015	.106
Component x Motion-onset/Motion-offset	.011	1	.011	15.124	.002
Component x Motion-onset/offset x Diagnosis	.002	1	.002	2.871	.114
Component x Recording Site	.009	1	.009	9.982	.008
Component x Recording Site x Diagnosis	.001	1	.001	1.509	.241
Motion-onset/offset x Recording Site	.002	1	.002	3.967	.068
Motion-onset/offset x Recording Site x Diagnosis	.001	1	.001	1.480	.245
Component x Motion-onset/Motion-offset x Recording Site	.003	1	.001	2.965	.028
Component Motion-onset/offset x Recording Site x Diagnosis	.001	1	.001	2.965	.109

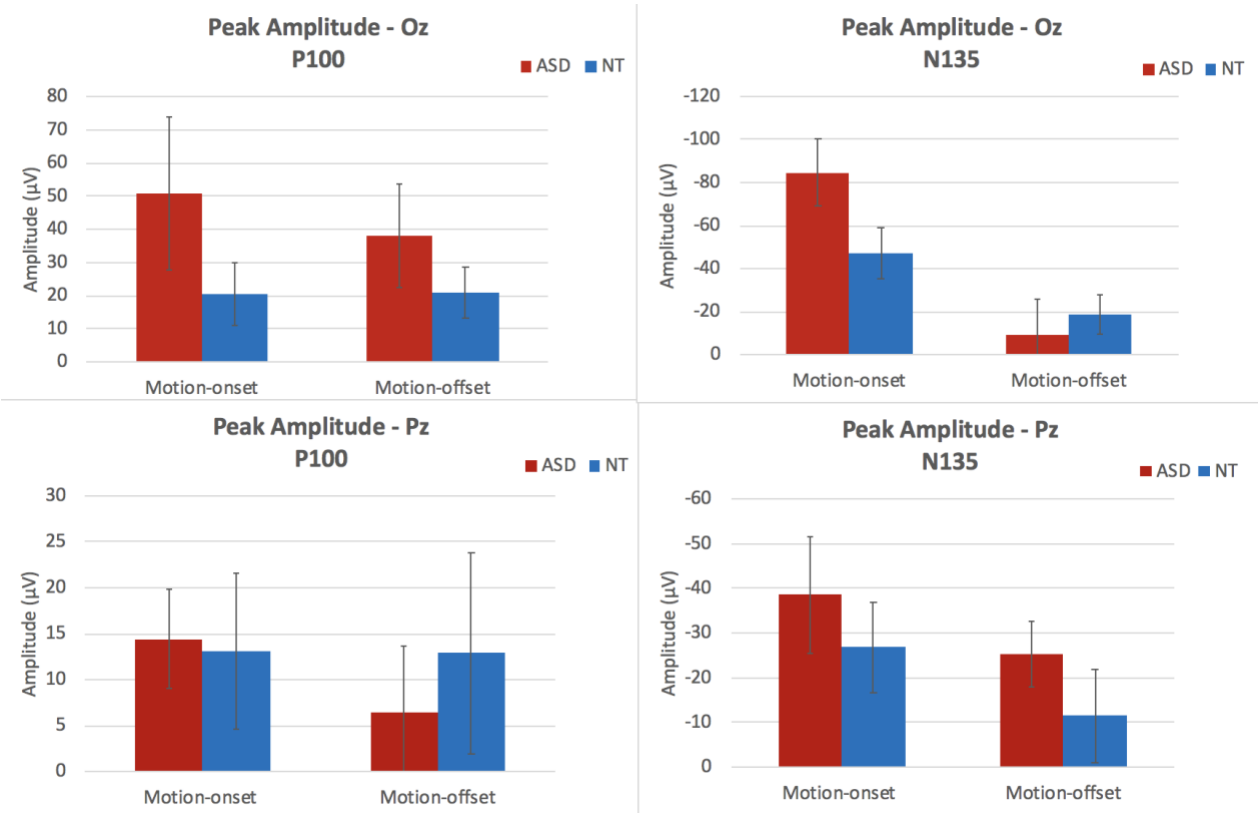

Figure 29. Peak amplitude measurement for responses for motion-onset/offset at electrode site Oz and Pz for component P100 and N135 for ASD and NT subjects. Error bars represent SEM.

Motion-Onset and Offset Peak Latency

To further examine motion-onset and offset responses, peak latencies were evaluated in a model that included diagnosis, recording site, component type, and movement type (onset vs offset; Table 16). Only a fully expected main effect for the component latency (P100 vs. N135) was found to be statistically significant ($F_{(1,13)} = 75.924$, $p < .001$). In this model, all other main effects and interactions were non-significant including those that involved diagnosis as a factor. There was, however, a large effect size for motion-offset at component N135 ($d = .7$), where ASD subjects show a delay in the component peak. Despite this delay (see Figure 30), all other latency

measures do not distinguish between ASD and NT subjects and may not be suitable for identifying the members of each group.

Table 16. ANOVA for peak latency for ASD and NT groups.

Criteria	SS	Df	MS	F-value	P-value
Diagnosis	232.143	1	232.143	.280	.606
Component	50891.525	1	50891.525	75.924	<.001
Component x Diagnosis	142.625	1	142.625	.213	.652
Motion-onset/offset	833.733	1	833.733	.940	.350
Motion-onset/offset x Diagnosis	823.900	1	823.900	.929	.353
Recording Site	455.208	1	455.208	1.107	.312
Recording Site x Diagnosis	1488.775	1	1488.775	3.622	.079
Component x Motion-onset/offset	247.250	1	247.250	.349	.565
Component x Motion-onset/offset x Diagnosis	12.950	1	12.950	.018	.895
Component x Recording Site	292.918	1	292.918	.536	.477
Component x Recording Site x Diagnosis	1453.218	1	1453.218	2.657	.127
Motion-onset/offset x Recording Site	90.304	1	90.304	.121	.734
Motion-onset/offset x Recording Site x Diagnosis	25.137	1	25.137	.034	.857
Component x Motion-onset/offset x Recording Site	11.091	1	11.091	.013	.910
Component x Motion-onset/offset x Recording Site x Diagnosis	3.857	1	3.857	.005	.947

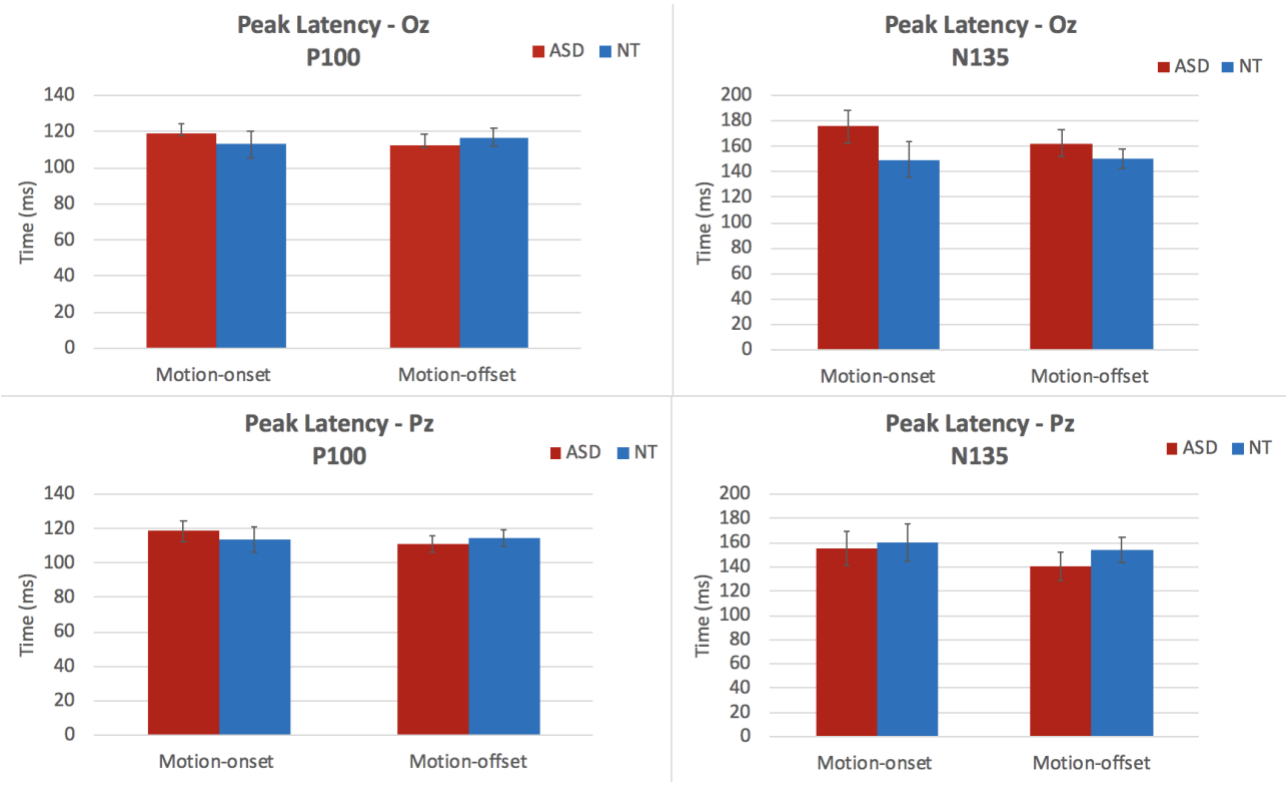

Figure 30. Peak latency measurement for responses for motion-onset/offset at electrode sites Oz and Pz for component P100 and N135 for ASD and NT subjects. Error bars represent SEM. No significant differences between latencies were found in the model (see pp. 53-54, Motion-Onset and Offset Peak Latency); the largest group difference appears for long latencies at electrode site Oz for component N135, whereas ASD subjects show longer average latencies.

Although the current results do not show that motion-onset and offset responses are capable of reliably distinguishing between ASD and NT groups, some effect-size values and qualitative findings call for further study, most notably, the increased amplitude of the N135, and potentially increased latency, for motion-onset stimuli (see Figure 27.A). Although significant effects of diagnosis were not present, the large effect size (d = 1.0) for component N135 in response to motion-onset at site Oz indicates a consistent characteristic of ASD responses.

3.5. Do mean amplitude and fractional-area latency measures differ from peak amplitude and peak-latency measures in their assessment of the VEP?

Unfortunately, there is no gold standard for determining which types of measures should be used to quantify any given set of VEP data measuring amplitudes and latencies. The best approach may be to employ measures of mean amplitude and fractional area latency when there is concern about specific types of artifacts (e.g. averaging of individual waveforms with varying latencies and attempts to reduce the influence of adjacent components on the component of interest). Fractional-area latency is less sensitive to noise; does not depend on the shape of the waveform, which could present more than one peak; and measures the whole component of interest (Luck, 2005; Kiesel et al., 2008; Woodman, 2010). Here we re-examine the results of our data utilizing *mean* amplitude and *fractional area* latency. The results will be compared to previously presented results of the more traditional measures of *peak* amplitude and *peak* latency.

3.5.1. Mean Amplitude of the N75 and P100 for Reversing Checkerboards

Similar to the model for peak amplitudes of the checkerboard stimuli, we examined the influence of diagnosis, check size, and contrast on both the N75 and P100 components. The mean amplitude of component N75 ANOVA results (Table 17) showed a main effect for check size ($F_{(1,12)} = 13.966$, $p = 0.003$; see figures 7 and 8), a main effect for contrast ($F_{(3,36)} = 4.569$, $p = 0.008$), and a significant interaction between check size and contrast ($F_{(3,36)} = 5.068$, $p = 0.005$). All main effects and interactions that involved diagnosis were not significant. Despite this, for the large checkerboard at 0.025 contrast a large effect for diagnosis ($d = 0.8$) was present (Figure 31). ASD subjects had small mean amplitude values relative to the NT subjects for the large check sizes at low

contrast, but not at 0.98 contrast (d = 0.4; see Figure 31). For the small check size ASD subjects mean amplitudes were similar to those found in the NT group (see Figure 32).

Table 17. ANOVA for mean amplitude checkerboards for component N75 at electrode site Oz between ASD and NT groups.

Criteria	SS	Df	MS	F-value	P-value
Diagnosis	.001	1	.001	.396	.541
Check Size	.019	1	.019	13.966	.003
Check Size x Diagnosis	.000	1	.000	.177	.682
Contrast	.026	3	.009	4.569	.008
Contrast x Diagnosis	.000	3	.000	.085	.968
Check Size x Contrast	.008	3	.003	5.068	.005
Check Size x Contrast x Diagnosis	.003	3	.001	2.202	.105

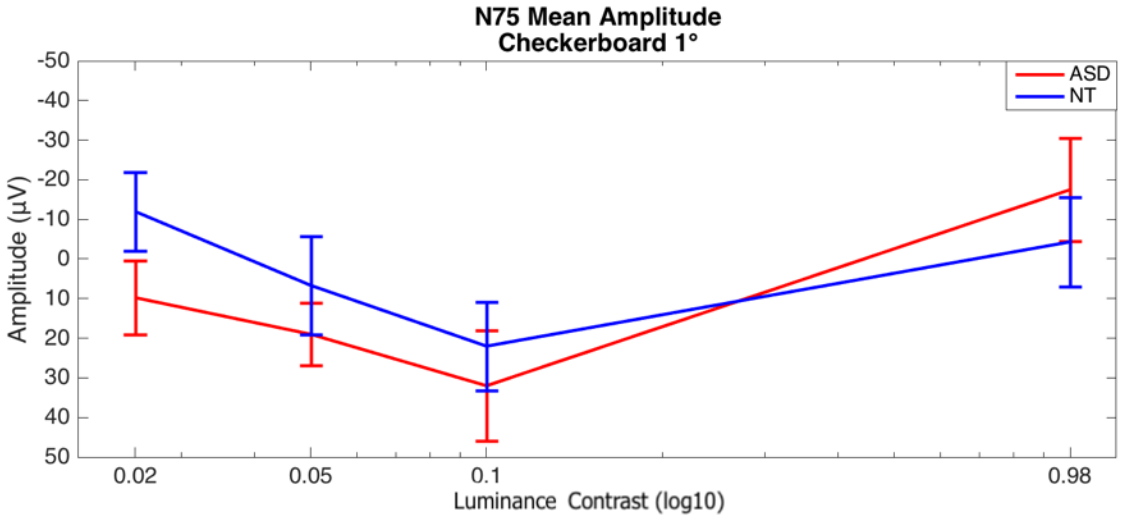

Figure 31. Contrast-response function for component N75 mean amplitudes for ASD versus NT subjects at checkerboard size 1° visual angle for the four contrasts (0.025, 0.05, 0.1, and 0.98). Error bars represent SEM.

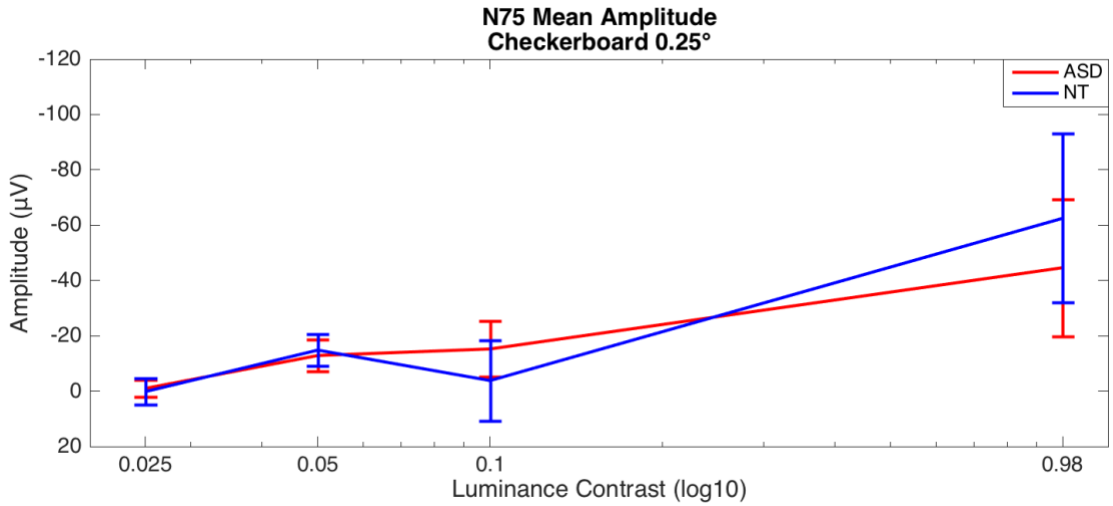

Figure 32. Contrast-response function for component N75 mean amplitudes for ASD versus NT subjects at checkerboard size 0.25° visual angle for the four contrasts (0.025, 0.05, 0.1, and 0.98). Error bars represent SEM.

A comparison between the mean amplitude and peak amplitude results for the N75 component show the same pattern of results: main effects of both check size and contrast, as well as a significant interaction between the two (see tables 2 and 17). For both measures, amplitudes at 0.98 contrast were always greater than those found at lower contrast levels (see Table 19). In sum, the pattern of the ANOVA results for peak amplitude and mean amplitude measures of the N75 were largely indistinguishable.

Mean Amplitude of the P100

The ANOVA analysis for the mean amplitudes of the P100 (Table 18) indicated a main effect for check size ($F_{(1,12)} = 17.862$, $p = 0.001$) as well as a main effect for contrast (at Oz ASD: 44 ± 34 μV; NT: 8 ± 15 μV; $F_{(3,36)} = 5.026$, $p = 0.005$; see Figure 7.A). Of interest, there was also a three-way interaction for check size, contrast, and diagnosis ($F_{(3,12)} = 4.310$, $p = 0.011$; see figures 7 and 8, and for plotting see figures 33 and 34). The ASD subjects showed more uniform amplitudes through the four contrast

levels for the large check sizes compared to the small checks, where amplitudes stayed smaller relative to the NT subjects (see figures 33 and 34).

Table 18. ANOVA for mean amplitudes for component P100 electrode site Oz between ASD and NT groups.

Criteria	SS	Df	MS	F-value	P-value
Diagnosis	.001	1	.001	.667	.430
Check Size	.025	1	.025	17.862	.001
Check Size x Diagnosis	.002	1	.002	1.408	.258
Contrast	.016	3	.005	5.026	.005
Contrast x Diagnosis	.001	3	.000	.346	.793
Check Size x Contrast	.002	3	.001	.927	.438
Check size x Contrast x Diagnosis	.010	3	.003	4.310	.011

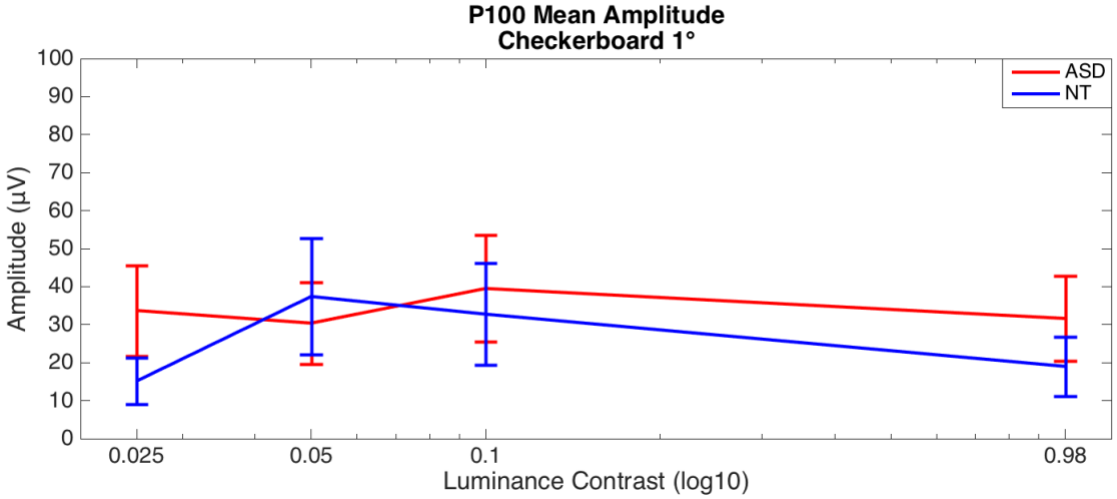

Figure 33. Contrast-response function for component P100 mean amplitudes for ASD versus NT subjects at checkerboard size 1° visual angle for the four contrasts (0.025, 0.05, 0.1, and 0.98). Error bars represent SEM.

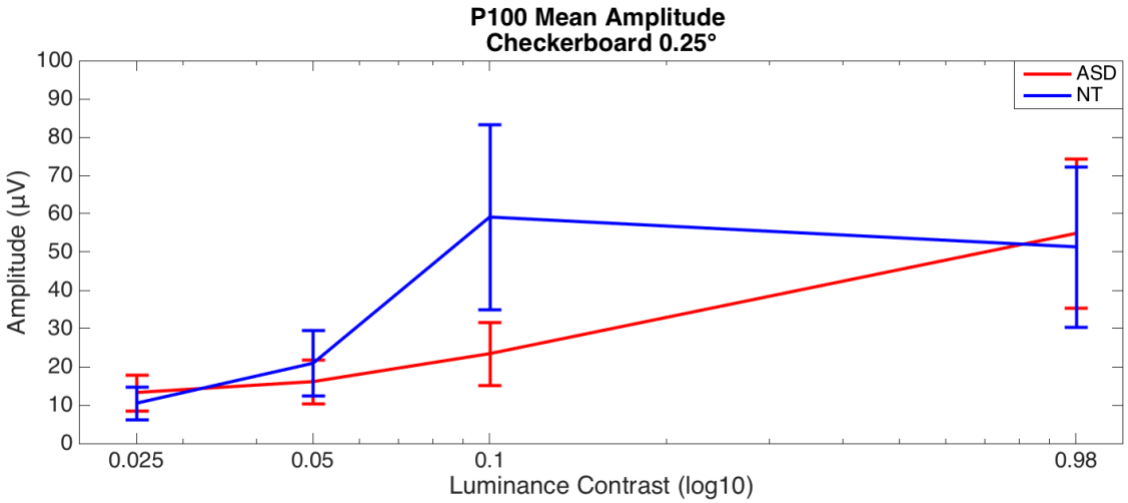

Figure 34. Contrast-response function for component P100 mean amplitudes for ASD versus NT at checkerboard size 0.25° visual angle for the four contrasts (0.025, 0.05, 0.1, and 0.98). Error bars represent SEM.

If we compare the mean amplitude analysis to the peak amplitude analysis already performed for the P100, the ANOVA results differ in an important respect. The peak amplitude analysis shows only a two-way interaction between check size and contrast, while the mean amplitude analysis shows only a three-way interaction between check size, contrast, and diagnosis (Table 19). A visual inspection of the relevant graphs (figures 33 and 34) shows a different pattern of results for the diagnosis x contrast displays given at each checkerboard size. These graphed responses are not consistent with those found for peak amplitude measures (cf. figures 33 and 34 to figures 11 and 12). Differences between the ASD subjects for the large check size at the lowest contrast value do indicate a hyperresponsivity in the magnocellular system; however, the two groups converge at the 0.05 contrast level. In contrast, peak amplitude measures at this contrast level showed a large effect size (d = 1.09) but non-significant group differences in the ANOVA analysis.

Table 19. Comparing significant results between peak amplitude and mean amplitude for components N75 and P100 at electrode site Oz for pattern-reversal.

Peak Amplitude		**Mean Amplitude**	
Component N75		**Component N75**	
Criteria	**P-value**	**Criteria**	**P-value**
Check Size	.001	Check Size	.003
Contrast	.001	Contrast	.008
Check Size x Contrast	.001	Check Size x Contrast	.005
Component P100		**Component P100**	
Criteria	**P-value**	**Criteria**	**P-value**
Check Size	.005	Check Size	.001
Contrast	.001	Contrast	.005
Check Size x Contrast x Diagnosis	NS	Check Size x Contrast x Diagnosis	.011

Fractional-Area Latency of the N75

Fractional-area latency for the component N75 showed no significant main effects or interactions (see figures 32 and 33 and Table 20) for any of the factors, including diagnosis. There were, however, several medium to large effect sizes when comparing the ASD to the NT subjects. Large effect sizes were present for the large checkerboard (1° visual angle) at 0.025 contrast (d = 0.7), 0.05 contrast (d = 0.9), 0.1 contrast (d = 1.49) and 0.98 contrast (d = 0.7). For the small checkerboard (0.25° visual angle), large to medium effect sizes were found at 0.05 contrast (d = 0.7), 0.1 contrast (d = 0.6), and 0.98 contrast (d = 0.8).

By comparison, the previously described peak latency measures showed a main effect of check size (see Table 5) that was not present for the fractional-area latency measure (see Table 20). Despite this difference, the results between the two methods are largely similar, with diagnosis showing non-significant effects with both techniques and comparable effect sizes between ASD and NT subjects across the two measurement methods.

Table 20. Fractional area latency of the N75 for reversing checkerboards at location Oz.

Criteria	SS	DF	MS	F-value	P-value
Diagnosis	6434.120	1	6434.120	1.731	.213
Check Size	13.872	1	13.872	.401	.538
Check Size x Diagnosis	87.769	1	87.769	2.538	.137
Contrast	163.365	3	54.455	.998	.405
Contrast x Diagnosis	34.334	3	11.445	.210	.889
Check Size x Contrast	40.204	3	13.401	.642	.593
Check Size x Contrast x Diagnosis	68.856	3	22.952	1.099	.362

Fractional-Area Latency of the P100

For the P100, the ANOVA for fractional-area latency measures (Table 21) found a significant effect for contrast (at Oz, ASD: 111.3 ± 4.73 ms, NT: 109.8 ± 10.4 ms, $F_{(3,12)} = 6.038$, $p = 0.002$; see Figure 8.C), along with a two-way interaction between check size and contrast ($F_{(3,12)} = 6.503$, $p = 0.001$). Once again, diagnosis did not show a significant main effect or interaction with the other variables. A large group-driven effect size was present for the large checkerboard (1° visual angle) at 0.1 contrast ($d = 0.7$). For the large checkerboard, ASD subjects present longer latencies at the lower contrast values

(0.025 and 0.05), while at the 0.1 and .98 contrast values, ASD subjects showed shorter latencies (see Figure 35). For the small checkerboard, ASD subjects present shorter latencies at lower contrasts (0.025 and 0.05). At the higher levels of contrast (0.1 and 0.98), ASD subjects present longer latencies.

Table 21. ANOVA for fractional area latency for component P100 electrode site Oz.

Criteria	SS	DF	MS	F-value	P-value
Diagnosis	.012	1	.012	.000	.990
Check Size	.964	1	.964	0.15	.904
Check Size x Diagnosis	8.679	1	8.679	.136	.718
Contrast	1044.446	3	348.149	6.038	.002
Contrast x Diagnosis	21.161	3	7.054	.112	.946
Check Size x Contrast	891.470	3	297.157	6.503	.001
Check Size x Contrast x Diagnosis	103.899	3	34.633	.758	.525

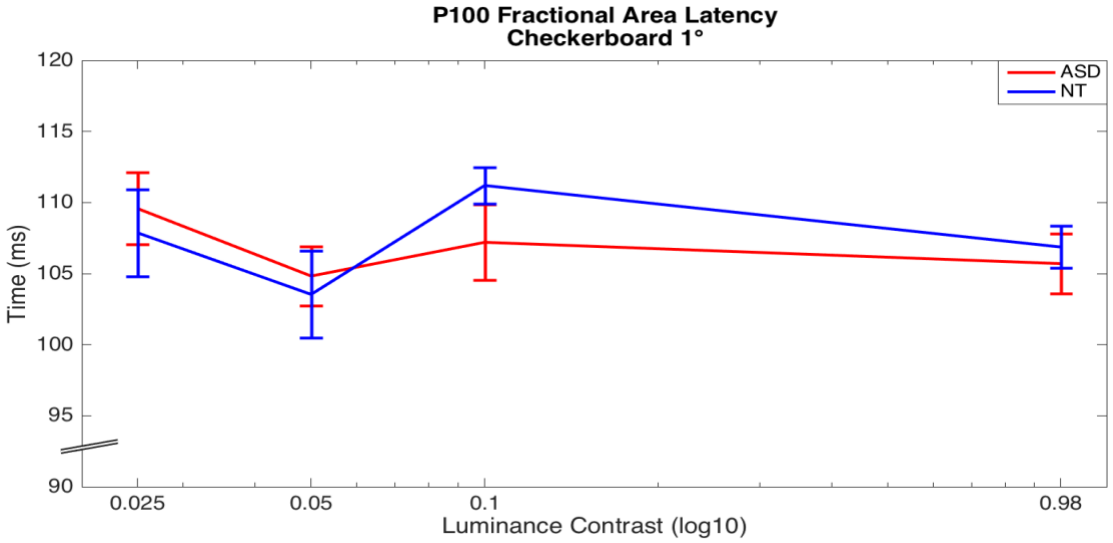

Figure 35. Contrast-response function for component P100 fractional-area latency for ASD versus NT at checkerboard size 1° visual angle at electrode Oz for the four contrasts (0.025, 0.05, 0.1, and 0.98). Error bars represent SEM.

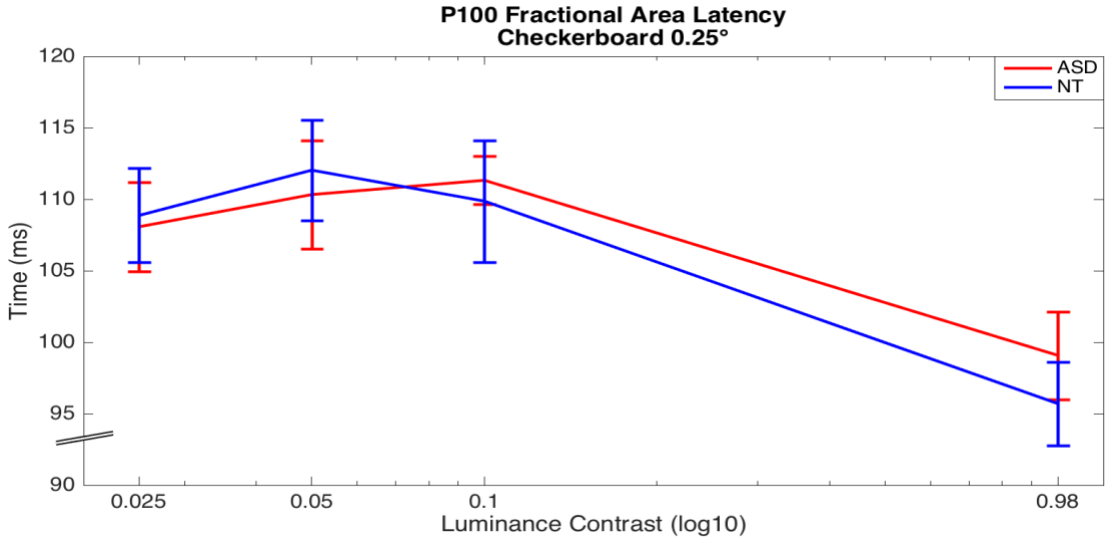

Figure 36. Contrast-response function for component P100 fractional-area latency for ASD versus NT at checkerboard size 0.25° visual angle at electrode Oz for the four contrasts (0.025, 0.05, 0.1, and 0.98). Error bars represent SEM.

P100 latencies from this data show similar patterns regardless of whether they are measured with peak latency or fractional area latency (see Table 22). Fractional-area latency does, however, appear to be more sensitive to shifts in the distribution of values associated with the P100 that are correlated with changes in contrast (cf. figures 35 and 36). This is likely due to the general mathematical nature of the measure: one is a point measure (peak latency) while the other considers the distribution of values across a wider window (fractional-area latency). As with the peak latency measures (see pp. 31–35), fractional area latency differences do not seem to have practical utility for distinguishing between the ASD and NT groups.

Table 22. Comparing significant results between peak latency and fractional area latency for components N75 and P100 at electrode site Oz for pattern-reversal.

Peak Latency		**Fractional Area Latency**	
Component N75		**Component N75**	
Criteria	**P-value**	**Criteria**	**P-value**
Check Size	.012	Check Size	NS
Component P100		**Component P100**	
Criteria	**P-value**	**Criteria**	**P-value**
Contrast	.004	Contrast	.002
Check Size x Contrast	.023	Check Size x Contrast	.001

3.5.2. Movement-Onset and Offset: Mean Amplitude and Fractional Area Latency Measures.

Mean amplitudes and fractional-area latencies were also calculated for the movement onset and offset stimuli. Comparison of the different results between these measures and the traditional measures of peak amplitude and latency (see pp. 51–56) are presented here.

Mean Amplitude of the P100 and N135

As with the peak amplitude analysis for motion-onset and offset, an ANOVA model examined the effects of component type (P100 and N135), recording site (Oz vs. Pz), motion type (onset vs. offset) and diagnosis on the mean amplitude values. This analysis (Table 23) revealed a three-way interaction between component type, motion type (onset v. offset), and recording site ($F_{(1,13)} = 5.016$, $p = .043$), as well as a two-way interaction between the component type (P100 v. N135) and motion type (onset v. offset; $F_{(1,13)} = 5.457$, $p = .036$; see figures 27 and 28). Motion-onset, component N135, showed

large amplitudes in ASD subjects relative to the NT subjects at both Oz and Pz (at Oz, 21 ± 37 μV) compared to the NT subjects (at Oz, 3 ± 17 μV). For motion-offset at electrode site Oz, component N135 continued to show larger amplitudes for the ASD subjects (at Oz, -13 ± 33 μV) relative to the NT group (at Oz, -2 ± 24 μV; see figure 37). There was, however, a medium effect size at electrode site Oz for motion-onset at component N135 (d = .7), where ASD subjects show a larger mean amplitude. Despite these qualitative differences, main effects and interactions for diagnosis were not significant.

Table 23. ANOVA for mean amplitude for component P100 and N135 between ASD subjects and NT group for electrode site Oz and Pz.

Criteria	SS	Df	MS	F-value	P-value
Diagnosis	2.934E-5	1	2.934E-5	.019	.893
Component	.000	1	.000	1.393	.259
Component x Diagnosis	.000	1	.000	.591	.456
Motion-onset/ offset	.001	1	.001	.451	.514
Motion-onset/offset x Diagnosis	.000	1	.000	.235	.636
Recording Site	.001	1	.001	3.982	.067
Recording Site x Diagnosis	.001	1	.001	2.194	.162
Component x Motion-onset/offset	.001	1	.001	5.457	.036
Component x Motion-onset/offset x Diagnosis	.000	1	.000	1.436	.252
Component x Recording Site	.000	1	.000	1.559	1.559
Component x Recording Site x Diagnosis	1.101E-5	1	1.101E-5	.103	.753
Motion-onset/offset x Recording Site	.001	1	.001	1.677	.218
Motion-onset/offset x Recording Site x Diagnosis	.001	1	.001	2.517	.137
Component x Motion-onset/Motion-offset x Recording Site	.000	1	.000	5.016	.043
Component x Motion-onset/offset x Recording Site x Diagnosis	6.921E-5	1	6.921E-5	.905	.359

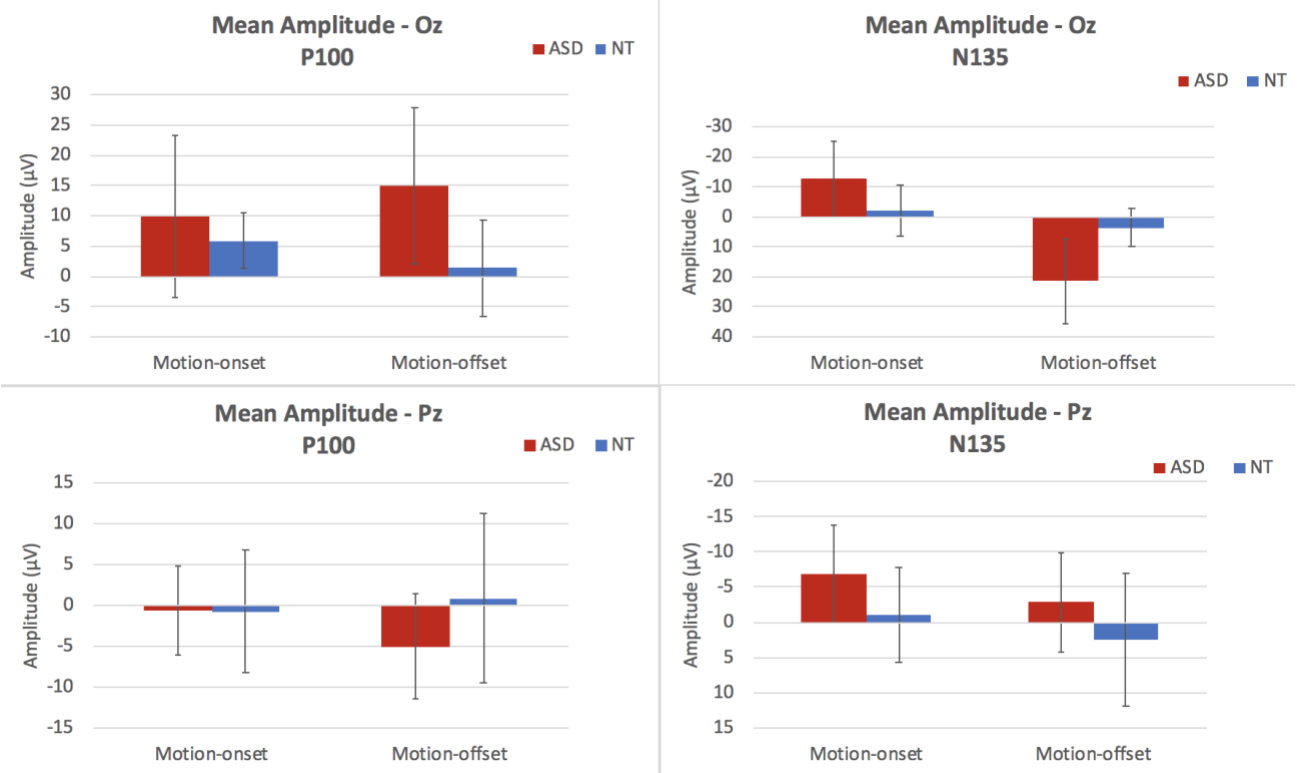

Figure 37. Mean amplitude responses for motion-onset/offset at electrode site Oz and Pz for component P100 and N135 for ASD subjects and NT subjects. Error bars represent SEM.

When the peak and mean amplitude analyses are directly compared (Table 24), there is some substantial overlap in the results. In both cases the three-way interaction between component, motion onset/offset, and recording site was significant. Although additional effects were found when using peak amplitude, these lower order effects (main effects and two-way interactions) are subsumed by the more complex three-way interaction that both analyses shared.

Table 24. Comparing significant effect between peak amplitude and mean amplitude for motion-onset/offset.

Peak Amplitude		**Mean Amplitude**	
Criteria	**P-value**	**Criteria**	**P-value**
Component x Type of Motion	.002	Component x Type of Motion	.036
Component x Type of Motion x Recording site	.028	Component x Type of Motion x Recording Site	.043
Component x Recording Site	.008	Component x Recording Site	NS
Component	.001	Component	NS

Fractional Area Latency

As seen in Table 25, the ANOVA analysis for fractional area latency revealed an expected main effect for the component ($F_{(1,13)} = 175.019$, $p < .001$), as well as a main effect for recording site ($F_{(1,13)} = 7.427$, $p = .017$).

Table 25. ANOVA table for fractional area latency between ASD subjects and NT group.

Criteria	SS	Df	MS	F-value	P-value
Diagnosis	29.863	1	29.867	.233	.638
Component	64566.801	1	64566.801	175.019	<.001
Component x Diagnosis	9.601	1	9.601	.026	.875
Motion-onset/offset	178.101	1	178.101	2.490	.139
Motion-onset/offset x Diagnosis	4.101	1	4.101	.057	.815
Recording Site	268.8	1	268.8	7.427	.017
Recording Site x Diagnosis	7.467	1	7.467	.206	.657
Component x Motion-onset/offset	37.202	1	37.202	.239	.633
Component x Motion-onset/offset x Diagnosis	152.402	1	152.402	.978	.341
Component x Recording Site	35.148	1	35.148	.446	.516
Component x Recording Site x Diagnosis	45.015	1	45.015	.572	.463
Motion-onset/offset x Recording Site	.648	1	.648	.005	.944
Motion-onset/offset x Recording Site x Diagnosis	15.048	1	15.048	.120	.735
Component x Motion-onset/offset x Recording Site	3.621	1	3.621	.065	.803
Component x Motion-onset/offset x Recording Site x Diagnosis	154.821	1	154.821	2.779	.119

Once again main effects and interactions were nonsignificant for diagnosis, but we found large between group effect sizes for motion-onset at electrode site Oz

component P100 (d = 0.7; see figure 38). For motion-offset we found a medium between group effect at electrode site Oz (d = 0.6) for component P100. As before, relative to the peak latency findings, the fractional area latency analysis showed similar, but not identical outcomes (Table 26). While both component and recording site showed main effects for fractional area latency measures, in the peak latency analysis only component showed a main effect. The effects involving diagnosis were nonsignificant in for both measures of component latency.

Table 26. Comparing significant effects between peak latency and fractional area latency for motion-onset/offset.

Peak Latency		**Fractional Area Latency**	
Criteria	**P-value**	**Criteria**	**P-value**
Component	.001	Component	.001
Recording Site	NS	Recording Site	.017

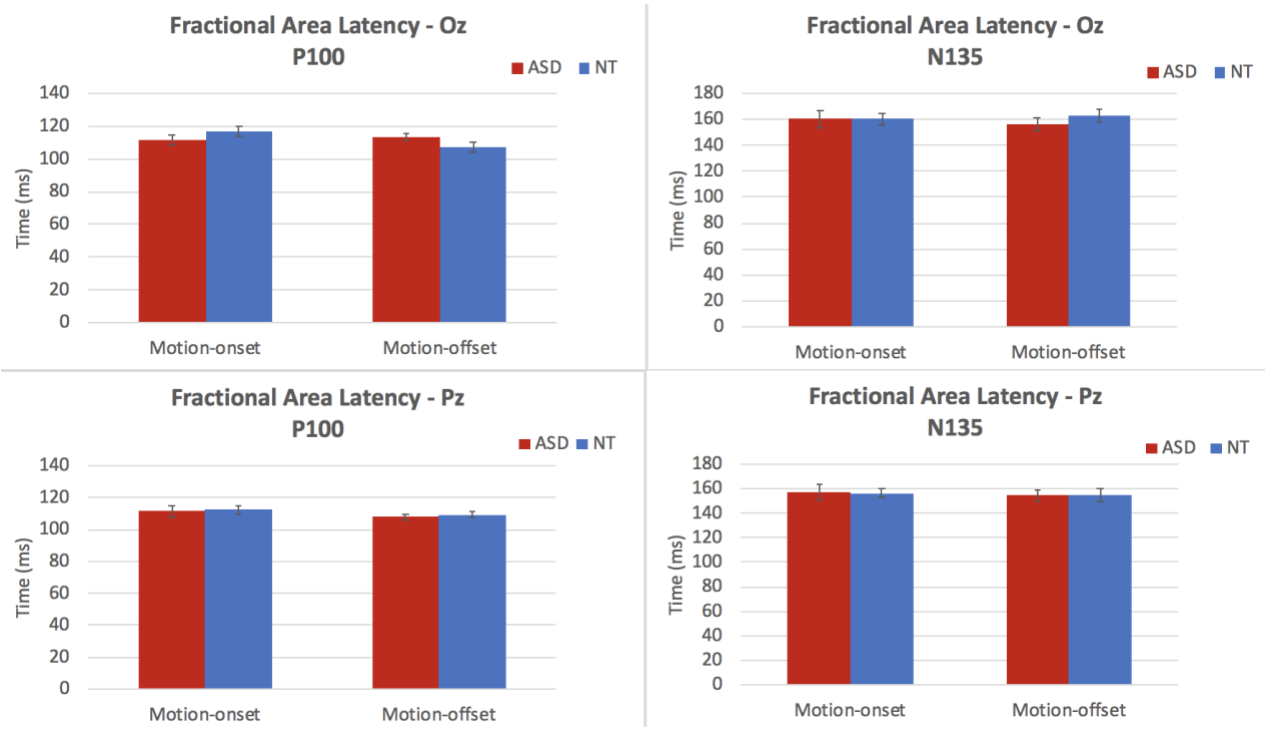

Figure 38. Fractional area latency measurement responses for motion-onset/offset at electrode site Oz and Pz for component P100 and N135 for ASD subjects and NT subjects. The error bars represent standard error of the mean (SEM).

In summary, when comparing the traditional waveform measures and those of mean amplitude and fractional area latency the outcomes were largely the same with some exceptions. The choice between the two outcome measures should largely be determined by the presence of the types of artifacts these measures are intended to solve (e.g.; in cases where there is high variability in the latency of the components or where adjacent components may distort the component of interest). Regardless of whether the type of method is chosen arbitrarily, or is chosen based upon visual inspection of the individual waveforms, a quantitative method should be specified prior to the actual data analysis. Otherwise, there is a danger of increasing the type I area rate associated with any specific comparison.

4. General Discussion

The aim of this study was to explore early visual responses in children with ASD and whether they consistently differed from NT individuals. To evaluate early visual functioning, VEPs were recorded from the cortex with a checkerboard pattern-reversal paradigm that included two different sizes checks (1° and 0.25°) and four different levels of contrasts (0.025 contrast, 0.05 contrast, 0.1 contrast and 0.98 contrasts). These black and white stimuli were focused on evaluating the integrity of the magnocellular pathway in ASD, since evidence has suggested that ASD subjects have difficulties with tasks that rely on the magnocellular pathways, such as evaluating moving stimuli. We further attempted to assess the magnocellular pathway with a moving stimulus so that we could specifically assess responses to motion-onset and motion-offset stimuli. Although a small sample size made it difficult to find statistically significant effects, there were several notable outcomes:

1. When evaluating the reversing checkerboards there was a lack of group differences between the ASD and NT subjects for the earliest visual component: the N75. This was true regardless of the check size or contrast of the stimuli. This lack of significant effects for diagnosis, either as a main effect or as interaction with other factors, indicates that the N75 component may not readily distinguish between ASD and NT subjects.
2. In contrast, for the P100 greater, but nonsignificant, positive amplitudes were found in the ASD subjects at a combination of the largest check size and at the lowest contrast values. This could suggest hyper-responsiveness in the P100 that can be attributed to the M-pathway (Figure 11). This contention is supported by

smaller differences between the groups at both the highest contrast level for the large check size and at almost all the contrast levels of the small check size (Figure 12). These results suggest that responses to low contrast low spatial frequency stimuli may have some utility in distinguishing between the ASD and NT groups. Despite these qualitative differences, main effects and interactions for diagnosis were not significant and the notable effect sizes further highlight the lack of power due to low sample size.

3. Latency measures did not identify clear differences between the ASD subjects for either the N75 or the P100 components. These unclear differences between the two groups and their latency might be due to the size of the windows that we used to extract these measurements (see section 4.6, Planned Improvements).
4. Motion onset/offset stimuli were used to further explore differences between the ASD and NT groups responses to visual motion for both the P100 and N135 components. There was a qualitative increase in the peak amplitude of the N135, along with potentially increased latency of this component, for motion-onset stimuli in the ASD subjects (see Figure 27. A). Even though the study was underpowered we found a large effect size of peak latency ($d = 1.0$) for component N135 for motion-onset at electrode site Oz. This large effect size, coupled with the nonsignificant effects of diagnosis, clearly suggest that greater power (more subjects) are needed to fully assess this result.
5. Since VEP waveforms have been proposed in the past to be a potential early marker of ASD, we also evaluated whether this would be a viable option with these types of visual stimuli. Despite some large effect sizes for the differences

between ASD and NT subjects, differences between the ASD and NT subject groups were largely insignificant. Furthermore, an examination of the individual subject waveforms suggests a level of variability that precludes the use of these measures for early identification of ASD risk in individual subjects.

6. To determine if symptom severity was related to early visual responses in individual subjects, correlations were calculated between various quantitative measures of the VEP components and individual subject symptom severity as assessed by the GARS-2. Due to the low power in the study, these values were never significant. Adjusted R squared (R^2) value did, however, indicate that in some cases over 25 percent of the variance in the quantitative results could be explained by the symptom severity scores.
7. Traditional point measures of each component of interest (peak amplitude and peak latency) and measures of larger segments of these components (mean amplitude and fractional area latency) were compared for both the reversing checkerboards and the motion-onset/offset stimuli. These measures were often very similar, but not identical. Although there is no objective criterion for selecting the most appropriate measure, whole component measures might be most appropriate where component point values are known to substantially vary within a specific subject group. This may especially be true of patient groups.

4.1. The Visual Pathways and their Contribution to Early Visual Responses

The visual system segregates information at early stages into parallel streams: the M and the P pathways. These two parallel pathways start at the level of the retina where distinct types of ganglion cells show different response properties to visual stimuli. The

M-pathway has been linked to low spatial frequencies while the P-pathway processes higher spatial frequencies (Kothari et al., 2014; Livingstone & Hubel, 1988). In our study, we used two different types of checkerboards that include both types of frequencies. The large (1° visual angles) checkerboard likely favors the M-pathway (Ellemberg et al., 2001), where our results show differences in amplitudes between ASD and NT subjects. For the higher frequency small (0.25° visual angle) checks may preferentially activate the P-pathway (Leonova et al., 2003). In addition, stimuli with hard edges also include high spatial frequencies, regardless of the stimulus size, that would be expected to activate the M pathway.

To stimulate and isolate the M-pathway low contrast motion or flicker is best, while isoluminant and color patterns are optimal for preferentially activating the P and the small-cell koniocellular (K) pathways (Livingstone & Hubel, 1987). It could be concluded that the differences we found in our study between check sizes among ASD and NT subjects could potentially point to a dysfunction of the M-pathway. It is crucial to identify differences in visual responses between high and low frequencies between ASD groups and NT subjects in order to better assess the retinogeniculate visual pathway. Understanding differences in responses could potentially help to create an electrophysiological neuromarker based on early visual responses.

Standardized stimuli used in clinical settings consist of two checkerboards 0.25° and 1.0° of visual angle presented at 0.98 contrast. Considering the results of just these stimuli, ASD subjects showed a large P100 peak amplitude effect size for the small, but not the large checkerboard (see Figure 10). Although these effect sizes are notable, they were not significant in our statistical analysis. This is due to a lack of power in the

experiment and the variability amongst subjects. Latency values at 0.98 contrast did not differ between groups for either the N75 or the P100.

In the present study, for pattern-reversal, the negative component N75 which occurs between 60-100 ms was found to behave similarly in the ASD group compared to NT subjects at electrode site Oz. The first negative component in VEPs has been proposed to be mostly generated in the primary visual cortex (striate cortex; Kovarski et al., 2016). This first negative component is not often reported in VEPs studies of ASD subjects, and studies that have reported responses on this component have been inconsistent. In a research study by Siper et al., (2016), where they used a reversing checkerboard at high contrast, they reported finding a main effect for smaller peak amplitudes at the component N75 and P100, between ASD and NT subjects, but no significant effects in latencies between NT and ASD subjects. Sayorwan et al., (2018), used stimuli similar to Siper et al., (2016), and found that amplitude and latency of the N75 component was slightly reduced compared to a control group. In our results the N75 does not show differences in amplitudes and latencies between the ASD and NT participants at these early stages of visual processing. These findings largely match the results reported in the studies cited above, however a larger sample size may have better been able to evaluate some of the larger effect sizes that were found. This early negative component in ASD and NTs subjects needs to be reported not only to analyze and understand how early visual processing at these early stages differed among the groups, but also because it is very close in time to the P100 and may affect the absolute amplitude of that component. Peak-to-trough values (the difference between the N75 and the P100 amplitude) can be reported as another control for drift of the recording from the baseline.

In this study, the peak-to-trough amplitude results basically mirrored those found for the P100 amplitudes. Namely, some differences between ASD and NT subjects at the lower contrast values of the large checkerboard stimuli.

The later positive P100 peaks around 80-130 ms. This first positive component has been proposed to measure retino-striate conduction time and recorded responses are strongest from the midline electrodes (Bach & Ullrich, 1996). Although nonsignificant, there were large effect sizes at the lower contrast levels for the large checkerboard when evaluating the amplitude of the P100. At these lower contrast levels ASD subjects consistently showed higher amplitudes relative to the control subjects (see Figure 6). In contrast, these differences at low contrast were not apparent for the P100 elicited from the small checkerboard. Peak latency measures also did not appear to distinguish between the groups.

The P100 component is highly sensitive to changes in contrast, and increases in amplitude as contrast increases, while showing longer latencies as contrast decreases (Jemel et al., 2010; Kubavá eta al., 1995). Besides the significant effect for contrast, for mean amplitude, there was also a three-way interaction between checkerboard size, contrast, and diagnosis. For the large checkerboard ASD subjects tended to show more uniform amplitudes across the different contrasts while the NTs amplitudes decreased at the lower contrast levels. For the small checkerboard ASD subjects' amplitudes were more similar to the NT group. Past studies have not always shown this pattern of results; however, measures of mean amplitudes are rarely used. Kovarski et al., (2016) used the same paradigm of a reversing black-and-white checkerboard at a 100 percent contrast and found that ASD subjects' P100 *peak* amplitudes were smaller than those found in their

NT subjects. In another study by Constable et al., (2012), using two types of contrast (98 percent and 10 percent), no differences were found in the positive component P100 either in amplitudes or latencies. These studies do not match our findings, where our results between ASD subjects and NTs differed in P100 amplitudes for the largest checkerboard. As stated, in the current study ASD subjects continue to show a predominant P100 with large amplitudes for the large checkerboard (see Figure 7). The NT subjects' P100 wave behaved as Kubavé et al., (1995) reports, showing lower amplitude and longer latencies at the lowest contrast levels for the large checkerboard. It has been suggested previously that these differences in the P100 amplitudes in ASD subjects may be caused by specific neural abnormalities that are related to low-level visual processing (Walsh et al., 2005).

Other studies exploring early visual responses have utilized nonclinical stimuli, such as sine wave grating stimuli that can be varied in frequency, amplitude (an analog for contrast) and luminance (Bertone et al., 2005; Dakin & Hess, 1997). In a study by Jemel et al., (2010) they used VEPs along with grating stimuli at different cycles per degree of visual angles (cpd) and looked at low (0.8 cpd), medium (2.8 cpd) and high (8 cpd) spatial frequencies. They found that ASD subjects showed a reduction in responses for medium (2.8 cpd) and higher (8 cpd) spatial frequencies compared with controls, but had similar responses at the lowest (0.8 cpd) spatial frequency. In these studies differences in contrast sensitivity and frequency responses in ASD subjects seem to point instead to a disruption of the P-pathway and not exclusively to problems within the M-pathway. Considering the high contrast sensitivity of the P-pathway and low contrast sensitivity of the M-pathway (Kubová et al., 1995; Foxe et al., 2008), and the differences in responses to contrasts between ASD and NT subjects found in our study. These results

with nonclinical stimuli suggest that additional VEP studies of neural processing in motion and contrast are very much needed in ASD groups.

4.2. Individual VEP Waveforms and Symptom Severity

Past ERP studies in ASD have explored whether ASD subjects show higher response variability to both auditory and visual stimuli. Results from these studies are contradictory. Some studies show no substantive differences between ASD subjects and controls in terms of response variability (Butler et al., 2017), while others find greater variability in ASD subjects (Kovarski et al., 2019). The neural unreliability hypothesis proposes greater variability in moment-to-moment cortical representation of environmental events where responses might show greater trail-to-trial variability in individuals with ASD compared to NTs (Haigh et al., 2015; Butler et al., 2017). Our results are equivocal in regards to this hypothesis. On the one hand, individual waveforms do not seem to provide a basis for early diagnosis. On the other hand, results of Levene's test do not indicate higher variability in ASD subjects. The outcome of these variance analysis are tempered both by the low power in our study and the inability to conclude that a null statistical result means that there are no differences between the groups. It is still important to explore inter-trial variability at early visual responses among ASD subjects for the development of individualized therapeutic treatments (Kovarski et al., 2019).

Only a few studies have explored individual VEP waveforms in ASD subjects. Most of these studies grouped patients depending upon the severity of their symptoms (low versus high; Sayorwan et al., 2018; Sutherland & Crewther, 2010) or language abilities (DiStefano et al., 2019). These studies proposed that the inconsistency in

findings between severity and their responses might be due to variability (Kovarski et al., 2019; Milne, 2011) and the relatively small sample sizes used, similar to our study. We found that in some cases VEP responses were related to symptom severity assessed by the GARS-2. In the ASD group, negative correlations between the amplitude of the P100 and symptom severity as assessed by the GARS-2 in the ASD subjects could, in some cases, account for over 25 percent of the variance in these measures. Although intriguing, due to low power, these correlations never reached significance. Individual waveform variability limits the use of VEPs as a neuromarker; there is some potential relationship to symptom severity that deserves further study. As with most patient groups, the variability in the individual waveforms was striking and correlations between individual averages and measures of severity in the ASD group were never significant. In aggregate, this suggests that VEPs, although easy to measure in a clinical setting, are likely not useful as a potential diagnostic tool for either the presence or severity of an ASD diagnosis. One potential explanation is the heterogeneity in ASD subjects at the genetic and phenotypic levels (Dickinson et al., 2018; Eapen et al., 2013).

4.3. Motion-Onset and Offset Responses

Although diagnosis did not show any main effects or interactions in response to motion onset and offset, there were several notable effect size differences between the groups. Perhaps the clearest of these were higher amplitudes in the ASD group for the P100 for both motion-onset and motion-offset, and larger negative amplitudes for the N135 for motion onset, but not offset.

The expanding and contracting ‘dartboard’ stimulus employed here was used specifically to assess scalp responses to motion onset and offset. In contrast, to assess the

hypothesis that ASD subjects present disadvantages of the M-Pathway many of the visual motion studies in ASD have focused on motion-coherence and biological-motion, but little is known how ASD subjects process motion at early visual stages as assessed by VEPs. Behaviorally, ASD subjects are better on detail-focused perceptual tasks where they are faster at detecting single targets (Plaisted et al., 1998), while for motion-coherence and/or biological-motion tasks, they tend to do worse than their NT peers (Dakin & Firth, 2005). The literature in motion processing in ASD is largely in agreement that motion processing is disrupted (Dakin & Firth, 2005; van Boxtel et al., 2016), and that patients with an ASD diagnosis see this aspect of the world differently.

4.3.1. Motion-Onset Responses in ASD

Many studies use a radial motion stimulus moving in all direction (Bertone et al., 2003, 2005), and random dots to assess coherence thresholds in ASD subjects. In this study we used Bach and Hoffman's (1999) approach to explore both motion-onset and motion-offset responses using a radial ring which expands and contracts for stimulation of the M-pathway in ASD patients. We analyzed the onset and offset responses to motion for the P100 and N135 at midline electrode sites Oz and Pz. In motion-onset studies, the negative N135 component displays the largest amplitudes and has been linked to the activity of the M-pathway (Kuba et al., 2007). This second negative component in ERP averages represents motion mechanisms (Bach and Ullrich, 1996) that fluctuate between 150-205 ms, and has been associated with extrastriate areas with high-contrast sensitivity (Kuba et al., 2007; Kubová et al.,1995). A study by Constable et al., (2012) where they study motion-onset responses using VEPs and a contracting and expanding concentric rings (33.3% duty cycle at 10 percent contrast) found that ASD subjects had a

significantly larger N135 peak amplitude for motion-onset VEPs compared to NTs subjects. In another study by Yamasaki et al. (2011), using random dots to measure motion-coherence, they found in adults with ASD a significantly prolonged N135 and P100 latencies for radial optic flow, but not for horizontal motion. The present results show similar outcomes for motion-onset at component N135, where ASD subjects present larger amplitudes and longer latencies compared to NT subjects although these differences did not reach significance. Although a larger subject group is needed, these findings suggest that early visual processing of motion stimuli impacts the processes of motion perception (Dakin & Firth, 2005).

4.3.2. Motion-Offset Responses in ASD

Motion-offset was followed by a period of 1500 ms where the dartboard remained stationary. Many studies have focused on motion-onset, but there is a notable lack of research exploring motion offset and adaptation to movement in ASD subjects. In studies of neurotypicals recording VEPs in response to a contracting and expanding stimulus, responses to motion onset are typically larger and more uniform compared to motion offset responses (Bach & Ullrich, 1993). Past research has recommended using a stationary period of around 1000 ms, along with this type of stimuli, in order to prevent adaptation to motion which can result in a predominant P100 and a reduction in amplitude of the subsequent N135 component. These N135 responses have been linked to parietal-occipital regions while the P100 component is tied to occipital locations alone (Kuba et al., 2007; Bach & Ullrich, 1993). In our study we found a medium effect size for peak amplitude at component N135 for motion offset at electrode site Pz (between subject group $d = 5$) which could suggest that ASD subjects are less sensitive to motion

adaptation compared to NT subjects. These results, however, never reached significance. Van Boxtel et al., (2015) measured adaptation to biological motion using two different types of action stimuli (walking versus running) to compare performance between ASD and NT subjects. The ASD group did not show significant adaptation to either action, relative to the NT group. Their finding suggests that ASD patients present decreased sensitivity to motion and motion adaptation. Understanding how ASD patients respond to motion offset is lacking, and studies of motion-onset and motion-offset stimuli are essential to our understanding of how ASD subjects not only perceive motion in daily life, but also how they adapt to a variety of moving stimuli such as facial expressions.

4.4. Comparison of mean amplitude and fractional area latency measures to peak amplitude and peak latency measures

This is perhaps the most difficult question to firmly answer given that there is no gold standard for quantification of individual components in the VEP waveform. Peak amplitudes and peak latency are the most commonly reported measures, but whether there might be potentially less biased methods of extracting amplitude and latency values is unknown. In our study mean amplitude and fractional area latency often yielded similar, but not identical, results when analyzing data. In the end, a qualitative visual examination of the individual waveforms and their relation to the average waveform of the subject group might be the best indicator of when such alternative measures might be helpful. For example, in the case where peak latency variability might artificially depress the amplitude of the averaged component (for further discussion about these measurements review: Clayson et al., 2013 and Luck, 2005). If alternative measures are

to be considered for use, criteria for their implementation should be established *a priori*. The exact nature of these criteria remains to be determined.

4.5. Implications for Early Detection

Because early behavioral intervention is associated with better long-term outcomes in ASD individuals, finding a neuro- or biological marker as an adjunct to the currently utilized behavioral criterion is a fundamental goal of a great deal of ASD research. The diagnosis of ASD can potentially be detected at 18 months or younger, but a diagnosis by experienced professionals is typically given around age two (CDC, 2020). Some of the onset behaviors in infants at risk to develop ASD include a delay in motor milestones, abnormal fidgety movements, less goal-directed actions, and reduction in adopting the role of a social actor in interactions with parents and caregivers (Yirimiya & Charman, 2010). Many of these behaviors are linked to social communication and any type of early disruption to visual input could cause a cascade of symptoms that could be linked to ASD. Whether VEPs could be used in a clinical setting to target ASD at early stages in very young infants is still a somewhat open question not fully addressed by the current work. Given the individual variability in response to the checkerboard stimuli in the present study, it may be that motion-onset stimuli (i.e., the expanding and contracting dartboard stimulus) might hold the most potential promise for assessing risk for ASD in young children. Despite this, the variability of individual subject responses suggest that such measures would likely have to be only one of several potential risk factors utilized in early assessments. Whether VEPs provide unique predictive utility for an ASD diagnosis remains to be addressed with multivariate analyses. The present study only

used children already diagnosed with ASD and does not speak to the question of whether differences in responses to motion-onset are present at earlier ages.

4.6. Planned improvements in upcoming studies

The present study relates differences between ASD subjects and NT group for the P100 components and their amplitudes to contrast responses. For latencies these differences were less clear between the two groups (ASD vs. NT) and might be due to the sizes of the window we used to extract their values (for the checkerboard P100: 80-130 ms and dartboard P100: 85-135 and N135: 100-205). These results did not represent the peak latencies when their peaks did not fall between the two fixed measurement points. To better ensure that the peak latencies fall in that specific measurement window for the component P100 we will make these windows larger to assess latencies differences between the two groups. Larger windows can also create problems for peak latency extraction and Luck (2005) suggests using the *local peak* option that can be found within the *measurement tool* of ERP lab to assess the window used and the component of interest to ensure that the peak of interest falls within the window.

In future studies we are planning to use a high density EEG system with 125 channels to explore the electrocortical activity across brain regions. Multiple sensors can help identify potential hemispheric differences in early visual signals in ASD and could provide better insights into regional differences in the early VEP signals. Additional sensors could also be used to examine neural oscillatory information between cortical locations. One additional advantage of having more sensors is that 'scalp current density' (SCDs) can be used to possibly disentangle neural sources. For our planned follow up studies we have coded our pattern-reversal and motion stimuli in Matlab 2015 (The

Mathworks, Natick, MA, United States) and have added different contrasts to our expanding and contracting dartboard (0.025, 0.05, 0.1, and 0.98). Although we studied moving stimuli, a notable shortcoming of the current work is that we did not assess different contrast levels with the expanding and contracting dartboards. Lower contrast stimuli could maximize stimulation of the M-pathway and provide better insight into the question of whether the M-pathway is specifically impaired in ASD. In terms of recruiting more participants, Reno has a large community of Spanish speakers and we have extended our research for participants that speak Spanish, translating our consent forms to make our study more inclusive. We are also using the Raven's Progressive Matrices Test to measure non-verbal, abstract and cognitive functions of participants with ASD and NT subjects that speak English and/or Spanish since this test is designed to have no cultural or ethnic bias. Recruiting more participants will increase the power to detect differences between ASD subjects and NT subjects, and our preliminary findings reported here can be used in an *a priori* power analysis to select a sample size that gives enough power to detect medium to large effect sizes. We are also measuring handedness of the participants and confirming that participants have normal, or corrected to normal vision, using the Freiburg Vision Test ('FrACT) to measure acuity. To improve detection of eye movement artifacts, electrodes will be placed above, below and lateral to the eyes. In the current study electrodes were only placed lateral to the eyes. These additional electrodes will allow for better detection of non-horizontal eye movements as well as eye closures.

4.7. Future study directions: The role of alpha band in early visual processing in ASD subjects

Cortical oscillations have been suggested to play an active role in network coordination and communication between distant brain areas (Khan et al., 2013). In ASD, specific impairments have been reported, including difficulty integrating perceptual and sensory information, which may be associated with a disruption of interareal brain networks (Simon & Wallace, 2016). The hypothesis of connectional change suggests that ASD subjects have both long-range, functional hypoconnectivity and short-range hyperconnectivity. Long-range connections are typically associated with top-down functions and rely on slower rhythms in the delta (~.1- 4 Hz), theta (~4 - 6 Hz), and alpha (~7-15 Hz) bands. Short-range connectivity has been functionally linked to bottom-up cognitive functions and runs at faster rhythms such as the beta (~15 - 30 Hz), and gamma (~30 - 100+ Hz) bands (O'Reilly et al., 2017). For these frequencies to integrate sensory information and higher cognitive processes, intact long-range connections are required. ASD cortical connectivity changes could result in the alpha band abnormalities that have been reported in the past (Dickinsons et al., 2018; Larraín-Valenzuela et al., 2017). These alterations have the potential to affect higher cognitive processes that are related to social perception (Khan et al., 2013). The lack of research in this area leaves a gap in how the alpha band acts in sensory visual perception in ASD, which could be key to understanding the already documented structural changes to connectivity found in ASD.

4.8. The Role of Alpha-Band in Visual Perception Tasks

In future studies we would also like to explore the role of alpha band activity in the visual responses of ASD subjects. Little is known about how the alpha band acts in visual perception in ASD. The alpha band is the dominant rhythm in the brain and has a frequency between 7-15 Hz. It is most active in parietal-occipital regions during resting

states and in pre-stimuli onset (Jessen and Kotz, 2011; Edgar et al., 2015). Recent studies have investigated the role that the alpha band plays in behaviors that make up the core characteristics in autism. Alpha oscillations act in sensory perception, social communication, and emotional processing (Lefebvre et al., 2018; Fitzpatrick et al., 2019, Jessen & Kotz, 2011; Klimesch, 2012). Early reports in this frequency have been described in ASD subjects, at the group level, with a decrease in peak alpha frequency and reduced power in ASD compared to NT subjects (Dickinsons et al., 2018; Larraín-Valenzuela et al., 2017). A study by Edgar et al., (2015) measured alpha frequency in a resting state paradigm and found that the alpha band activity in ASD subjects was increased in primary motor cortex as well as somatosensory and parietal multimodal areas. The alpha band has also been proposed to modulate the transfer of information in thalamo-cortical and cortico-cortical networks (Kilmesch et al., 2007). These past findings indicate that early sensory visual processing and alpha oscillations in ASD are important avenues for future exploration. The hypothesis being that early visual disruption in ASD, could impact the binding of visual information as mediated by the alpha band. In a future study, to better understand how the alpha band acts in visual processing, we are using electroencephalogram (EEG) recordings along with a two-flash fusion stimulus during a visual discrimination task. Performance will be compared to their resting state measures. To extract the rhythms of alpha we will use time frequency analysis to correlate alpha-band activity during the resting state and prior to stimulus onset (for paradigma information see: Samaha and Postel, 2015).

Scalp-recorded occipital alpha-band oscillations reflect phasic information transfer in thalamocortical neurons projecting from the LGN to primary visual cortex

(Lörincz et al., 2009). Animal studies in cats, monkeys and rats have shed some light on how the LGN might be modulating transmission of visual information to V1 utilizing these alpha frequencies. These studies have reported that the alpha band is linked to the LGN mediating corticogeniculate feedback processing during resting states and during natural wakefulness states (Lörincz et al., 2009; Bastos et al., 2014). Reports in ASD subjects during resting states indicate that altered power in the alpha band could indicate abnormalities in corticothalamic projections that could be linked to altered thalamic volumes in ASD (Dickinson et al., 2018; Edgar et al., 2015). A past study by Chen et al., (2016) demonstrated impaired thalamo-cortical information transmission in ASD and suggested that atypical development of thalamo-temporal connections may result in interareal communication deficits in ASD.

In summary, the alpha band plays a role in social communication as well as sensory visual perception. It is associated with the LGN's role of sending and modulating both feedback and feedforward visual information to and from area V1.

4.9. Overall Conclusion

In conclusion, early visual processing in ASD as assessed by VEPs shows altered responses in subjects with ASD compared to NT subjects. In our results, ASD subjects show larger P100 amplitudes for the large check sizes at lower contrast values. Individual waveforms in ASD subjects are likely too variable to be used as a reliable early neuromarker. In the ASD group, negative correlations between the amplitude of the P100 and symptom severity as assessed by the GARS-2 in the ASD subjects could, in some cases, account for over 25 percent of the variance in these measures. However, these correlations never reached significance. For motion onset, ASD subjects present large

amplitudes for components P100 and the N135 at electrode site Oz. For motion offset, ASD subjects continue to show large amplitudes, but only for the P100 component. Considering our findings, we could conclude that ASD subjects show a marked disruption at early visual processing stages that likely impact the M-pathway causing a cascade of symptoms that could impair social perception. Future studies should be better tailored to specifically evaluate group differences and whether specific measures of the ASD waveforms might produce better differentiation of individual subjects.

References

Allen, D., Norcia, A. M. and Tyler, C. W. (1986). Comparative study of electrophysiological and psychophysical measurement of the contrast sensitivity function in humans, *Amer. J. Optometry Physiol. Optics* 63, 442 – 449.

American Psychiatric Association, & American Psychiatric Association. DSM-5 Task Force. (2013). *Diagnostic and statistical manual of mental disorders: DSM-5* (Fifth ed.).

Bach, M., & Hoffmann, M. B. (1999). Visual motion detection in man is governed by non-retinal mechanisms. *Vision Research, 40*(18), 2379-2385. doi:10.1016/S0042-6989(00)00106-

Bach, M., & Ullrich, D. (1997). Contrast dependency of motion-onset and pattern-reversal VEPs: Interaction of stimulus type, recording site and response component. *Vision Research, 37*(13), 1845-1849. doi:10.1016/s0042-6989(96)00317-3

Bakroon, A., & Lakshminarayanan, V. (2016). Visual function in autism spectrum disorders: A critical review: Visual function in autism spectrum disorders. *Clinical and Experimental Optometry, 99*(4), 297-308. doi:10.1111/cxo.12383

Bastos, A. M., Briggs, F., Alitto, H. J., Mangun, G. R., & Usrey, W. M. (2014). Simultaneous recordings from the primary visual cortex and lateral geniculate nucleus reveal rhythmic interactions and a cortical source for γ-band

oscillations. *The Journal of Neuroscience, 34*(22), 7639-7644. doi:10.1523/JNEUROSCI.4216-13.2014

Bertone, A., Mottron, L., Jelenic, P., & Faubert, J. (2003). Motion perception in autism: A "Complex" issue. *Journal of Cognitive Neuroscience, 15*(2), 218-225. doi:10.1162/089892903321208150

Bertone, A., Mottron, L., Jelenic, P., & Faubert, J. (2005). Enhanced and diminished visuo-spatial information processing in autism depends on stimulus complexity., *128*(10), 2430-2441. doi:10.1093/brain/awh561

Blake, R., Turner, L. M., Smoski, M. J., Pozdol, S. L., & Stone, W. L. (2003). Visual recognition of biological motion is impaired in children with autism. *Psychological Science, 14*(2), 151-157. doi:10.1111/1467-9280.01434

Brown, A. C., Chouinard, P. A. & Crewther, S. G. V. (2017). Vision research literature may not represent the full intellectual range of autism spectrum disorder. *Front Hum. Neurosci.* 11, 57.

Brown, A. C., Peters, J. L., Parsons, C., Crewther, D. P., & Crewther, S. G. (2020). Efficiency in magnocellular processing: A common deficit in neurodevelopmental disorders. *Frontiers in Human Neuroscience, 14*, 49-49. doi:10.3389/fnhum.2020.00049

Butler, J. S., Molholm, S., Andrade, G. N., & Foxe, J. J. (2017). An examination of the neural unreliability thesis of autism. *Cerebral Cortex*, *27*(1), 185-200. https://doi.org/10.1093/cercor/bhw375

Callaway, E.M. (2005), Structure and function of parallel pathways in the primate early visual system. The Journal of Physiology, 566: 13-19. https://doi.org/10.1113/jphysiol.2005.088047

Chen, H., Uddin, L. Q., Zhang, Y., Duan, X., & Chen, H. (2016). Atypical effective connectivity of thalamo-cortical circuits in autism spectrum disorder. *Autism Research, 9*(11), 1183-1190. doi:10.1002/aur.1614

Clayson, P. E., Baldwin, S. A., & Larson, M. J. (2013). How does noise affect amplitude and latency measurement of event-related potentials (ERPs)? A methodological critique and simulation study. *Psychophysiology, 50*(2), 174–186. https://doi.org/10.1111/psyp.12001

Constable, P. A., Gaigg, S. B., Bowler, D. M., & Thompson, D. A. (2012). Motion and pattern cortical potentials in adults with high-functioning autism spectrum disorder. *Documenta Ophthalmologica, 125*(3), 219-227. doi:10.1007/s10633-012-9349-7

Dakin, S. C., & Hess, R. F. (1997). Absence of contour linking in peripheral vision. *Nature, 390*(6660), 602-604. doi:10.1038/37593

Dakin, S., & Frith, U. (2005). Vagaries of visual perception in autism. *Neuron, 48*(3), 497-507. doi:10.1016/j.neuron.2005.10.018

Dickinson, A., DiStefano, C., Senturk, D., & Jeste, S. S. (2018). Peak alpha frequency is a neural marker of cognitive function across the autism spectrum. *The European Journal of Neuroscience, 47*(6), 643-651. doi:10.1111/ejn.13645

DiStefano, C., Senturk, D., & Jeste, S. S. (2019). ERP evidence of semantic processing in children with ASD. *Developmental Cognitive Neuroscience*, *36*, 100640–100640. https://doi.org/10.1016/j.dcn.2019.100640

Eapen, V., Crnčec, R., & Walter, A. (2013). Exploring Links between Genotypes, Phenotypes, and Clinical Predictors of Response to Early Intensive Behavioral Intervention in Autism Spectrum Disorder. *Frontiers in human neuroscience*, *7*, 567. https://doi.org/10.3389/fnhum.2013.00567

Edgar, J. C., Edgar, J. C., Heiken, K., Heiken, K., Chen, Y., Chen, Y., Roberts, T. P. L. (2015). Resting-state alpha in autism spectrum disorder and alpha associations with thalamic volume. *Journal of Autism and Developmental Disorders, 45*(3), 795-804. doi:10.1007/s10803-014-2236-1

Ellemberg, D., Lewis, T. L., Liu, C. H. and Maurer, D. (1999). Development of spatial and temporal vision during childhood, *Vision Res.* 39, 2325–2333.

Fitzpatrick, P., Mitchell, T., Schmidt, R. C., Kennedy, D., & Frazier, J. A. (2019). Alpha band signatures of social synchrony. *Neuroscience Letters, 699*, 24-30. doi:10.1016/j.neulet.2019.01.037

Foxe, J. J., Strugstad, E. C., Sehatpour, P., Molholm, S., Pasieka, W., Schroeder, C. E., & McCourt, M. E. (2008). Parvocellular and magnocellular contributions to the initial generators of the visual evoked potential: High-density electrical mapping of the "C1" component. *Brain Topography*, *21*(1), 11-21. https://doi.org/10.1007/s10548-008-0063-4

Frey, H., Molholm, S., Lalor, E. C., Russo, N. N., & Foxe, J. J. (2013). Atypical cortical representation of peripheral visual space in children with an autism spectrum

disorder. *The European Journal of Neuroscience, 38*(1), 2125-2138. doi:10.1111/ejn.12243

Fujita, T., Yamasaki, T., Kamio, Y., Hirose, S., & Tobimatsu, S. (2011). Parvocellular pathway impairment in autism spectrum disorder: Evidence from visual evoked potentials. *Research in Autism Spectrum Disorders, 5*(1), 277-285. doi:10.1016/j.rasd.2010.04.009

Gepner, B., & Mestre, D. (2002). Rapid visual-motion integration deficit in autism. *Trends in Cognitive Sciences, 6*(11), 455-455. doi:10.1016/S1364-6613(02)02004-1

Greenaway, R., Davis, G., & Plaisted-Grant, K. (2013). Marked selective impairment in autism on an index of magnocellular function. *Neuropsychologia, 51*(4), 592-600. doi:10.1016/j.neuropsychologia.2013.01.005

Haigh, S. M., Haigh, S. M., Heeger, D. J., Heeger, D. J., Dinstein, I., Dinstein, I., Minshew, N., Minshew, N., Behrmann, M., & Behrmann, M. (2015). Cortical variability in the sensory-evoked response in autism. *Journal of Autism and Developmental Disorders, 45*(5), 1176-1190. https://doi.org/10.1007/s10803-014-2276-6

Howard, P. L., Zhang, L., & Benson, V. (2019). What can eye movements tell us about subtle cognitive processing differences in autism? *Vision, 3*(2), 22. doi:10.3390/vision3020022

Jemel, B., Mimeault, D., Saint-Amour, D., Hosein, A., & Mottron, L. (2010). VEP contrast sensitivity responses reveal reduced functional segregation of mid and

high filters of visual channels in autism. *Journal of Vision, 10*(6), 13-13. doi:10.1167/10.6.13

Jessen, S., & Kotz, S. A. (2011). The temporal dynamics of processing emotions from vocal, facial, and bodily expressions. *NeuroImage 58*(2), 665-674. doi:10.1016/j.neuroimage.2011.06.035

Kaplan, E., & Shapley, R. M. (1986). The primate retina contains two types of ganglion cells, with high and low contrast sensitivity. *Proceedings of the National Academy of Sciences - PNAS, 83*(8), 2755-2757. doi:10.1073/pnas.83.8.2755

Khan, S., Gramfort, A., Shetty, N. R., Kitzbichler, M. G., Ganesan, S., Moran, J. M., Kenet, T. (2013). Local and long-range functional connectivity is reduced in concert in autism spectrum disorders. *Proceedings of the National Academy of Sciences - PNAS, 110*(8), 3107-3112. doi:10.1073/pnas.1214533110

Klimesch, W. (2012). Alpha-band oscillations, attention, and controlled access to stored information. *Trends in Cognitive Sciences, 16*(12), 606-617. doi:10.1016/j.tics.2012.10.007

Kothari, R., Singh, S., Singh, R., Shukla, A. K., & Bokariya, P. (2014). Influence of visual angle on pattern reversal visual evoked potentials. *Oman journal of ophthalmology, 7*(3), 120–125. https://doi.org/10.4103/0974-620X.142593

Kovarski, K., Malvy, J., Khanna, R. K., Arsène, S., Batty, M., & Latinus, M. (2019). Reduced visual evoked potential amplitude in autism spectrum disorder, a variability effect? *Translational Psychiatry, 9*(1), 341-9. doi:10.1038/s41398-019-0672-6

Kovarski, K., Thillay, A., Houy-Durand, E., Roux, S., Bidet-Caulet, A., Bonnet-Brilhault, F., & Batty, M. (2016). Brief report: Early VEPs to pattern-reversal in adolescents and adults with autism. *Journal of Autism and Developmental Disorders, 46(10),* 3377-3386. doi:10.1007/s10803-016-2880-8

Kremláček, J., Kuba, M., Kubová, Z. *et al.* Motion-onset VEPs to translating, radial, rotating and spiral stimuli. *Doc Ophthalmol* 109, 169–175 (2004). https://doi.org/10.1007/s10633-004-4048-7

Kuba, M., Kubová, Z., Kremláček, J., & Langrová, J. (2007). Motion-onset VEPs: Characteristics, methods, and diagnostic use. *Vision Research, 47*(2), 189-202. doi:10.1016/j.visres.2006.09.020

Kubová, Z., Kuba, M., Spekreijse, H., & Blakemore, C. (1995). Contrast dependence of motion-onset and pattern-reversal evoked potentials. *Vision research, 35*(2), 197-205.

Larraín-Valenzuela, J., Zamorano, F., Soto-Icaza, P., Carrasco, X., Herrera, C., Daiber, F., Aboitiz, Billeke, P. (2017). Theta and alpha oscillation impairments in autistic spectrum disorder reflect working memory deficit. *Scientific Reports, 7*(1), 14328-11. doi:10.1038/s41598-017-14744-8

Laycock, R., Crewther, S. G., & Crewther, D. P. (2007). A role for the 'magnocellular advantage' in visual impairments in neurodevelopmental and psychiatric disorders. *Neuroscience and Biobehavioral Reviews, 31*(3), 363-376. doi:10.1016/j.neubiorev.2006.10.003

Lefebvre, A., Delorme, R., Delanoë, C., Amsellem, F., Beggiato, A., Germanaud, D., Dumas, G. (2018). Alpha waves as a neuromarker of autism spectrum disorder:

The challenge of reproducibility and heterogeneity. *Frontiers in Neuroscience, 12,* 662-662. doi:10.3389/fnins.2018.00662

Leonova, A., Pokorny, J., & Smith, V. C. (2003). Spatial frequency processing in inferred PC- and MC-pathways. *Vision Research, 43*(20), 2133-2139. https://doi.org/10.1016/S0042-6989(03)00333-X

Little, J. (2018). Vision in children with autism spectrum disorder: A critical review: Vision in children with autism. *Clinical and Experimental Optometry, 101*(4), 504-513. doi:10.1111/cxo.12651

Liu, C. J., Bryan, R. N., Miki, A., Woo, J. H., Liu, G. T., & Elliott, M. A. (2006). Magnocellular and parvocellular visual pathways have different blood oxygen level-dependent signal time courses in human primary visual cortex. *American Journal of Neuroradiology: AJNR, 27*(8), 1628-1634

Livingstone, M. S., & Hubel, D. H. (1987). Psychophysical evidence for separate channels for the perception of form, color, movement, and depth. *Journal of Neuroscience, 7*(11), 3416-3468.

Livingstone, M., & Hubel, D. (1988). Segregation of form, color, movement, and depth: Anatomy, physiology, and perception. *Science (American Association for the Advancement of Science), 240*(4853), 740-749. doi:10.1126/science.3283936

López-Calderón, J., & Luck, S. J. (2014). ERPLAB: An open-source toolbox for the analysis of event-related potentials. *Frontiers in Human Neuroscience, 8*, 213-213. doi:10.3389/fnhum.2014.00213

Lörincz, M. L., Kékesi, K. A., Juhász, G., Crunelli, V., & Hughes, S. W. (2009). Temporal framing of thalamic relay-mode firing by phasic inhibition during the alpha rhythm. *Neuron, 63*(5), 683-696. doi:10.1016/j.neuron.2009.08.012

Luck, S. J. (2005). An introduction to the event-related potential technique. *Cambridge, Mass: MIT Press.*

Milne, E. (2011). Increased intra-participant variability in children with autistic spectrum disorders: evidence from single-trial analysis of evoked EEG. *Frontiers in Psychology*, *2*, 51–51. https://doi.org/10.3389/fpsyg.2011.00051

Milne, E., Swettenham, J., Hansen, P., Campbell, R., Jeffries, H., & Plaisted, K. (2002). High motion coherence thresholds in children with autism. *Journal of Child Psychology and Psychiatry*, *43*(2), 255–263. https://doi.org/10.1111/1469-7610.00018

O'Reilly, C., Lewis, J. D., & Elsabbagh, M. (2017). Is functional brain connectivity atypical in autism? A systematic review of EEG and MEG studies. *PloS One, 12*(5), e0175870-e0175870. doi:10.1371/journal.pone.0175870

Odom, J. V., Bach, M., Brigell, M., Holder, G. E., McCulloch, D. L., Mizota, A., International Society for Clinical Electrophysiology of Vision. (2016). ISCEV standard for clinical visual evoked potentials. *Documenta Ophthalmologica, 133*(1), 1-9. doi:10.1007/s10633-016-9553-y

Plaisted, K., O'Riordan, M., & Baron-Cohen, S. (1998). Enhanced visual search for a conjunctive target in autism: A research note. *Journal of Child Psychology and Psychiatry*, *39*(5), 777-783. https://doi.org/10.1017/S0021963098002613

Samaha, J., & Postle, B. (2015). The speed of alpha-band oscillations predicts the temporal resolution of visual perception. *Current Biology, 25*(22), 2985-2990. doi:10.1016/j.cub.2015.10.007

Sayorwan, W., Phianchana, N., Permpoonputtana, K., & Siripornpanich, V. (2018). A study of the correlation between VEP and clinical severity in children with autism spectrum disorder. *Autism Research and Treatment, 2018*, 1-8. doi:10.1155/2018/5093016

Shigeto, Tobimatsu, S., Yamamoto, T., Kobayashi, T., & Kato, M. (1998). Visual evoked cortical magnetic responses to checkerboard pattern reversal stimulation: A study on the neural generators of N75, P100 and N145. *Journal of the Neurological Sciences*, *156*(2), 186–194. https://doi.org/10.1016/S0022-510X(98)00026-4

Simon, D. M., & Wallace, M. T. (2016). Dysfunction of sensory oscillations in autism spectrum disorder. *Neuroscience and Biobehavioral Reviews, 68*, 848-861. https://doi.org/10.1016/j.neubiorev.2016.07.016

Siper, P. M., Zemon, V., Gordon, J., George-Jones, J., Lurie, S., Zweifach, J., Kolevzon, A. (2016). Rapid and objective assessment of neural function in autism spectrum disorder using transient visual evoked potentials. *PloS One, 11*(10), e0164422-e0164422. doi:10.1371/journal.pone.0164422

Spencer, J., O'Brien, J., Riggs, K., Braddick, O., Atkinson, J., and Wattam-Bell, J. (2000). Motion processing in autism: evidence for a dorsal stream deficiency. *Neuroreport* 11, 2765–2767.

Sutherland, A., & Crewther, D. P. (2010). Magnocellular visual evoked potential delay with high autism spectrum quotient yields a neural mechanism for altered perception. *Brain, 133*(Pt 7), 2089-2097. doi:10.1093/brain/awq122

Thye, M. D., Bednarz, H. M., Herringshaw, A. J., Sartin, E. B., & Kana, R. K. (2018). The impact of atypical sensory processing on social impairments in autism spectrum disorder. *Developmental Cognitive Neuroscience, 29*, 151-167. doi:10.1016/j.dcn.2017.04.010

Todorova, G.K., Hatton, R.E.M. & Pollick, F.E. (2019). Biological motion perception in autism spectrum disorder: a meta-analysis. *Molecular Autism* 10, 49 https://doi.org/10.1186/s13229-019-0299-8

Ung, D., Selles, R., Small, B. J., & Storch, E. A. (2014). A systematic review and meta-analysis of cognitive-behavioral therapy for anxiety in youth with high-functioning autism spectrum disorders. *Child Psychiatry and Human Development, 46*(4), 533-547. doi:10.1007/s10578-014-0494-y

Van der Hallen, R., Manning, C., Evers, K., & Wagemans, J. (2019). Global motion perception in autism spectrum disorder: A meta-analysis. *Journal of Autism and Developmental Disorders, 49*(12), 4901-4918. doi:10.1007/s10803-019-04194-8

Walsh, P., Kane, N., & Butler, S. (2005). The clinical role of evoked potentials. *Journal of Neurology, Neurosurgery and Psychiatry, 76* (suppl 2), ii16-ii22. doi:10.1136/jnnp.2005.068130

Woodman G. F. (2010). A brief introduction to the use of event-related potentials in studies of perception and attention. *Attention, perception & psychophysics*, *72*(8), 2031–2046. https://doi.org/10.3758/APP.72.8.2031

Yamasaki, T., Fujita, T., Kamio, Y., & Tobimatsu, S. (2011). Motion perception in autism spectrum disorder. *Advances in psychology research, 82*, 197-211.

Yamasaki, T., Maekawa, T., Fujita, T., & Tobimatsu, S. (2017). Connectopathy in autism spectrum disorders: A review of evidence from visual evoked potentials and diffusion magnetic resonance imaging. *Frontiers in Neuroscience, 11*, 627-627. doi:10.3389/fnins.2017.00627

Zane, E., Yang, Z., Pozzan, L., Guha, T., Narayanan, S., & Grossman, R. B. (2019). Motion-capture patterns of voluntarily mimicked dynamic facial expressions in children and adolescents with and without ASD. *Journal of Autism and Developmental Disorders, 49*(3), 1062-1079. doi:10.1007/s10803-018-3811-7